8-25-2017 12:00 AM

Planform Change and Bedload Transport in Braiding Rivers

Lara Middleton
The University of Western Ontario

Supervisor
Peter Ashmore
The University of Western Ontario

Graduate Program in Geography
A thesis submitted in partial fulfillment of the requirements for the degree in Master of Science

Abstract

Proglacial gravel-bed braided rivers have a dynamic planform composed of multiple unstable channels and ephemeral bars. The planform position is seen to change during high flows as the position of channels and bars changes. These changes are produced as pulses of bedload are mobilized and transported downstream, causing an observable change in the river planform and morphology. While it is known that bedload transport, morphological change and planform change in a braided river are inter-related the relationships have not been quantified. The first component of this research was to build on previous results by re-analyzing daily areas of planform change on a proglacial reach of the Sunwapta River, Alberta. The second component was to extend the field data by replicating selected hydrographs from Sunwapta River in a small-scale physical model in which simultaneous measurements of bedload transport, morphological change and equivalent areas of planform change were measured. Planform change, morphological change and bedload transport were all found to increase in relation to an increase in peak discharge of the experimental hydrographs, with some variability among repeated hydrographs. Total bedload transport, area of planform change, and volumes of erosion and deposition, were significantly correlated. This result contributes to the overall understanding of braided river planform dynamics and provides a potential surrogate method for measuring rates of bedload transport in gravel-bed braided river systems using event-based area of planform change.

Keywords

Braided rivers, gravel-bed rivers, planform adjustment, bedload transport, experimental modelling

Acknowledgements

First and foremost, I would like to extend my sincere thanks to my thesis advisor, Dr. Peter Ashmore. I greatly appreciate all the support, guidance and wisdom as well as the love and passion for braided rivers. Your continued encouragement and support throughout my undergraduate and graduate degrees has been exceptional. Thank you for understanding and fully supporting my love of field work and constant need to be in a pair of waders.

Thank you to the rest of the fluvial lab for the constant encouragement, advice and support. To Dr. Pauline Leduc specifically, this project would not have been possible without your coding and other computer skills. I can't thank you enough for taking the time to explain and teach me not only on coding, but gardening and cooking as well, your friendship has been invaluable. I also want to thank Sarah Peirce, who provided support in the field, flume and at conferences, I have many fond memories of the endless hours we have spent together.

Thank you to everyone who helped in the completion of field work including Dr. Darren Sjogren, Dr. Joe Wheaton, Wally Macfarlane and Dr. Chris Hugenholtz. I also want to thank Danielle Barr, Dr. Matilde Welber, Elizabeth Sutherland and Erika Hill for their help in the flume.

I would also like to thank the staff in the Geography Department including Joe Smrekar, Karen Vankerkoerle and Lori Johnson for all your help and support. A special thank you to Dr. Chris Smart and Dr. Brian Luckman for the encouragement and interest in this project.

Lastly, I want to thank my friends and family for the continued love and support. To the 'grad-club crew' thank you for all the laughs and memories throughout the past two years. In particular, Julia Howett, I cannot thank you enough for the constant support and friendship. Finally, to my parents, brothers and partner, Chris, thank you for the unwavering love and support.

Table of Contents

Abstract i
Table of Contents iii
List of Figures v
List of Tables viii
1 Introduction 1
1.1 Research Problem 1
2 Background 3
2.1 Characteristics of Gravel-Bed Braided Channels 3
2.2 Planform dynamics of braided rivers 6
2.3 Bedload transport in braided rivers 9
2.4 Experimental Geomorphology 10
2.5 Rationale for Research 12
3 Field Methods 15
3.1 Study Location 15
3.2 Data Collection 18
3.2.1 Time-lapse Imagery 18
3.2.2 Study Reach Discharge 21
3.3 Measurement of Planform Change 27
3.3.1 Rectification of Oblique Images 27
3.3.2 Planform Measurement 29
3.3.3 Manual Analysis 31
3.3.4 Automated Analysis 33
4 Laboratory Methods 38
4.1 Experimental Setting 38
4.1.1 Discharge 41
4.1.2 Sediment 41
4.2 Experimental Design 43
4.3 Experimental Data Collection 46
4.3.1 Time-lapse imagery 48
4.3.2 Photogrammetry 48

4.3.3 Width and Depth Measurements 49
4.3.4 Bedload Samples 49
4.4 Experimental Data Processing 49
4.5 Measurements 51
4.5.1 Planform Change Measurement 51
4.5.2 Measurement of Morphological Change 55
4.5.3 Measurement of Bedload Transport 56
5 Field Results 57
5.1 Description of Data 57
5.2 Analysis of Sunwapta River Discharge 57
5.3 Analysis of Sunwapta River Channel Planform Change 63
5.4 Automated Image Analysis 70
5.5 Planform Change and Wetted Area 77
5.6 Field Results Summary 79
6 Laboratory Results 81
6.1 Description of Data 81
6.2 Analysis of Flume Discharge 81
6.3 Measurements 83
6.3.1 Planimetric Measurements 83
6.3.2 Morphological Measurements 85
6.3.3 Bedload Measurements 95
6.3.4 Measurements Summary 109
6.4 Laboratory Results Summary 109
7 Discussion 111
7.1 Field and Laboratory Comparison of Planform Change 111
7.2 Extension of Field Analysis 118
7.3 Planform change and active width 122
7.4 Planform change and bedload in gravel-bed braided rivers 123
8 Summary and Conclusions 126
8.1 Implications and Future Research 127
8.2 Concluding Statements 129
Appendix A - Structure from Motion Photogrammetry 137

Appendix B Bubbler Sensor System 140
Appendix C Slope 141
Appendix D Estimation of Flume Discharge 142
Appendix E Summary of Linear Correlation 143
Appendix F Summary of Boxplots 146

List of Figures

Figure 2.1: Planimetric features of braided rivers 5
Figure 2.2: A confluence and bifurcation unit. 6
Figure 3.1: The location of the study reach 16
Figure 3.2: The grain size distribution of sediment samples collected from the field 18
Figure 3.3: Set up of the time-lapse cameras 20
Figure 3.4: The rating curve #16 used by the WSC 22
Figure 3.5: Rating curve developed for this study to estimate the discharge 22
Figure 3.6: The relationship between field measurements by the WSC and the estimated discharges using the rating curve developed for this study. 23
Figure 3.7: The rating curve derived to determine discharge at the study reach 26
Figure 3.8: Location of the 10 GCP used to rectify the time-lapse photos. 27
Figure 3.9: An example of the orthorectification of field time-lapse images 28
Figure 3.10: The comparison between distances measured between ground control points in the rectified images (adjusted for photo scale) and on the ground in the GPS datum. 28
Figure 3.11: The channel planform position at the field site with the UAV photograph underneath and the ortho-rectified time-lapse image overlaid on top. 29
Figure 3.12: The relationship between original planform change measurements and re-measured areas of planform change. 33
Figure 3.13: An example of successive time-lapse imagery every half hour with changes to the reflection and lighting. 35
Figure 3.14: An example of two subsequent daily binary images and the resulting subtraction . 36
Figure 4.1: An image of the physical model of the Sunwapta River. 39
Figure 4.2: The layout of the flume 40
Figure 4.3: The grain size distribution of the field site at the Sunwapta River and the physical model 42
Figure 4.4: Selected representative Sunwapta hydrographs with the intended replicated scaled flume experimental hydrographs 44
Figure 4.5: Flume hydrograph experimental runs 47
Figure 4.6: The frequency distribution of elevation error on DEMs of Difference. 50
Figure 4.7: An example of (a) a flume stitched orthophoto 52
Figure 4.8: An example of a cropped ortho-image from the flume 54

Figure 4.9: An example of a DEM and DoD generated from hydrograph experiment runs. 55
Figure 5.1: The analysis of Sunwapta discharge 58
Figure 5.2: 15-minute discharge readings for the study periods of 2012 and 2013..... 60
Figure 5.3: The relationship between the maximum and total discharge 61
Figure 5.4: An example of a sequence of typical daily hydrographs..... 61
Figure 5.5: The relationship between discharge and temperature 62
Figure 5.6: The minimum, average, maximum and historical discharge values for 2012 in relation to the measurements of planform change 64
Figure 5.7: The minimum, average, maximum and historical discharge values for 2013 in relation to the measurements of planform change 65
Figure 5.8: The relationship between planform change and discharge 66
Figure 5.9: The relationship between two discharge groups. 67
Figure 5.10: An example of small area of planform change recorded at a lower discharge analyzed 68
Figure 5.11: An example of small area of planform change recorded at a higher peak discharge analyzed 69
Figure 5.12: An example of a high peak that resulted in large areas of planform change 70
Figure 5.13: The relationship found between peak daily discharge and area of planform change using automated image analysis..... 71
Figure 5.14: The relationship between areas of planform change documented using automated analysis and manual analysis methods..... 72
Figure 5.15: Measurement of planimetric change using automated image analysis and the different detection produced due to inherent differences in time lapse imagery..... 74
Figure 5.16: Measurement of planimetric change using manual image analysis 75
Figure 5.17: An example of channel avulsion 76
Figure 5.18: The relationship between the wetted area and discharge 77
Figure 5.19: Examples of images at different stages. 78
Figure 5.20: The relationship between peak discharge and the normalized area of planform change. 79
Figure 6.1: The range of discharges in Sunwapta River for both 2012 and 2013 with the representative hydrographs selected 82
Figure 6.2: The relationship between planform change and peak discharge in the flume..... 84
Figure 6.3: The relationship between peak discharge and the area of change as a proportion of peak flow wetted area. 85
Figure 6.4: The volumes of erosion, deposition, and the sum of the two. 86
Figure 6.5: DEMs of Difference for each hydrograph experiment. 87
Figure 6.6: The total volume of erosion and deposition in relation to the peak discharge. 88
Figure 6.7: The relationship between planform and morphological change 89
Figure 6.8: An example of small areas of planform and morphological change documented at the lowest peak discharge 90
Figure 6.9: An example of small areas of planform and morphological change documented at the second lowest peak discharge 91

Figure 6.10: An example of large planform and morphological changes documented at the second highest peak discharge. 93
Figure 6.11: An example of large planform and morphological changes documented at the highest peak discharge. 94
Figure 6.12: The relationship between the bedload transport rate of individual samples and discharge. 96
Figure 6.13: The ABI in relation to the bedload sample weight 96
Figure 6.14: The rate of bedload transport in relation to discharge and hydrograph stage. 97
Figure 6.15: The relationship between average sediment weight transported during an experimental run in relation to the peak discharge in the flume. 98
Figure 6.16: The relationship between the D_{10}, D_{50} and D_{90} of individual sediment samples and discharge. 101
Figure 6.17: The sediment distribution of individual sediment samples 102
Figure 6.18: The summary statistics of the D_{50} 103
Figure 6.19: The relationship between weight of a bedload sample and the size of D_{10}, D_{50} and D_{90}. 103
Figure 6.20: The temporal relationship between bedload transport and grain size distribution. 104
Figure 6.21: The relationship between total bedload transport weight and areas of planform change 106
Figure 6.22: An example of run 11 108
Figure 7.1: The relationship between areas of planform change and peak discharge for equivalent areas of the field prototype and the physical model 112
Figure 7.2: An example of planform changes over a daily hydrograph with a peak below 11 m^3s^{-1} in the field and the flume 114
Figure 7.3: An example of planform changes over a daily hydrograph with a peak below 11-17 m^3s^{-1} in the field and the flume 115
Figure 7.4: An example of planform changes over a daily hydrograph with a peak greater than 17 m^3s^{-1} in the field and the flume 117
Figure 7.5: The relationship between the area of planform change/wetted area and peak discharge for equivalent areas of the field and physical model. 118
Figure 7.6: An example small morphological change detected where no planform change was observed 120
Figure 7.7: The current braided configuration of the Sunwapta River. 121
Figure 7.8: The relationship between active width/wetted area for previous measurements in 1999, 2003 and developed for this research for 2012 and 2013. 123
Figure B.1: A diagram of the typical model of a Pressure Bubbler Sensor operating system.... 140

List of Tables

Table 4.1: The summary statistics of the water input from the sediment sorter. 43
Table 4.2: The summary of the experimental conditions and time of the four different hydrograph experimental runs, designed to replicate Sunwapta hydrographs. 45
Table 4.3: The absolute threshold values applied to DoDs for removal of points..... 51
Table 6.1: The summary statistics from the individual sediment samples collected..... 100
Table 6.2: P-values of the correlation between total bedload transport and areas of planform change 107
Table 6.3: The PCC and significance of the relationship between areas of planform change, volumes of morphological change and total bedload transport weight. 109
Table D.1: The relative error in discharge measurements in the flume..... 142
Table E.1: Summary of statistics of the original areas of planform change measured and the same daily hydrograph re-measured. 143
Table E.2: Summary of statistics for the areas of planform change measured in the field on daily hydrographs with peaks below 11 m^3s^{-1} 143
Table E.3: Summary of statistics for the areas of planform change and volumes of morphological change over hydrographs in the physical model. 144
Table E.4: Summary of statistics for the areas of planform change and total bedload transported over hydrograph experiments 1-12 in the physical model. 144
Table E.5: Summary of statistics for the areas of planform change and total bedload transported over hydrograph experiments 1-10 in the physical model. 145
Table F.1: Summary of statistics for the sediment weights transported at different observed Active Braiding Intensities. 146

Chapter 1

1 Introduction

1.1 Research Problem

Gravel-bed braided rivers are characterized by their multi-thread planform composed of unstable channels and ephemeral bars. The dynamic nature of the planform geometry of gravel-bed braided rivers is related to rates of bedload transport, altering the morphology and thus planform position. These rivers are commonly found in mountainous proglacial environments in which glacier melt controls the hydrological regime due to seasonal and daily variation in temperature impacting the rate of meltwater produced, and water discharge. This temporal temperature-driven variation in discharge affects rates of bedload transport and morphological change because they are reliant on a critical discharge to initiate bed-load transport, required for morphological processes such as bar development and erosion, local scour and fill, bank erosion, and channel migration and avulsion to occur. The rate of planform development of the river is therefore tightly linked to the rate of bed load transport and the threshold discharge at which these changes occur.

The prediction of bedload transport is complicated by the highly dynamic nature of braided rivers influencing the spatial and temporal relationship between bedload transport, morphology and planform change. Laboratory experiments on physical models of braided rivers have shown considerable variability in bedload transport rates even at a constant discharge in relation to bedload pulses produced as the intrinsically unstable river morphology continually changes and the variability increases with increases in the rate of bedload transport and morphological change (Ashmore 1988; Ashmore, 1991; Goff & Ashmore, 1994; Shvidchenko & Kopiliani, 1998).

The morphological method has been used as an alternative method to directly measuring sediment transport rates in braided rivers to try and encompass the dynamic nature, inferring rates of bedload transport to changes in channel topography over time (Ashmore & Church, 1998; Chandler et al. 2002). Changes in river morphology and rates of morphological change are determined by the measurement of areas of erosion and deposition over repeated cross-sectional surveys or repeat surveys of the digital elevation data. This allows for a better understanding of the spatial and temporal patterns of bedload transport and morphological change by focussing on measured changes in the river topography.

Monitoring and measuring bedload transport is fundamental to a process-based understanding of river morphology in general. Because bedload transport in braided rivers, in particular, is tightly connected to rapid morphological changes, this relationship can be explored over a short temporal scale, with complex processes of channel formation and change altering the river planform rapidly. Measurements of morphological change and bedload transport have often used images of the braided planform to understand spatial and temporal changes in a braided river but these changes have not been related to quantified measurements of planform change. If there is a close correlation between water discharge, rate of planform change and bedload transport rate, the measurement of areas of planform change could provide important information on braided river dynamics as well as a possible low cost surrogate method for continuous monitoring of bedload flux in braided channels using time-lapse imagery of planform change. Understanding of the bedload-planform connection in braided rivers may be generalized to other rivers and longer time scales. Therefore, the research in this thesis focusses on the following objectives:

1) Quantify areas of planform change in a proglacial river over a range of discharge conditions to describe the relationship between discharge and planform change and its known variability.

2) Replicate hydrographs from the field in a physical model to obtain a comparable data set to allow for planform measurement and comparison between the field prototype and physical model.

3) Characterize the relationship between planimetric change, morphological change and bedload transport in the physical model to extend the analysis to an assessment of the prediction of bedload transport rate from planform change.

Specific research questions are developed at the end of Chapter Two.

Chapter 2

2 Background

2.1 Characteristics of Gravel-Bed Braided Channels

Braided rivers exist in a wide range of environments such as mountainous regions, alluvial fans and lower gradient coastal or continental plains. Many different factors have been investigated to explain the occurrence of a braided channel such as slope, bed material grain size, discharge, vegetation, and the variation in discharge (Ashmore, 2013). Overall, sediment supply is a key factor in the transition from a single thread to braided channel with a heavy sediment load found to be critical for braiding development in all environments (Church & Gilbert, 1975; Mueller & Pitlick, 2014). In proglacial settings specifically, braiding is common because of the availability of coarse non-cohesive (gravel) sediment, glacial meltwater discharge, high energy flows and limited vegetation (vegetation tends to inhibit braiding development) (Church & Gilbert, 1975; Tal et al. 2004; Tal & Paola, 2010). Typically braiding is the result of the high sediment supply as well as low bank and bed resistance to erosion in relation to stream energy, and high stream power relative to the erodibility of the dominant particle sizes. These characteristics lead to a river planform and morphology that is very dynamic and can be drastically altered over a few hours when flow conditions are high (Ashmore, 2013; Wheaton et al. 2013). This is evident in Figure 2.1 showing the minimum stage on either end of a daily hydrograph period, highlighting the change in planform and morphology on the exposed bed in a twenty four hour period on the Sunwapta River, Alberta. Changes in a braided river planform are also evident as the flow increases, with the wetted width found to almost solely account for increases in discharge with little change evident in the river depth (Sauks & Ashmore, 2006) and the active width to act as a major control on bedload, rather than shear stress (Bertoldi et al. 2009). The planform of gravel-bed braided rivers is thus the result of interactions between the bed topography, bedload transport and flow. Flows capable of eroding bedload particles are seen to adjust the river planform through mid-channel bar development, lateral migration and channel bifurcation (Ashmore, 2013).

These planform changes documented in Figure 2.1, of the Sunwapta River, Alberta, were studied over a range of discharges during the meltwater seasons of 2012 and 2013 (Middleton, 2015). The results of this study yielded interesting results and raised future research questions such as how

changes to the river planform are related to morphological change and bedload transport, setting up the research questions for this study, discussed further below. Middleton (2015) documented common planimetric features and the changes experienced through flow periods as the planform adjusted through features such as unit bars developing within a single channel of a braided system, an active and temporary feature often seen to migrate along braided channels (Smith, 1974; Ashmore, 1981). The morphology of a unit bar is dictated mainly by depositional processes. Complex bars are a more permanent feature of a braided system, separating channels and resulting from multiple erosional and depositional events (Robert, 2003; Ashmore, 2013). The planimetric change from one erosional/depositional event is evident in the complex bar seen in Figure 2.1.

While high rates of planimetric change are possible over a short time, these changes often do not occur over the entire river width. This is seen in Figure 2.1 where the secondary channel sees little change, with the unit bar remaining in the same position from July 11, 2012 (a) to July 12, 2012 (b) while the primary channel sees a large change in planform. Over this daily hydrograph the complex braid bar in the primary channel seen in Figure 2.1a changes in planform with the development of a bifurcation, creating a new channel and diverting water through the complex braid bar, while depositing material and forming a new braid bar at the bifurcation until the channels rejoin (Figure 2.1 b).

A fundamental element of braided river morphology is the confluence-bifurcation unit. This consists of at least two channels combining at the confluence and a downstream bifurcation where bed material eroded from the confluence, and from upstream, is deposited forming a mid-channel bar, seen in Figure 2.2 a highlighted in red and black, respectively (Ashmore 1982; Ashmore, 1993; Hundey and Ashmore, 2009; Ashmore 2013). A DEM corresponding to the ortho-image seen in Figure 2.2a is provided in Figure 2.2b, with the associated morphological features of the confluence bifurcation unit. This is seen in the scour hole typically found downstream of a confluence, producing the erosion, highlighted in red and the bifurcation causing the channel to divide and deposit material forming a braid bar. The diversion of flow towards the outer bank around the braid bar produces local bank erosion highlighted in the black box (Figure 2.2b).

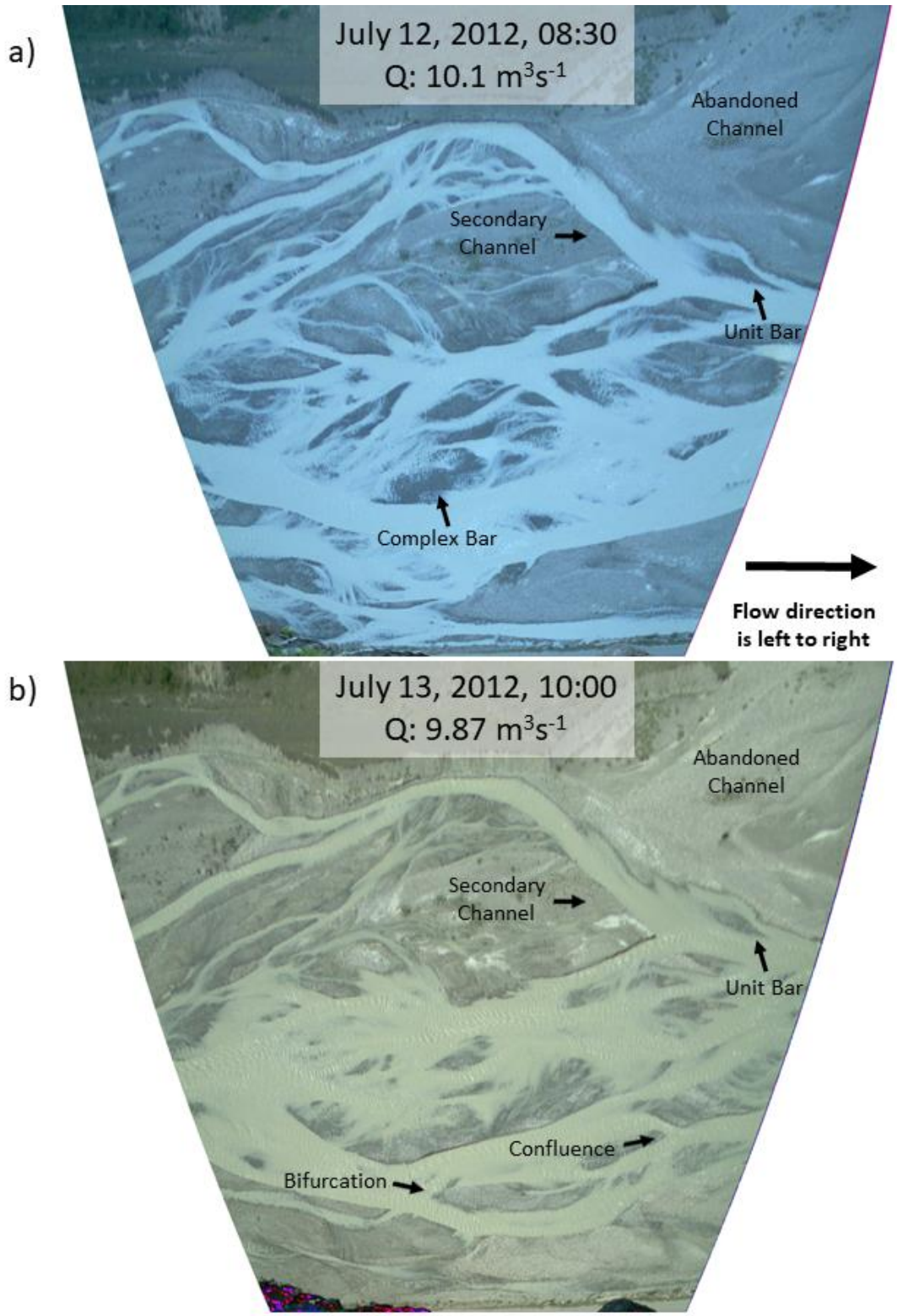

Figure 2.1: Planimetric features of braided rivers with the change in planform over a daily period seen from (a) July 12, 2012 to (b) July 13, 2012.

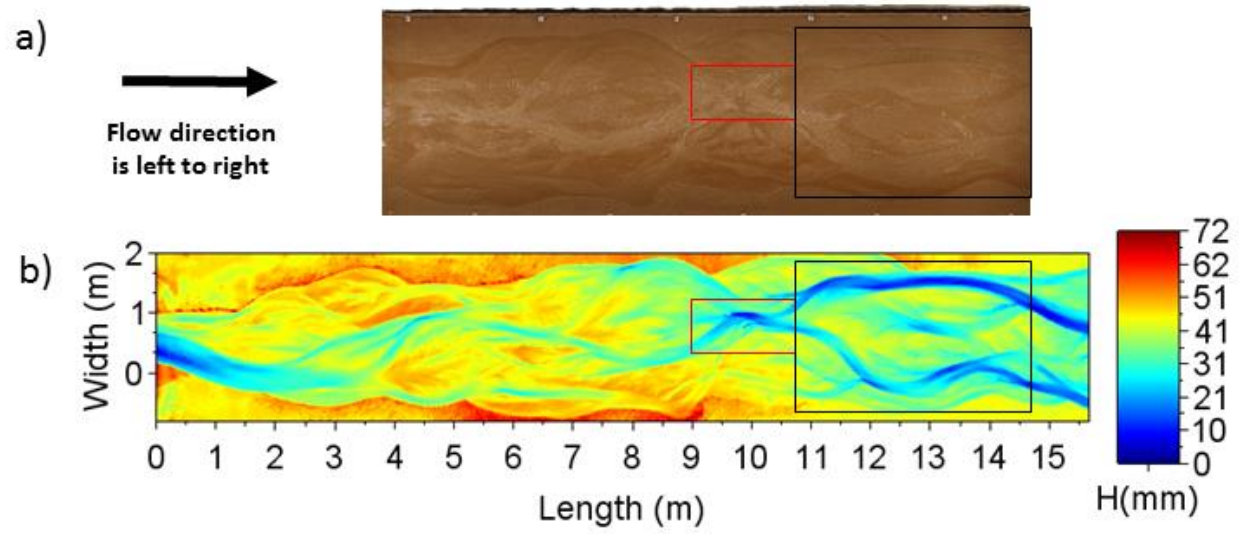

Figure 2.2: A confluence and bifurcation unit with the associated planform features (a) and morphological features (b), seen in a flume hydrograph experiment.

2.2 Planform dynamics of braided rivers

The river planform is defined simply as the shape of the river from overhead view, with braided rivers having a very dynamic planform, linked to changes in bedload transport and morphology. The overall planform position is the result of the interaction between flow, rates of bedload transport and the morphology that this creates. Monitoring the river planform provides a two-dimensional view of how a braided river develops and changes, providing a record of lateral widening or movement; bar formation and migration; and channel avulsion in different channels. Due to the complicated nature of braided rivers, monitoring a large area of the river planform can be difficult, limiting studies to focus on detailed planform mechanics over short time frames at high frequency documenting how planform features are altered in relation to individual flow events (Arscott et al. 2002; Bertoldi et al. 2009; Bertoldi, 2012; Middleton, 2015), or over a large spatial and temporal scale of years/decades observed at widely spaced intervals to document channel changes (Warburton et al. 1993; Luchi et al. 2007; East et al. 2017).

Planform features of a braided river have been investigated on small spatial scales such as the study of Bertoldi (2012) documenting changes to a single bifurcation unit in a gravel-bed braided river. The planform configuration of this bifurcation was recorded as it evolved through seven different flood events. Over slightly larger spatial scales, planform features have been documented throughout flood periods to better understand the relationship between different features and flood

events. Arscott et al. (2002) documented rates of turnover in aquatic habitats located in braided river floodplains at five different reaches to understand how habitats changed in relation to a changing braided morphology. Located on the same braided river, the Tagliamento in Northern Italy, the study of Bertoldi et al. (2009) mapped changes between flood periods to understand the relationship between river flows, sediment dynamics and vegetated landforms. All three of these studies were completed on different sections of braided reaches of the Tagliamento River, in which peak flows are driven mainly by infrequent rainfall events during the spring and fall. This allowed observations based on changes in river planform in relation to flood events to be made infrequently over a longer time-period due to the limited number of planform-altering floods. Middleton (2015) also documented changes to planform features in relation to individual flood events but was able to analyze an extended range of flood events due to the summer-melt water hydrologic regime of proglacial rivers, creating daily flow events. This allowed the area of planform change over a daily hydrograph period to be related to the peak daily discharge and determined a critical discharge above which planform changes were observed, with variability (Middleton, 2015). This study is the starting point of this research, with daily hydrograph measurements re-analyzed and the relationship extended to a physical model, discussed further below.

Due to the complicated nature and difficulty of capturing the river planform between individual flood events and the large spatial scale that these occur on, studies have also focused on the historical changes in river planform, using aerial imagery allowing observations to be made over a much longer temporal scale and larger spatial scale (Warburton et al. 1993; Luchi et al. 2007; East et al. 2017). Warburton et al. (1993) studied ten sets of planform images of the braided Ashley River in New Zealand, dating back to 1860 allowing the historical changes of this braided section to be documented. Luchi et al. (2007) documented areas of channel change on a gravel-bed proglacial braided river, Ridanna Creek, located in Italy. Five sets of aerial images were analyzed from 1982 to 2000 and then extended with the completion of morphological measurements between 2003-2005. The recent study of East et al. (2017) documented the planform-evolution of four different rivers using a 74-year long data set. This determined if the current morphology of these rivers was driven by physical characteristics or alternatively by ecological drivers, such as the large increase in elk populations in relation to wolves dying off.

Studying the braided river planform has also been used to compliment other methods of measuring and understanding topographic change in a braided river (Goff & Ashmore, 1994; Hicks et al. 2002; Chandler et al. 2002; Surian et al. 2009; Bertoldi et al. 2010). Surian et al. (2009) used aerial imagery to identify the movement of painted gravel particles in relation to single flood events and relate this movement to planform changes documented in images. Quantitative measures of bedload transport in a field setting have been extended to include qualitative observations of the river planform to understand variations in measured bedload samples (Goff & Ashmore, 1994; Hicks et al. 2002; Chandler et al. 2002; Bertoldi et al. 2010). Oblique imagery recording the river planform was collected during each of these studies or time-lapse video in the case of Hicks (2002), allowing adjustments to the river planform to be related to topographic changes in a braided river. The collection of other topographic measurements discussed further in Section 2.5.

The current knowledge of braided river planform is limited to long term extended studies (>10 years) of channel adjustment (Warburton et al. 1993; Luchi et al. 2007; East et al. 2017) or the short term study of detailed planform mechanics in relation to individual flow events (Arscott et al. 2002; Bertoldi et al. 2009; Bertoldi, 2012). Prior to Middleton (2015), studies focussing on the planform dynamics of a braided river have only been able to capture a limited number of flow events over a multi-year period (Bertoldi et al. 2009). Long-term studies have shown the dynamic nature of braided rivers with some features such as bars found to persist for an extended period of time (>10 years) and evidence of long-term channel adjustments and migration patterns (Warburton et al. 1993). Physical processes, such as bedload transport and the hydrologic regime (flood activity) were found to play a strong role in forming the morphology and planform position over an extended period of time (East et al. 2017). Measurements of channel planform adjustment over an extended period have been related to short-term subsequent morphological measurements in later years, at the same study reach (Warburton et al. 1993). Many studies measuring morphological change and bedload transport have used images of planform changes as an understanding of how a braided river adjusts to different flow events but the measurement of planform changes has not been quantified in relation to morphological measurements (Goff & Ashmore, 1994; Hicks et al. 2002; Chandler et al. 2002; Surian et al. 2009). This has lead to an understanding of the relationship between planform, morphology and bedload transport in braided rivers but a relationship that has not been quantified.

2.3 Bedload transport in braided rivers

Fluvial bedload transport, defined as the movement of larger grains that move by sliding, saltating and rolling on the river bed, has been studied extensively by engineers and geomorphologists for over a century (Gomez, 1991; Church, 2010). Bedload transport is fundamental to fluvial morphology and morpho-dynamics as the primary process responsible for channel formation and rates of channel development and morphological change, especially in gravel-bed rivers. In the case of braided rivers specifically, there is strong evidence of a close association between the morphological change and bedload transport processes: bar-scale channel morphology is a manifestation of local spatial and temporal variations in bedload transport rates (Ashmore, 1988; Ashmore, 1991; Hoey & Sutherland, 1991; Bridge, 1993; Goff & Ashmore, 1994; Bertoldi et al. 2006; Meunier et al. 2006; Wheaton et al. 2013).

Field measurements of bedload transport in braided channels have been limited to measurements of morphological change focusing on volumes of change with very few direct measurements of bedload transport (Meunier et al. 2006; Mueller & Pitlick, 2014). The majority of field work has measured rates of erosion and deposition using surveyed cross-sections and higher resolution Digital Elevation Models (DEM) of bed topographic change which are widely spaced in time (Kussner, 1995; Brasington et al. 2000; Varkaris, 2002; Hicks et al. 2003; Wheaton et al. 2013). Field observations of bed morphology and patterns of change using cross-section surveys and repeat digital elevation data (from GPS, remote sensing and terrestrial and airborne laser scans) show complex patterns of erosion and deposition along a braided channel and that over time can be tied to the local scour-deposition processes of bar formation, construction of large scale braid bars and channel avulsion and filling (Goff and Ashmore, 1994; Kussner, 1995; Varkaris, 2002; Ashmore et al. 2011; Wheaton et al. 2013; Williams et al. 2014). For practical reasons these studies have been limited to a few widely-spaced (in time) repeat surveys or intensive measurements over short time periods (few weeks) in the case of proglacial rivers with diurnal flow peaks during summer meltwater periods (Goff and Ashmore, 1994; Kussner, 1995; Varkaris, 2002; Ashmore et al. 2011). Rates of change increase with discharge but the relationship is often very scattered because of local variability in rates and instability of channel patterns. These rates of morphological change can be used to estimate bedload transport rates, with some simple assumptions about bedload transfer processes (Ashmore and Church, 1998). However, this method

requires very intensive field surveys and repetition at high frequency over long periods of time, which is not generally feasible.

Due to problems of measurement of direct bedload flux and of morphological change in the field, a large amount of current knowledge of bedload transport and morpho-dynamics of braiding has been derived from small-scale physical models (computational morpho-dynamic models are still at a preliminary stage of development and require field or model data for validation). In most cases the experiments were completed using a Froude-scaled physical model. Several model studies have documented rates of bed load transport over a range of braided river morphology and discharge (Ashmore 1982; Ashmore, 1988; Ashmore, 1991; Young and Davies, 1990; Schvidchenko and Kopaliani, 1998; Bertoldi et al. 2006, 2009; Ashmore et al. 2011). Even at constant discharge, rates of bedload transport are seen to fluctuate widely over time and space, with this variability seen to increase with increasing intensity of braiding. As formative discharge is increased there is a general increase in the rate of bedload transport (with considerable scatter) that follows a systematic relationship and can be predicted from overall hydraulics of the braided river reach (Ashmore 1982, 1988, 1991; Warburton, 1996; Bertoldi et al. 2006, 2009; Ashmore et al. 2011). Linking spatial and temporal variation in bedload to morphological change shows that, observationally and statistically, much of the variability relates to channel-scale morpho-dynamic processes (Ashmore 1982, 1988, 1991; Warburton, 1996; Bertoldi et al. 2006, 2009; Ashmore et al. 2011). It is reasonable to expect that the rate of planform change then also correlates with the rate of bedload transport. These studies have given insight into the relationship between discharge and the complexity of braiding morphology, the rates of bedload transport over a range of channel-forming discharges, the variability in bedload transport rates over time and space in relation to braiding processes, and morphological change and the processes of planform change and dynamics. What is missing in research however is direct measurements of bedload flux, planform change as a surrogate for volumetric change and the variation in rates of change and transport within/between event hydrographs.

2.4 Experimental Geomorphology

Experimental research and the use of physical models has played a crucial role in advancing geomorphic knowledge, allowing phenomena and processes to be observed and measured which may not be possible in a field setting. The use of physical models in fluvial geomorphology dates

back over a century to G.K. Gilbert in 1914 who was the first geomorphologist to use a flume (McKenna Neuman et al. 2013). While braided rivers pose many problems in a field setting, the ease and effectiveness with which they are modelled has lead to the completion of a wide base of research to be conducted using a physical model, from which knowledge about a range of braided river processes has been developed (Paola et al. 2009). The large spatial and temporal scale of braided rivers in a field setting makes the collection of data across the entire river bed difficult. The use of physical models is advantageous allowing the reduction of spatial and temporal scale, where complex variables at play such as bedload transport and morphology can be understood over the entire river width and in relation to one another (Peakall et al. 1996; McKenna Neuman et al. 2013; Wohl, 2013; Bennett et al. 2015).

The majority of experimental research on braided rivers has been conducted using a scaled model in which the physical model represents some key parameters of a braided river system. The most common approach to scaling is the use of Froude-scaled models, discussed below but other types have been used including kinematic similarity (Sapozhnikov & Foufoula-Georgious, 1997) and models based on scaling laminar flow (Metivier & Meunier, 2003; Lajeunesse et al. 2010).

A Froude-scaled model preserves the essential geometric, kinematic and dynamic similarity between a model and a prototype (Peakall et al. 1996). Gravel braided rivers have been modelled both generically (Ashmore, 1982, 1988, 1990, 1991a, 1991b; Warburton & Davies 1994; Warburton 1996; Young & Warburton, 1996; Gran & Paola, 2001; Ashworth et al. 2004, 2007; Mao, 2012) and using a specific prototype river (Young & Davies, 1990; Hoey & Sutherland, 1991; Egozi & Ashmore, 2008; Hundey & Ashmore, 2009; Ashmore et al. 2011; Gardner & Ashmore, 2011).

Mobile-bed theory predicts that braided channels which are undistorted and self-formed in coarse, poorly sorted sand would obey the Froude scaling law (Yalin, 1971). Froude scaling with water reduces Reynold's numbers but for gravel-bed rivers hydraulic and sediment transport similarity is preserved if the model is large enough to retain a rough, turbulent flow as in the full scale river. Froude-scaling retains non-dimensional bed shear stress (Shields parameter) which is fundamental to bedload transport processes (Ashmore, 1991; Peakall et al. 1996; Young & Warburton, 1996). To achieve full Froude-scaled modelling the complete grain size distribution must be scaled, but as particle size is reduced, the finer grains may become cohesive in a physical model. This can

lead to a ripple formation on the bed which is typical in sand-bed rivers but not in gravel-bed, destroying the bedform and dynamic similarity of the model (Young & Warburton, 1996; McKenna Neuman et al. 2013; Bennett et al. 2015). To avoid this most studies have either used noncohesive micro silica beads as sediment as opposed to the typical quartz sediment utilized, or have truncated the sediment distribution to avoid finer grained sediment in the distribution (Young & Warburton, 1996; McKenna Neuman et al. 2013).

2.5 Rationale for Research

Although considerable research has been done, much is still unknown related to the complexity of braided river systems and their complex morphology (Hicks et al. 2008). Analyzing the river planform at a high-frequency over a larger area provides new insights into braiding processes. The river planform is defined broadly as the shape of river from an overhead view. In a braided river context, this includes the full extent of the braid plain and visual topography, not just the location of individual channels. For the purpose of this study, the river planform is defined as the observable braided geometry from an aerial view including all areas of river bed, both inundated and dry areas. The planform position and changes between subsequent planform positions were identified through the position of submerged channels, previously occupied channels which were evident in the former bank and bar position, and the lateral migration, expansion and erosion of morphological features such as unit and braid bars.

The complicated nature of braiding river dynamics has also lead to the increased use of physical models to study braided river systems. This allows for control, with most research completed at a constant discharge. Although conducting experiments using a constant discharge is critical to understand how bedload transport occurs in a generic braided river, natural braided rivers have variable discharge and very few experiments have used simulations of natural hydrographs (Young & Davies, 1990). The complicated nature of braiding river dynamics has also limited the number of studies investigating the unsteady flow of braided rivers in the field (Bertoldi et al. 2010). This research aims to fill this research gap by analyzing planimetric processes of a braided river at an unsteady flow in the field and relate these planimetric and morphological processes of a braided river at an unsteady flow in a physical model, replicating daily hydrographs of a specific river, the Sunwapta River, Alberta. This will aid in the development of understanding how bedload transport

actually occurs in these systems and allow for an analysis of the full range of discharges of a proglacial braided river system.

The aim of this research is to investigate a surrogate method of measuring bedload transport and morphological change in the field for braided rivers based on rates of planform change. Middleton (2015) showed that the area of planform change increases with increasing peak flow and total flow of daily hydrographs on the proglacial Sunwapta River, with a clear threshold discharge below which no planform change occurs, and with considerable overall variability in these relationships. Previous work incorporating cross-section survey data from Sunwapta has shown that the active width (river bed extent over which measurable erosion/deposition occurs) also correlated with discharge of a daily hydrograph above a threshold discharge (Ashmore et al. 2011). Consequently, there are reasons to hypothesize that planform change, topographic change and bedload are strongly correlated. Questions remain about the accuracy of the previous planform measurements (Middleton, 2015) (see Chapter 3 and 4) and about the relationship between planform change and bedload transport rates. Bedload measurements and detailed daily mapping of topographic change are extremely challenging in the field therefore, in this thesis, these relationships are investigated by comparing field and model results for planform change, and then extending the model data to include topographic change and bedload for the same hydrographs.

The ultimate goal of this research is to determine whether measurements of planform change can be used as a surrogate method of predicting bedload transport in a proglacial braided river as well as describing ways in which the rate of planform change is controlled by the discharge of the river. Determining rates of bedload transport and the critical discharges needed to produce this transport will be beneficial knowledge in applied geomorphology, engineering and ultimately in managing these complex systems (Piégay et al. 2006; Ashmore, 2009).

Therefore, the research in this thesis focusses on four primary questions:

1) Are previous measurements of planform change from oblique time-lapse images (Middleton, 2015) accurate and can an automated image analysis method be reliably used instead of manual measurements?

2) Is area of planform change measured over a daily event hydrograph in the physical model correlated with simultaneous measurements of bedload transport and morphological change?

3) Are these areas of planform change made in the physical model over a replicated event hydrograph comparable to areas of planform change measured over a daily hydrograph in the field prototype?

4) Is measurement of planform change a reliable surrogate for directly measuring bedload transport in a braided river during multiple flow events over time periods of months to years?

The research will address these questions using a combination of time-lapse imagery and discharge records from a proglacial braided river and physical model experiments in a laboratory flume. This allows hydrographs from the field to be reproduced in the laboratory during which simultaneous planform change and bedload flux data can be collected to complement and extend interpretation of the field planform change data.

Chapter 3

3 Field Methods

This chapter focuses on the field location where the relationship of planform change and discharge could be studied over a high-frequency and range of discharge conditions. This relationship was studied using the collection of simultaneous time-lapse images and discharge measurements. The field site and the data set used for this research were developed by in Middleton, 2015. This thesis extends the original analysis of Middleton (2015) by trying to provide an automated method for measuring areas of planform change as well as relating these areas of change to the total wetted area at peak discharge. This extension of Middleton (2015) was completed to: 1. reduce the subjectivity of the visual analysis and 2. provide an area of change in proportion to the total area that could possibly change, normalizing measurements which allowed planform measurements to be compared to previous studies of measurements of morphological change, as well as other rivers. The study reach was originally selected as it allowed for the collection of continuous discharge measurements from a WSC gauging station and continuous time-lapse imagery collected from an adjacent cliff providing an accessible location for cameras and gave a high-angle view of the river. This location was also selected as it is the field prototype of a physical model where field hydrographs were replicated as experiments, discussed further in Chapter Four below.

3.1 Study Location

The Sunwapta River is a gravel bed proglacial river which originates at the outlet of Sunwapta Lake at Athabasca Glacier in Jasper National Park, Alberta (Figure 3.1) and is tributary to the Athabasca River. The Sunwapta River receives additional flow from the Dome Glacier meltwater stream 1km downstream from the Sunwapta Lake and 2.5km upstream of the study reach location. As well as Middleton (2015), this study reach has been the location of numerous other studies including Goff and Ashmore (1994); Chew and Ashmore (2001); Chandler et al. (2002); Varkaris (2002); Ashmore and Sauks (2006) and Ashmore et al. (2011) which provide useful background information and some complementary data. The Icefields Parkway (Alberta Highway 93) runs along the river which gives easy access to the study site for ground surveys.

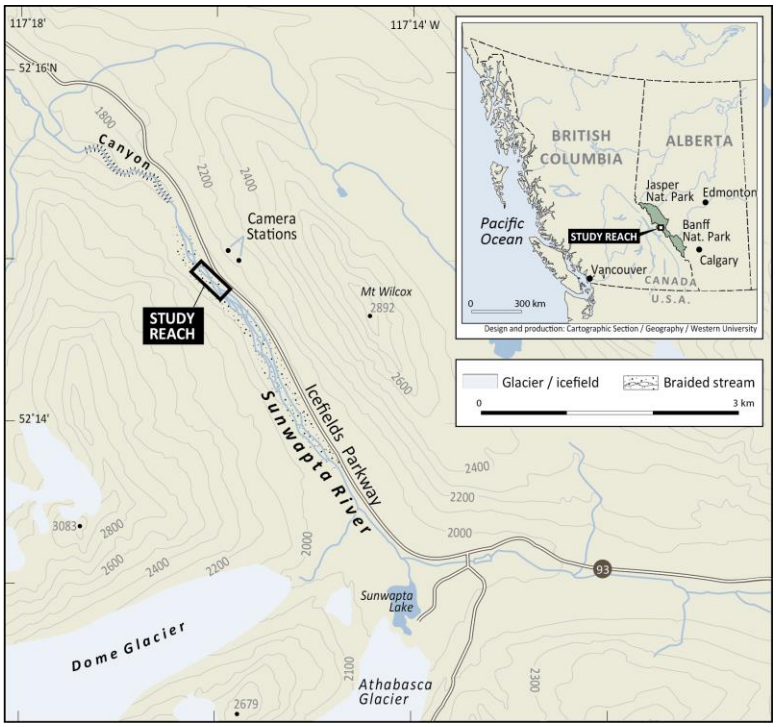

Figure 3.1: The location of the study reach in relation to the Icefields Parkway, the WSC gauge and within the province of Alberta, Canada.

The Sunwapta River experiences the highest flows, and therefore the most intense bedload transport and morphological change, during the summer melt-water period from late June to early September. The overall channel planform position can change from the beginning to the end of the season as the planform adjusts to high discharges and active braiding occurs. Prior observation shows that active braiding occurred in both 2012 and 2013 and over other years in previous studies (Goff & Ashmore, 1994; Chew & Ashmore 2001; Chandler et al. 2002; Varkaris. 2002; Ashmore & Sauks 2006; Ashmore et al. 2011; Middleton, 2015). The daily ice and snow melt cycle during this period produces a consistent daily hydrograph of discharge variation repeated on a daily cycle. These daily hydrographs have a similar shape and time base (approximately 24 hours) with some variation in the daily maximum and minimum flows, primarily related to synoptic weather conditions, especially air temperature and solar radiation (Ashmore & Sauks 2006; Ashmore et al. 2011). Rainfall events have only occasional and minor effects on this summer daily hydrograph cycle (Middleton, 2015). The summer melt cycle period is mainly a result of warmer air temperatures with discharges seen to fluctuate with a time lag of a few hours in relation to air temperature. This cycle creates individual daily flow hydrographs which typically peak in the evening with the minimum discharge typically

occurring during the early morning. Minimum discharges occur ~ 08:30 and maximum discharge at ~18:00. This pattern is most evident during July and August when flows are highest and the channel undergoes the majority of pattern change for the year. In addition to seasonal trends and daily hydrographs, flows tend to have periods of high/low flows with synoptic temperature patterns over time periods of the order of a week.

The Sunwapta is a gravel bed river, the study reach has an average grain size of approximately 0.04m (Figure 3.2) and a river gradient of approximately 1.5% (Chew and Ashmore, 2001; Varkaris, 2002; Ashmore and Sauks, 2006; Ashmore et al. 2011). The grain size distribution was measured in 1999 through spatial grain sampling which covered the width of the river bed. Over 2600 grains were collected from on bars and within channels to determine the average surface grain size distribution, discussed further in Varkaris (2002). The study reach is ~100 m long with a river width of ~120 m, determined by the fixed location of the camera viewpoint and the camera geometry.

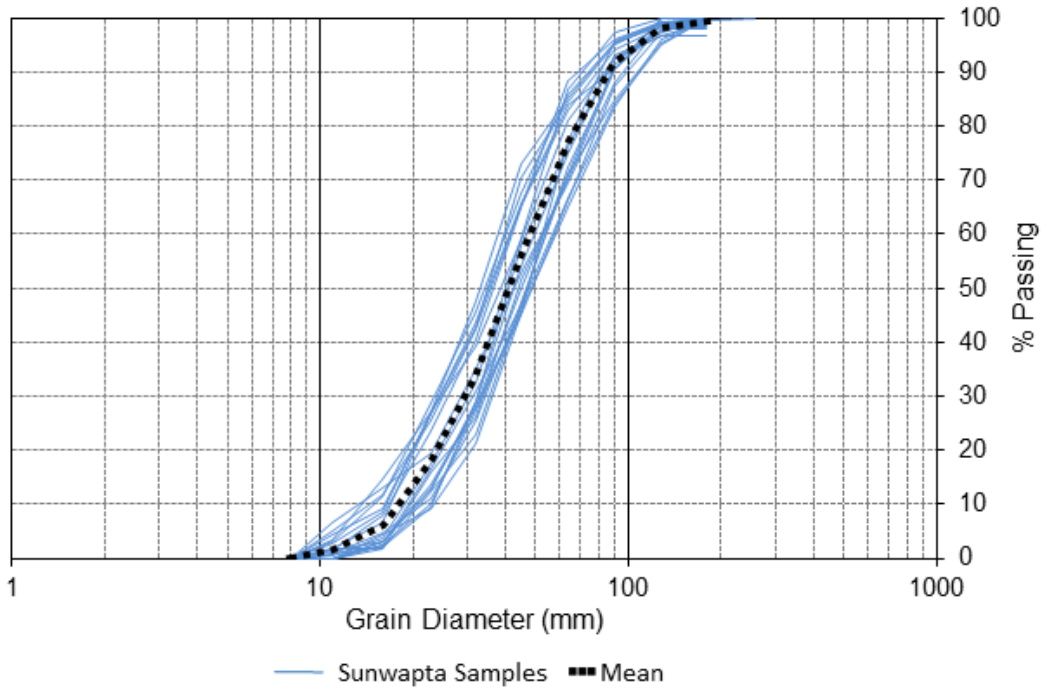

Figure 3.2: The grain size distribution of sediment samples collected from the field in relation to the average of samples surveyed (adapted from Varkaris, 2002). Samples were truncated at 8mm.

3.2 Data Collection

To determine the relationship between channel pattern change and discharge in the field, two types of data are required: 1. photographs to analyze the rate of channel pattern change and 2. wetted widths over a range of discharges including the daily peak. Specifically, this requires observations over an extended period of time to cover the full range of discharges and rates of channel pattern change experienced by the river and to measure variability in rates of change with respect to discharge and identify the possible threshold discharge for planform change. This included photographs acquired from time-lapse imagery from June-October 2012 and 2013 and discharge data from WSC with supplementary measurements, discussed below.

3.2.1 Time-lapse Imagery

Photographs were taken with two Reconyx Hyperfire 650 cameras installed on a cliff ledge approximately 90 meters above and 190 meters horizontally away from the middle of the river bed (Figure 3.3). The two cameras were located 30 m apart at the same elevation; one pointed slightly upstream relative to the other with a large area of overlap between the two. Cameras were mounted

on top of metal posts, hammered into the ground (Figure 3.3). Using two cameras ensured coverage of the melt-water season in case one camera failed. The downstream photographs were selected for analysis with the upstream used as a reference to the channel planform configuration upstream of the measurement section. The downstream images were selected due to the orientation of the camera with respect to the river and the control survey done from this location making the ortho-rectification process of the oblique images much easier. The cameras were programmed to take a picture every 30 minutes beginning at 0600 hours and ending at 2200 hours each day throughout the summer melt-water period of 2012 and 2013. This interval was selected to ensure there was a good selection of images covering a full range of discharges, documenting any planimetric changes throughout a daily hydrograph period. The high frequency of images allowed the planform to be captured at a comparable stage between daily hydrographs and allowed flexibility in image selection if weather and lighting conditions affected image quality. The 2012 time period covered June 7 to September 30 for a total of 3514 images. 2013 recorded June 7 to September 25 for a total of 3550 images. The images were 2048 x 1536 pixels at a resolution of 72 dpi covering the entire river width (~120 meters) and an ~ river length of 100 meters.

Quality of images varies during the day and from day to day because of several circumstances. Occasional issues included some vegetation growth in front of the camera, occasional wildlife blocking the view, and some slight shifts in camera position possibly from wind effects. Images that showed these effects were excluded from analysis. Due to the high-frequency of time-lapse images taken throughout the day, often another image could be selected. Only eight days were removed from analysis due to a shift in the camera position.

Figure 3.3: Set up of the time-lapse cameras with one viewing upstream (a, b) and the other downstream (c, d) with an area of overlap between the two.

3.2.2 Study Reach Discharge

To determine discharge, stage readings were acquired from the WSC gauging station (Station Number: 07AA007) located at the outlet of Sunwapta Lake. Stage has been recorded at the WSC station since 2005 (using a "Bubbler" sensor, described further in Appendix B). Prior to 2005 gauge data was collected using a stilling well and a mechanical chart recorder which operated from 1948-1997. The gauge was inactive from 1997-2005. While WSC stage and discharge were available at 15 minute intervals throughout the study period, some further analysis and measurements were needed to acquire a record of discharge at the camera site. Two main issues are involved: 1. adjustment of the WSC rating curve for stage-discharge conversion, 2. estimation of the tributary discharge (from Dome Glacier) contributed to the river between the WSC gauge and the camera site.

Stage-discharge Curve

The WSC gauging station records water stage at 15 minute intervals. Stage is converted to discharge using a rating curve established by doing on site velocity-area gauging several times per year. In the period of 2005-2013 there are 44 such calibration measurements used to establish WSC rating curve #16 for the gauge. Water Survey of Canada (Calgary office) provided 15 minute stage and discharge records along with the measured calibrated discharges and the rating table for curve #16. The Water Survey of Canada does not use a single-valued rating curve to calculate discharge. Discussion with Water Survey of Canada technical personnel confirmed that the rating curve is progressively 'shifted' through the year in order to align with the previous gauging measurement. This produces a systematic pattern of variation in the rating relationship during a year and between years and rating curve #16 (Figure 3.4) is, in effect, the minimum estimated discharge for a given stage. While this is appropriate for the purposes of WSC, for this research an alternative rating method was used to produce single-valued discharges for a given stage, with associated precision estimates, by fitting a single, continuous function to the 44 measured stage-discharge values (Figure 3.5). Therefore, the discharges used in this thesis are those calculated from published 15 minute stage data and the single 'best fit'; rating curve (instead of the 'shifting' rating curve used by WSC).

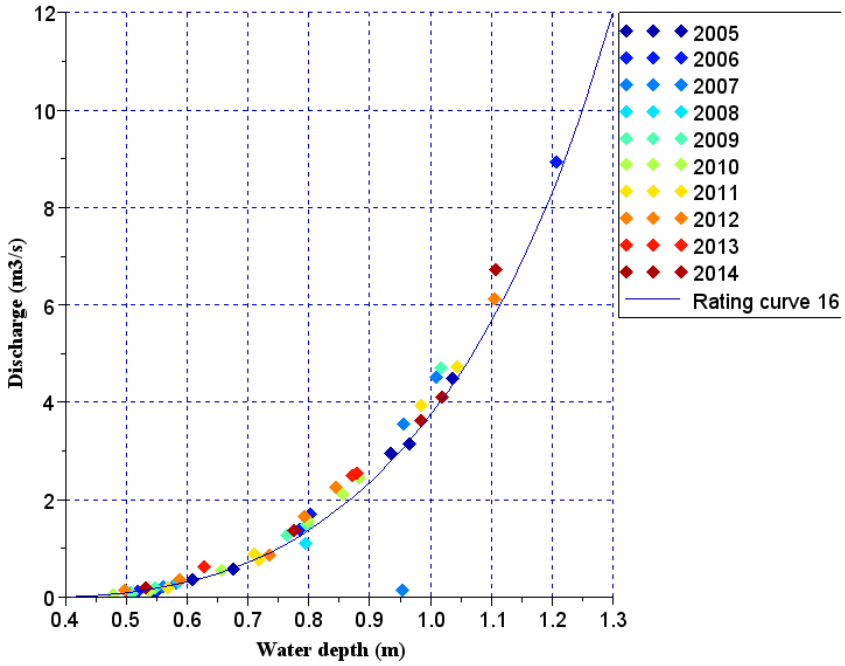

Figure 3.4: The rating curve #16 used by the WSC with gauging measurements identified for each year.

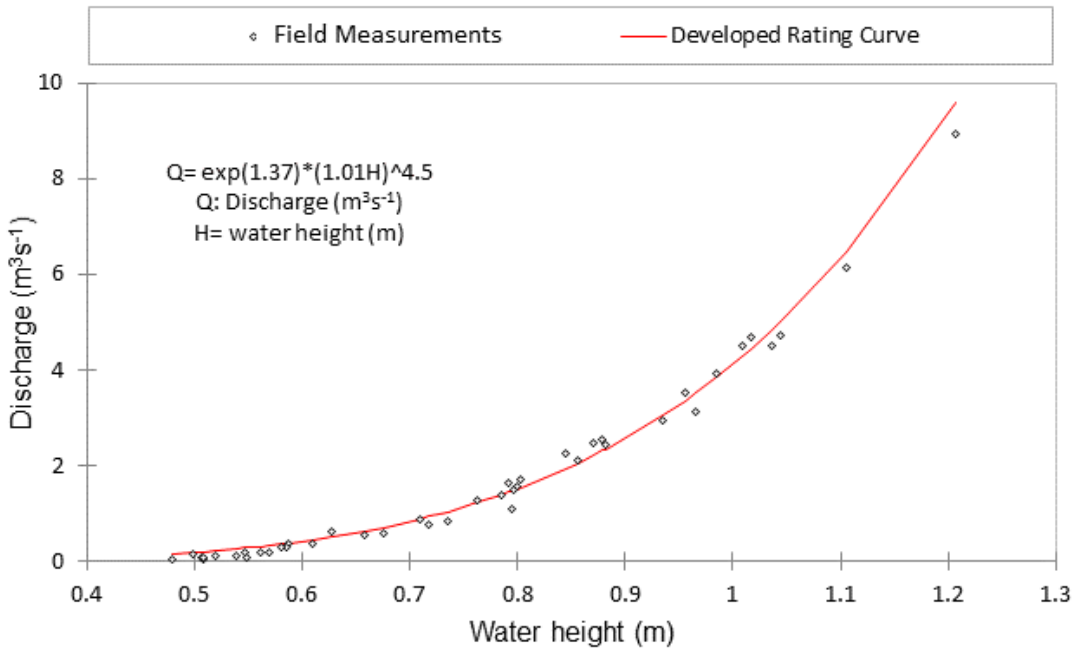

Figure 3.5: Rating curve developed for this study to estimate the discharge (m^3s^{-1}) based on stage (m) at the WSC gauge.

In Figure 3.5 it is clear that most of the measured discharges for the rating curve are at relatively low flow with only three surveys above a stage of 1.05 meters (equivalent to a discharge of approximately 5 m^3s^{-1}). This means that there is considerable uncertainty for discharges above this stage. These are the flow periods where the most channel planform change is seen (see below) and although the precision of the discharge is uncertain, this is the best possible estimate with available data. The relationship between measured discharges and the estimated discharges can be seen in Figure 3.6 with only one measurement exceeding 7 m^3s^{-1} at the WSC gauge.

The highest flow on record at the WSC gauge is 16.0 m^3s^{-1} in 2010 with the average annual maximum discharge from 1957-2012 being 11.4 m^3s^{-1}. A maximum discharge exceeding 14 m^3s^{-1} has a recurrence interval of about ten years. Daily discharge range is 2 m^3s^{-1} on average during lower flow months (early June and late September) and increases to a typical daily range of 6 m^3s^{-1} during the rest of the season. The inter-annual variability of these ranges is small due to the control by weather, specifically temperature and the peak flows being constrained by the rate of snow and ice melt that can occur given solar radiation input and air temperature.

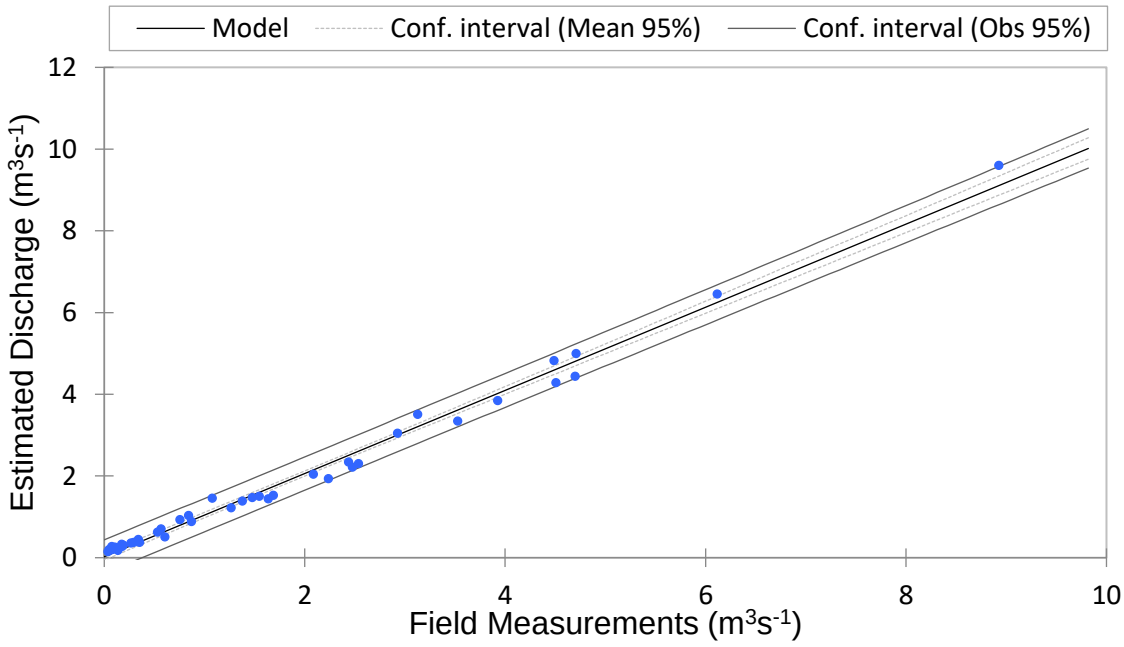

Figure 3.6: The relationship between field measurements by the WSC and the estimated discharges using the rating curve developed for this study.

Tributary Discharge Estimation

The WSC gauging station located downstream of Sunwapta Lake does not account for additional input from Dome Glacier melt-water which joins the Sunwapta River 500 meters downstream of the WSC gauge and upstream of the study reach. It was previously estimated that input of water from Dome Glacier increases the discharge from the WSC gauge by 30% at the study reach (Chew and Ashmore, 2001; Varkaris, 2002; Ashmore and Sauks, 2006; Ashmore et al. 2011).

To determine the additional input from Dome Glacier, velocity-area gauging was conducted in 2015 and 2016 using flow meters at both the study reach (where flow was confined to a smaller channel width because the river was confined to a single channel) and at the Dome Glacier melt-water stream. Additionally, a time lapse camera was installed to monitor the Dome Glacier melt-water stream during the entire melt-water season of 2015. Images were analyzed to determine the similarity in daily hydrograph cycles between the Dome and Athabasca Glaciers and allowed stage measurements to be derived from an image (Leduc et al. in press). The study of Leduc et al. (in press) showed the same pattern of variation over days and weeks throughout summer 2015.

In June 2015 velocity area gauging was conducted on two days at the Dome Glacier meltwater stream and an additional two days downstream of the Dome melt-water input into the Sunwapta where the flow was confined to one single channel. A second field campaign was completed in August 2016 to try and capture a higher flow period. At this time velocity area gauging was again conducted for two days at the Dome Glacier meltwater stream. There was no ideal section where the flow was confined to collect measurements as in the previous year. A site was selected with one wide main channel and two smaller channels located close together. As flows increased during the day the two smaller channels became one with the bar separating the two becoming inundated. Measurements were taken over a width of 33.5m where all the flow was within this area of the river bed, allowing one complete survey to be completed in under an hour. Due to the fast-changing nature of the proglacial discharger regime surveys needed to be completed within a small-time limit to measure a similar discharge across the river.

Discharge measurements completed in the summer field campaigns of 2015 and 2016 were combined with 2003 measurements and correlated with discharge at the WSC gauge allowing gauge measurements to the calculated and converted to discharges at the study reach (Figure 3.7a). The measurements collected in 2015 and 2016 extend the lower range of discharges and estimated

site discharges are almost 10% less than those made in 2003 (Figure 3.7b). The scatter seen in this relationship is caused by small differences in the rising and falling stage (Ashmore & Sauks, 2006).

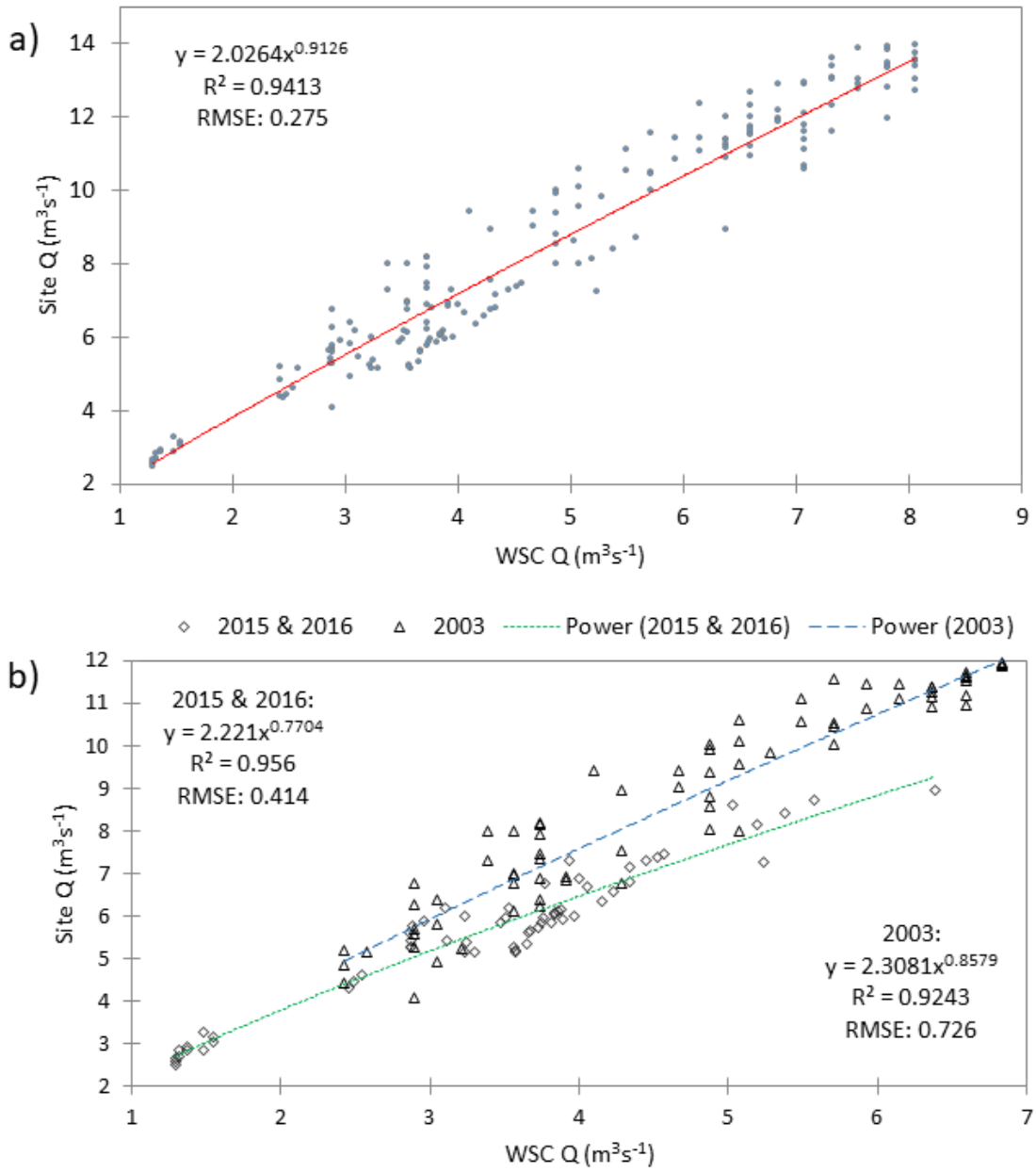

Figure 3.7: The rating curve derived to determine discharge at the study reach with (a) the overall relationship and power function used to estimate discharge and (b) the comparison between measurements completed in 2003 and field measurements completed for this study in 2015/2016, extending the lower range of discharges.

3.3 Measurement of Planform Change

Oblique photographs were taken from June to September in 2012 and 2013. Ten ground control targets, visible in the initial photographs for each year, were installed with high-precision GPS (cm-dm) at the beginning of each season tied to the local datum and the Water Survey of Canada benchmarks (survey completed by Dr. D. Sjogren, University of Calgary) (Figure 3.8). These were used to ortho-rectify the oblique images and assess the accuracy of the rectification.

Figure 3.8: Location of the 10 GCP used to rectify the time-lapse photos.

3.3.1 Rectification of Oblique Images

All photographs were ortho-rectified to account for the photographic distortion from the original oblique images. The rectification of photographs converts all parts of the image to an undistorted vertical view. Photographs were ortho-rectified using the known distances between the ten controlled target points. The number of pixels were calculated between each of the target points in the oblique photograph. From this a pixel-meter (distance) relationship was derived for all areas of the channel bed. This adjustment and conversion was applied to all oblique photographs with all work completed by Dr. Pauline Leduc (Figure 3.9).

Two different methods were used to determine the accuracy of the ortho-rectified photographs. The first compared the distances between each of the ten ground control target points in the rectified images and on the ground (Figure 3.10). The second compared the rectified Reconyx photograph with a UAV image in the same position by overlaying the Reconyx photo over the UAV (Figure 3.11). The UAV ortho-image mosaic provides an aerial viewpoint from an unmanned aerial vehicle (UAV) (acquired on the same days as the ground survey by Dr. Chris Hugenholtz, University of Calgary and Owen Brown, ISIS Geomatics).

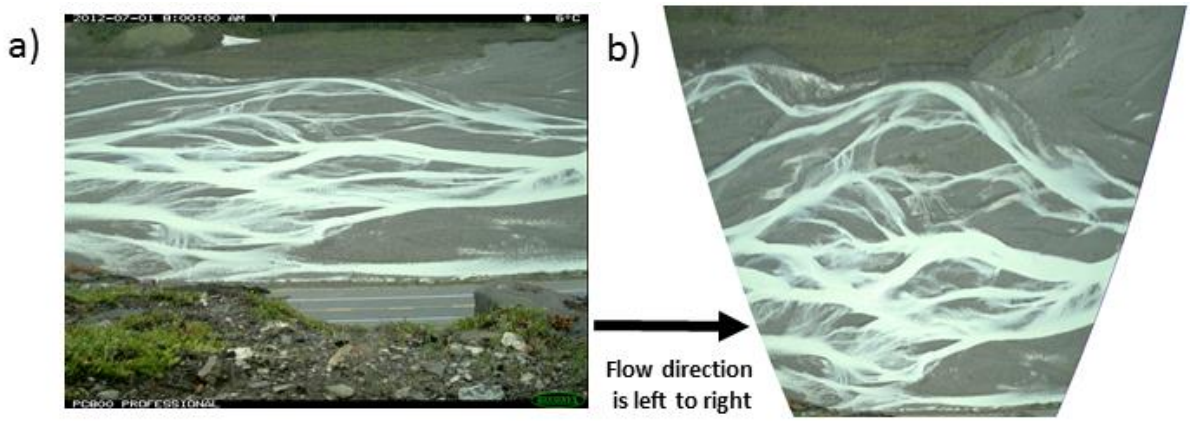

Figure 3.9: An example of the orthorectification of field time-lapse images, (a) original oblique view and (b) the orthorectified image. Original image taken on July 1, 2012, 08:30.

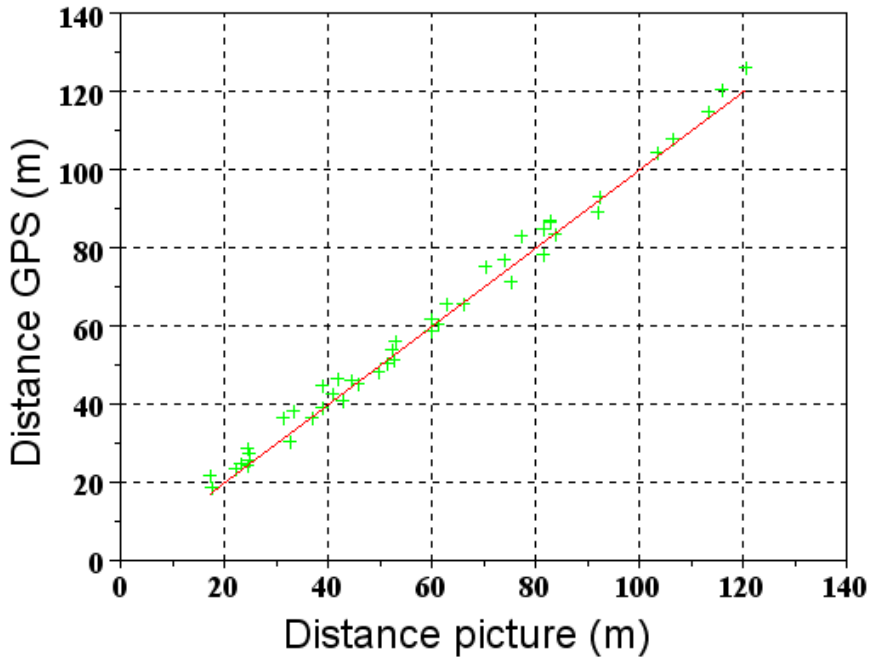

Figure 3.10: The comparison between distances measured between ground control points in the rectified images (adjusted for photo scale) and on the ground in the GPS datum.

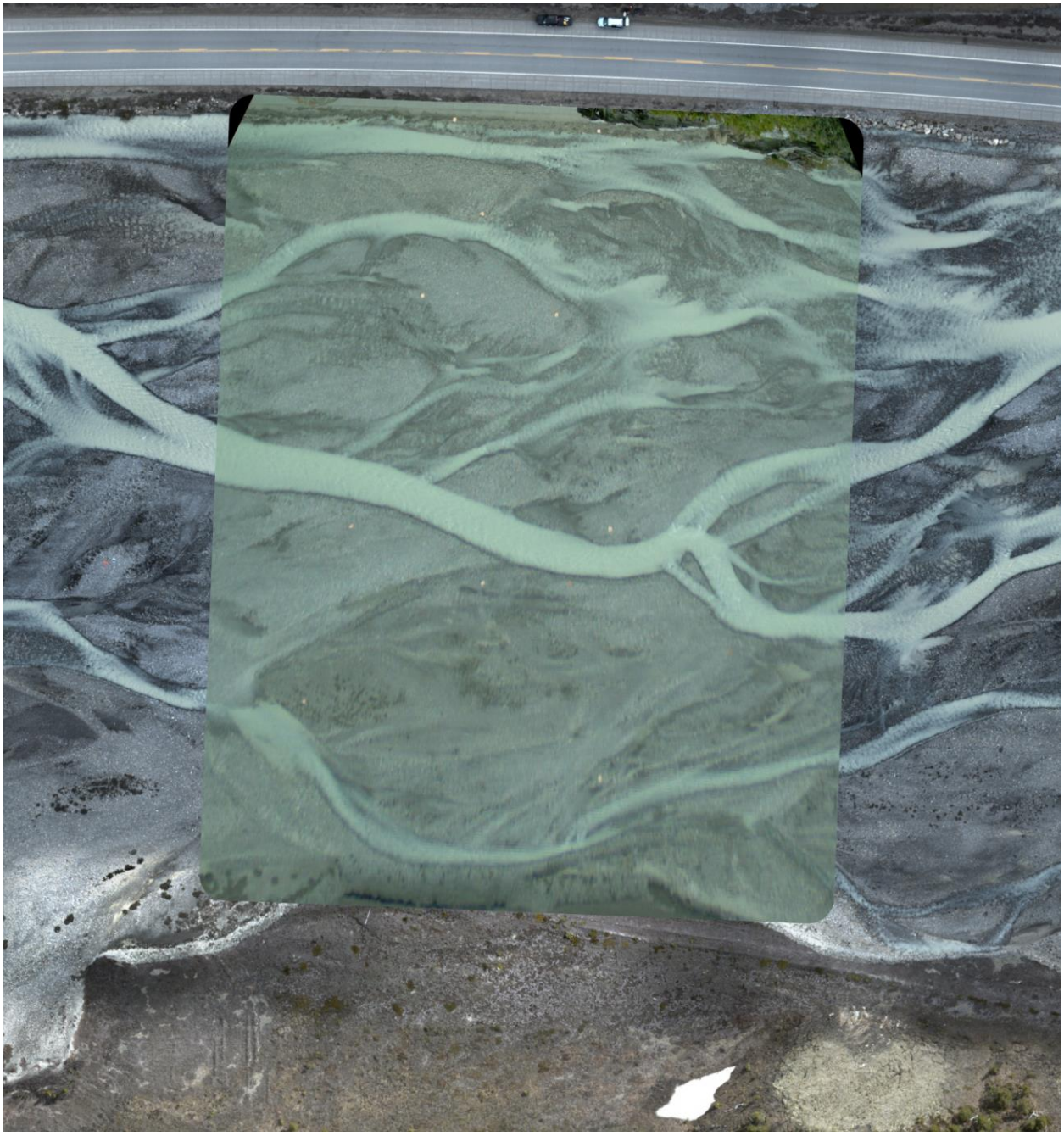

Figure 3.11: The channel planform position at the field site with the UAV photograph underneath and the ortho-rectified time-lapse image overlaid on top.

3.3.2 Planform Measurement

Very similar diurnal meltwater hydrographs made it possible to measure daily planform change over a wide range of daily peak and total discharges from June to September, each with the same

daily time base of morning low flow and evening high flow. Each daily hydrograph was analyzed as an individual flow event, with the amount of planform change produced driven by the peak or total discharge. It was apparent that any planform change occurred over a limited time period each day and not during daily low flow, even during the highest flow periods and not during daily low flows. Therefore, these flow events also represent separate planform change (and bedload transport) events. Daily hydrographs were first measured for areas of planform change in 2015 and re-analyzed for this study to improve the areas measured, automate the detection of changes and in relation to the wetted area, discussed further below.

Daily measurements of the areas of planform change were related to the energy which produced the planform change (peak or total discharge) and then further considered in relation to their potential to produce change. The wetted area was measured at peak discharges of daily hydrograph measurements to determine the total wetted area that had the potential to produce change in planform.

Initial assessment of changes was done by reviewing all the photos at 30 minute intervals covering the entire period of image acquisition in 2012 and 2013. By watching the time lapse sequences, and going back and forth through photographs over several days to detect change, observations were made on the type and extent of planform changes in this braided river and periods for more detailed measurements were selected.

Planform change measurements for a given daily hydrograph were made by selecting pairs of photographs on successive days at the lowest recorded comparable discharge during daylight (usually early in the morning each day because diurnal melt hydrographs were at a minimum in the morning, peaked in the early evening and were on the falling stage through the night). Low flow times were selected to minimize apparent effects of stage differences masking real channel changes, and to maximize the area of river bed visible. This was done by looking at the two daily minimum discharges. The day with the higher minimum discharge was selected and the image for the second day was selected for the time when the two discharges were comparable. WSC gauge was recorded every 15 minutes and photographs were taken only every 30 minutes. To account for this, if the discharge selected occurred at a time of quarter past or quarter to an hour they were not considered and the next closest discharge and time were used. Some day-to-day comparisons were not possible due to days that had no comparable discharge during the daytime from one day to the

next. These days were not analyzed because it was essential to have equivalent bed exposure in the two days to avoid the apparent extent of change being affected by flow stage rather than real planform change (ie. involving bar and channel erosion, deposition, bank erosion, channel avulsion etc.). The daily comparison of photographs allowed for a large amount of data to be analyzed over a wide range of discharge and channel pattern changes produced by the daily meltwater hydrographs of a proglacial river like the Sunwapta.

All possible day-to-day comparisons were analyzed however it was not possible for all days during the study periods. This was caused by two factors, first, a shift in the camera position during the beginning days of the 2012 study and set up of equipment; and second, days where there was no possible discharge close enough from one day to the next to compare without the influence of differences in flow stage. These two factors removed 7 daily hydrograph measurements with 216 remaining hydrograph measurements completed, 113 in 2012 and 103 in 2013.

Measurements of planform change were completed using two different methods. First the entire meltwater season of 2012 and 2013 was visually assessed to determine and measure areas of planform change from each daily hydrograph period using ImageJ software. Secondly any daily period which experienced measurable planform change based on manual analysis was then subsequently analyzed using an automated image classification routine in Scilab. An automated image analysis was completed to try and reduce the subjectivity of a visual analysis method.

3.3.3 Manual Analysis

The image analysis program ImageJ was used to manually measure areas of the river bed where the river planform had changed from one daily image to the next consecutive daily image. This method was used to improve the accuracy of areas of planform change compared to Middleton (2015). The manual analysis used for this study involved measurements of change made by the visual assessment of planform changes and manual delineation of areas of change in successive pairs of images.

Using the rectified images, areas of planform change could be measured as a known area of the river bed derived from the pixel-meter (distance) relationship (1m = 8.8125 pixels). To aid in this analysis a grid was applied to all rectified photographs which represented a known distance and area within the river bed. This outlined the study area, 96 x 120 meters.

Areas of planform change were visually determined and were then mapped, and measured as individual polygons. The areas of each individual polygon were accumulated to determine the total area of planform change for a daily hydrograph period between successive days. Planform change was determined to be any area where there was a change from water to gravel or gravel to water along with a change in the local river bed morphology (further discussed in Section 3.3.5). This included areas of erosion and deposition, partial avulsion, lateral migration of the channel, development of braid bars, cross channel bars and other changes resulting from active braiding processes.

Error and Precision

The manual measurement of planform change had a known subjectivity based on the user identifying planform changes and potentially between measurements made by one person. To better understand the subjectivity associated with manual measurements of planform change made by one person, measurements of planform change were re-measured from a daily hydrograph every week during the summer meltwater periods of 2012 and 2013 when planform changes were documented. 19 daily hydrographs were re-measured and showed a significant positive correlation (Figure 3.12), showing the high similarity between original and re-measured areas of change over a daily hydrograph period. Further details on the statistical significance can be found in Appendix E.

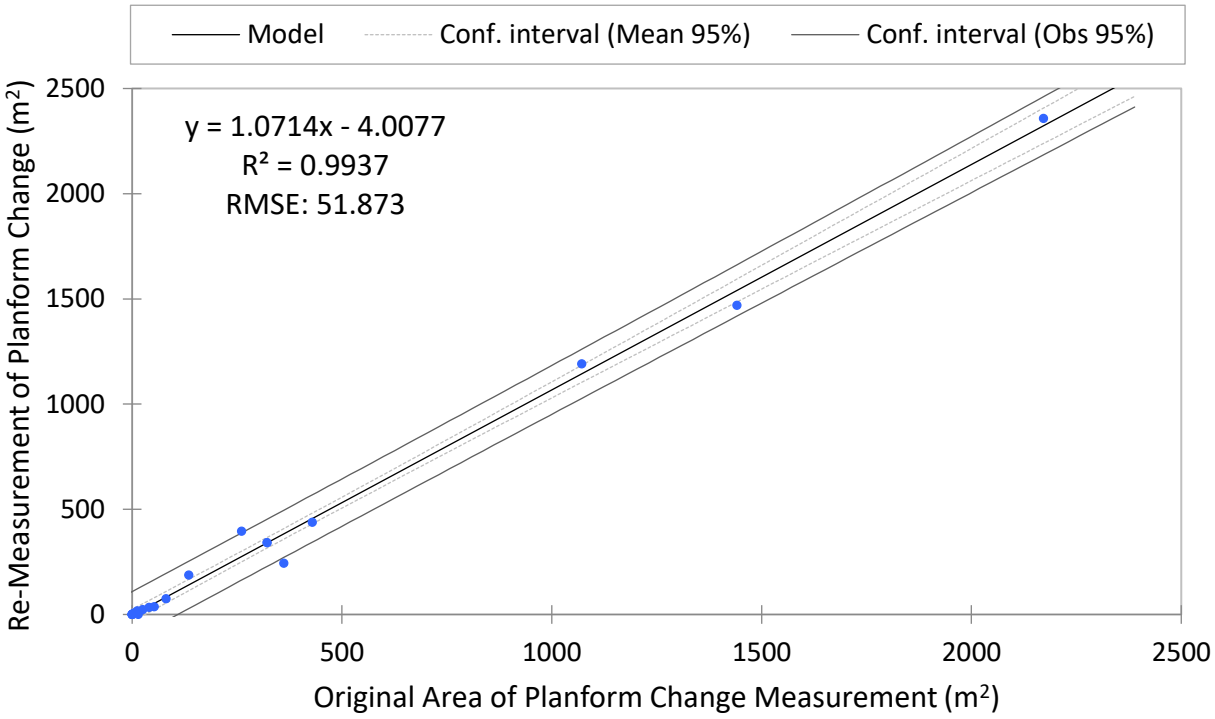

Figure 3.12: The relationship between original planform change measurements and re-measured areas of planform change.

3.3.4 Automated Analysis

The automated analysis was completed using Scilab software to automatically detect differences between water and gravel in a photo, using a script written by Dr. Pauline Leduc. This method was completed as part of the reanalysis to limit the subjectivity of the manual analysis method.

The automated analysis was completed for all daily hydrograph periods which experienced planform change, based on the results from manual analysis. Coloured rectified images were selected as inputs into the script and all areas of water were then manually selected by the user. Cells around the selected point with a RGB value of +/- 5% threshold were automatically detected as an area with water. Areas were selected differently based on the lighting in the photo causing the channel to appear more, or less similar in colour to the gravel (Figure 3.13). These changes in lighting and reflection of the water surface were also impacted by the shadow produced from the valley slope with large changes evident in the colour of the water surface over a small time-frame. This caused detection issues especially seen around the edges of channels and bars, and narrow and shallow channels, discussed more below in Section 5.6. After selecting all areas of water, areas

that were detected incorrectly could be manually removed by outlining a polygon on incorrect cells. Two filters were then applied, an erosion filter to remove any isolated individual water cells and then a dilate filter to merge groups of points. This smoothed out the picture removing any lonely points and then properly connected areas of water in the channel. The final output was a binary image, allowing consecutive daily photos to be subtracted from one another, giving an area of planform change based on transitions from water to gravel, or gravel to water (Figure 3.14). The subtraction of daily images was also completed using Scilab software and a second script developed by Dr. Leduc.

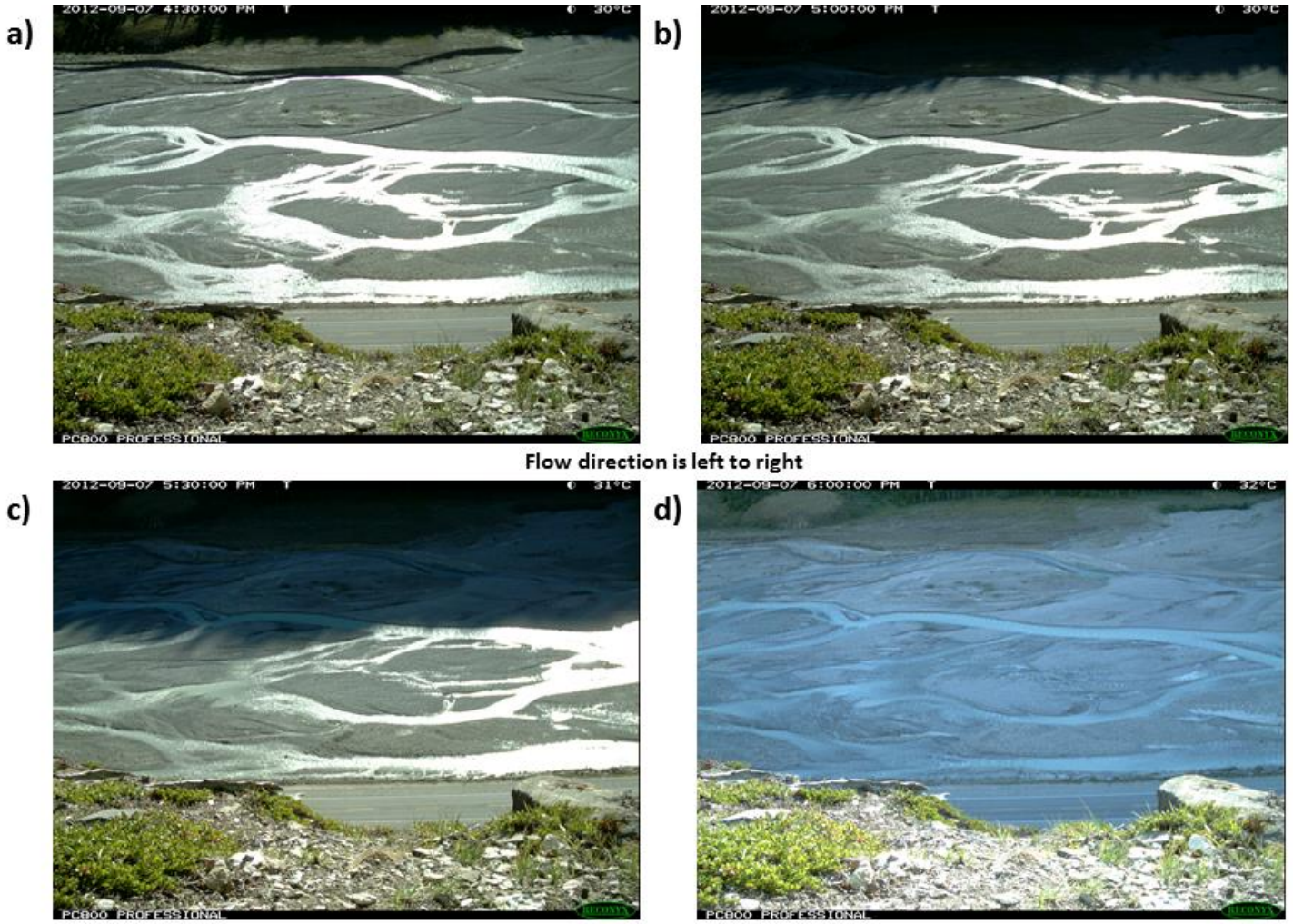

Figure 3.13: An example of successive time-lapse imagery every half hour with changes to the reflection and lighting. These changes seen over a short-time frame caused issues for the automated detection of the water surface due to differences in colour of the water surface between images.

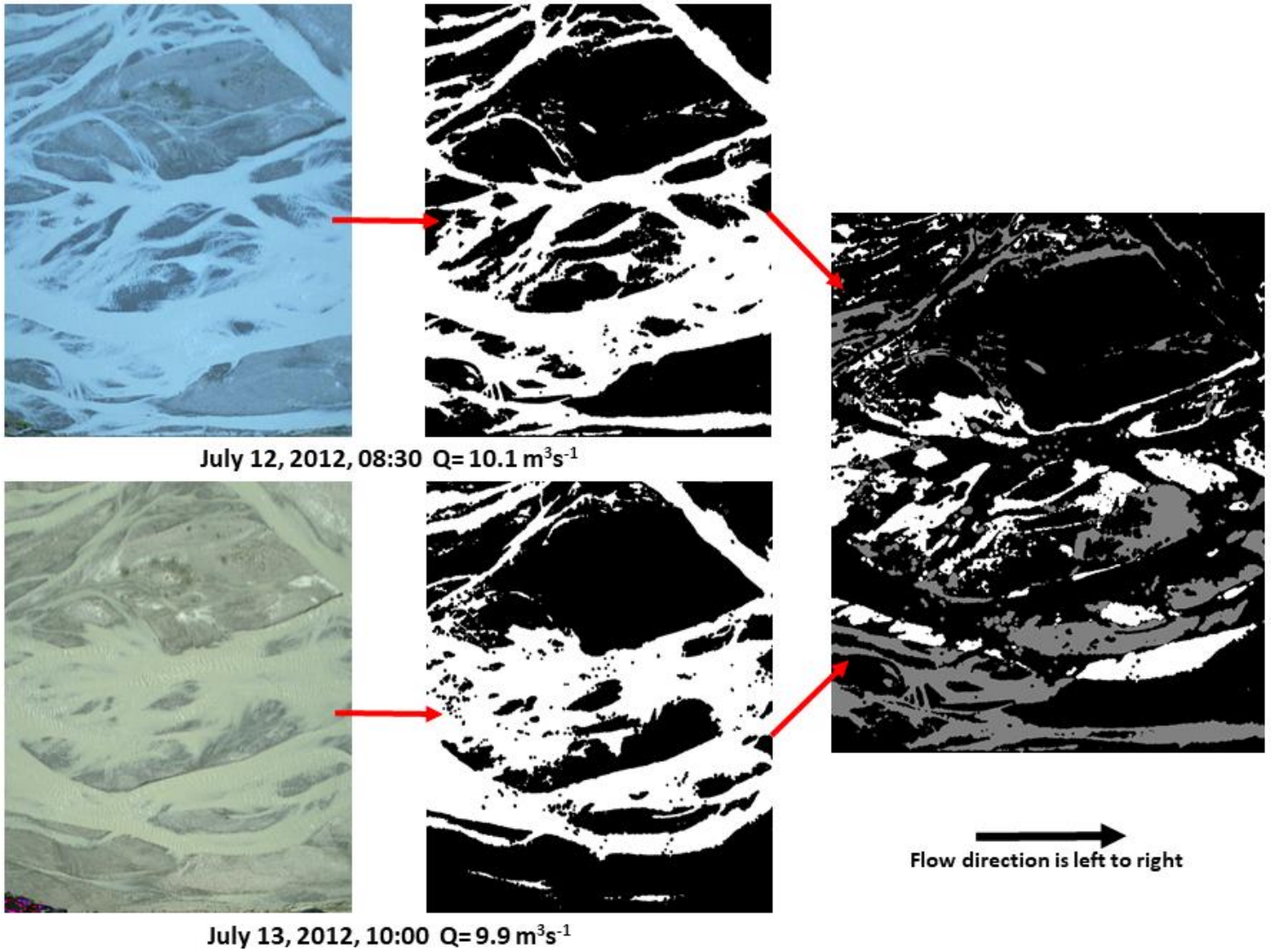

Figure 3.14: An example of two subsequent daily binary images and the resulting subtraction with a change in planform from gravel to water in white and from water to gravel in grey.

Wetted Area

The wetted area was measured at the peak flow of daily hydrographs to capture the maximum wetted area within which planform could have potentially changed. This allowed the area of planform change that was recorded to be normalized by the wetted area and to be related to the highest area of potential planform change. This makes the results comparable with physical model data and with any subsequent similar analysis on rivers of different scales.

The wetted area was determined using the automated analysis method discussed above in Section 3.3.4. The first script was run to automatically detect the differences and determine the area of water and gravel from an image with a binary output image created. This was completed for peak discharges of all daily hydrographs for which planform change occurred. The discharge wetted area relationship was extended to lower discharges by measuring the wetted area at the peak of one daily hydrographs at each discharge (1-2 m^3s^{-1}, 2-3 m^3s^{-1}, 3-4 m^3s^{-1}… etc.) for both 2012 and 2013.

Chapter 4

4 Laboratory Methods

The physical model experiments were designed to complement and assist in interpretation of the field data and assess aspects of the braided river dynamics that cannot be measured in the field. Specifically, the lab experiments allowed simultaneous measurements of planform dynamics, topographic change and bedload flux, as well as direct observation of bedload and morphological change because of clear water in the model. The intent of experiments was to assess whether bedload transport occurred independent of planform change and correlate planform change with morphological change through volumes of erosion and deposition.

Daily hydrographs on the Sunwapta with peak discharges known to produce planform change were scaled down and run in the flume. This control allowed four different peak discharges to be selected and then reproduced to try and capture the known variability in bedload transport in braided river systems. The ability to reproduce known hydrographs from the field also allowed a comparison to be made between field morphology and replicated morphologies in the flume.

4.1 Experimental Setting

Experiments were conducted in a river modelling flume using a small-scale physical model of a gravel-bed river. Previously located in the Boundary Layer Wind Tunnel Laboratory at the University of Western Ontario the physical model was approximately a 30:1 Froude scaled model of the Sunwapta River, scaled to the sediment caliber of the study reach location. The flume dimensions were 18.3m long and 3m wide with the ability to manipulate both the discharge and slope up to a maximum of 2.7 ls^{-1} and 2.5% respectively, with the slope set at 1.5% for experimental runs to reproduce field settings (Figure 4.1). This slope is the same as the Sunwapta study reach and the experimental model has the same slope as the field prototype with a Froude-scale. The slope was adjusted using the hydraulic lifts located under the flume and estimated to a 1.5% slope using a measure tape with known heights in relation to slope at the upstream end and then surveyed to check accuracy, with details found in Appendix C. This allowed hydrographs from the field to be run as experimental runs by scaling down both the discharge and time. Bedload transport samples were collected from five metal baskets spanning the width of the tail tank for each run (Figure 4.2).

Figure 4.1: An image of the physical model of the Sunwapta River.

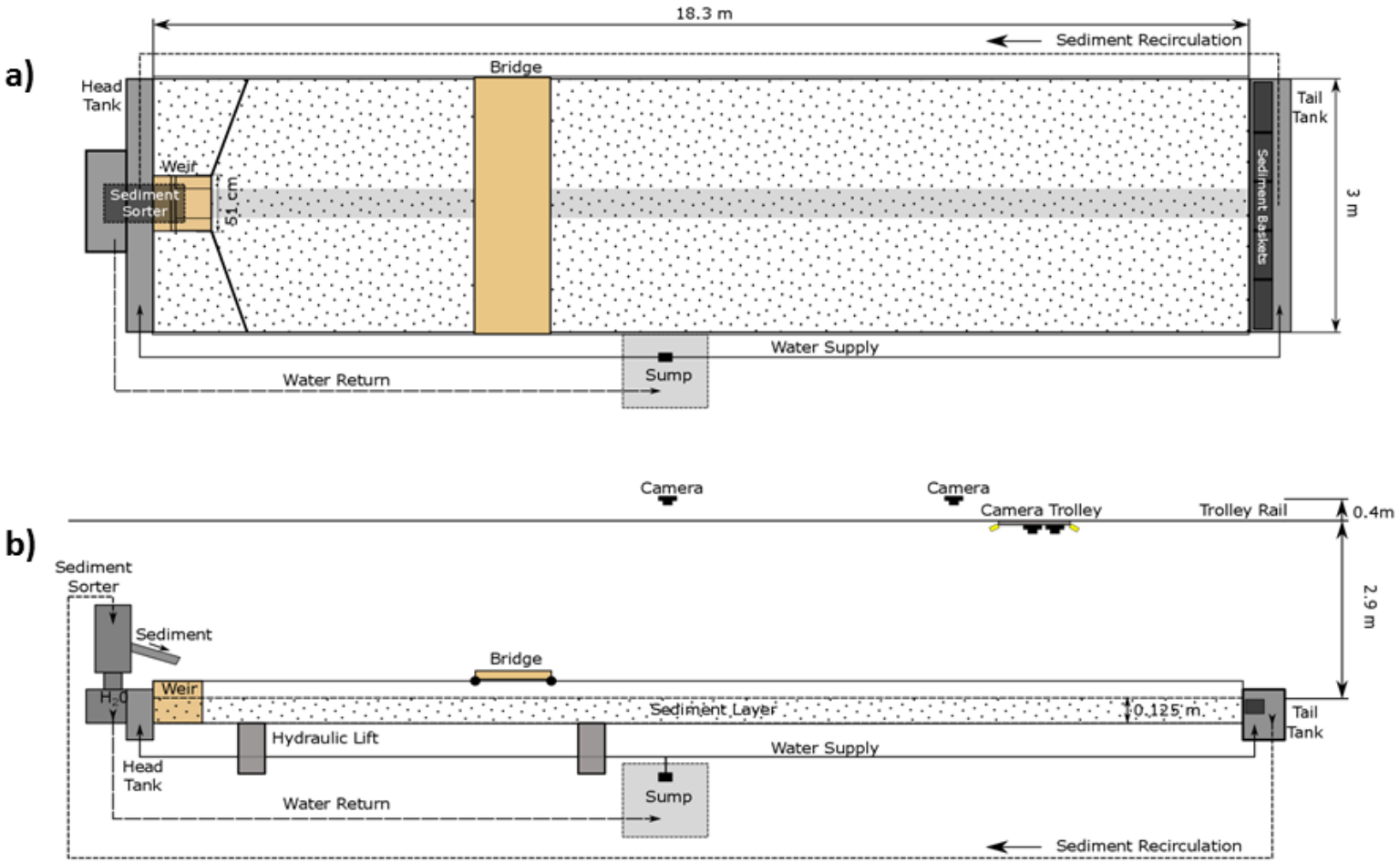

Figure 4.2: The layout of the flume seen from plan view (a) and side view (b), adapted from Peirce, 2017.

4.1.1 Discharge

The 1:33 Froude-scaled model yields a discharge scale of 1:6250. Discharge was adjusted during experimental runs using a valve situated at the sump pump, located underneath the flume (Figure 4.2). This altered the water level in the head tank, located at the upstream end of the flume. The water level in the in the head tank corresponded to a chosen discharge, calculated from a calibrated trapezoidal weir (see Appendix D).

4.1.2 Sediment

The grain size distribution from the flume was a 1:33 Froude-scale of the sediment distribution at the study reach on the Sunwapta River with a range of grain sizes from 0.18mm to 16mm. The field grain size distribution used was based on previous research completed in 2003 at the study reach. The median grain size of the flume sand is 1.18mm and the D_{10} and D_{90} are 0.18mm and 3.4mm respectively (Figure 4.3). The lower limit of the grain size distribution was truncated so that grains smaller than 0.18mm (equivalent to approximately 8mm in the field) were excluded, typical in a physical model of a gravel-bed river, as discussed in section 2.4.1.

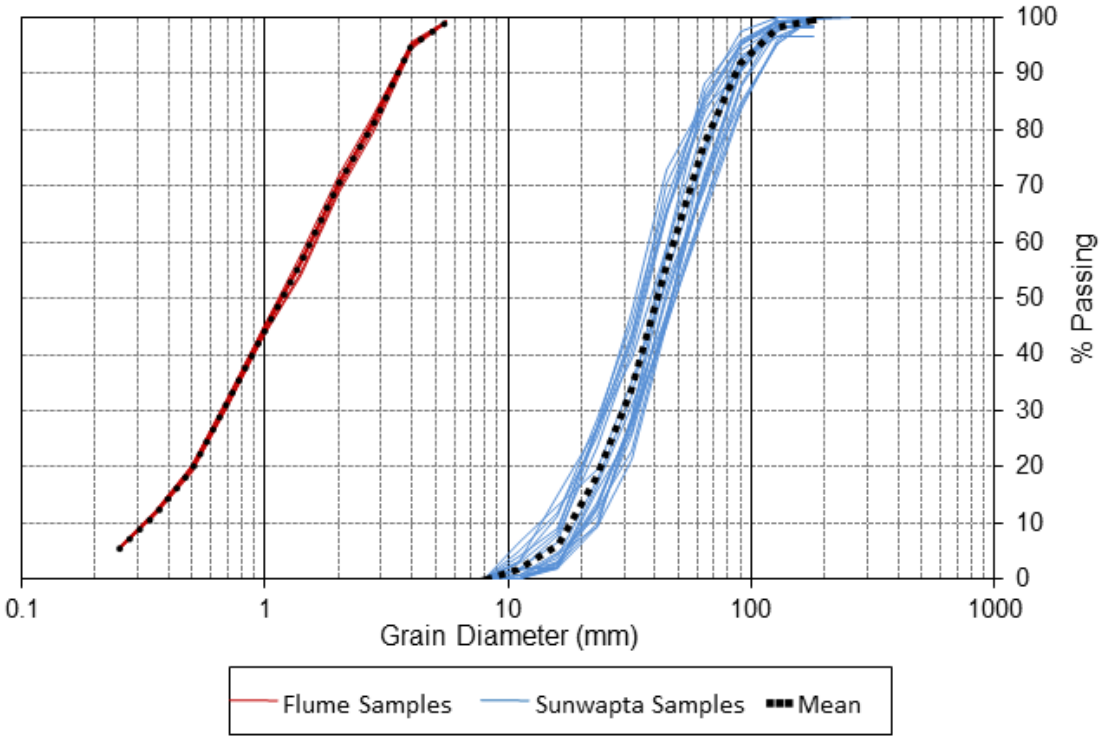

Figure 4.3: The grain size distribution of the field site at the Sunwapta River and the physical model.

An automated sediment recirculation system allowed sediment which was transported downstream into the tail tank to be returned upstream and be input at the head tank of the model river, maintaining an overall sediment balance during each experimental run. Water and sediment flowing into the tail tank at the downstream end were delivered upstream to a sediment sorter, located over the weir. Water was separated from sediment and returned to the head tank while sediment was deposited onto the sediment slide. A vibrator ensured that sediment did not build up on the slide and was continually input into the flume. Some additional water was not separated from the sediment sorter and entered the flume along the slide with the sediment input. This water input was measured at the end of experiments, summarized in Table 4.1 and determined the contribution on average was 0.12 ls^{-1}, below the error for discharge calibration, so no additional adjustments were added to the discharge.

Table 4.1: The summary statistics of the water input from the sediment sorter.

# of Samples	10
Mean Discharge (ls^{-1})	0.118
Standard Deviation (ls^{-1})	0.003

4.2 Experimental Design

Utilizing the WSC gauging station stage data and discharge measurements for the years of time-lapse observations, experiments were conducted to replicate a sequence of four daily hydrographs from the Sunwapta in the flume. These hydrographs were selected as representative daily hydrographs with four different daily maximum peak values (Figure 4.4). Equivalent discharge and time in the flume was calculated using a 1:33 Froude scale of measurements from the Sunwapta River as discussed in section 2.4.1. Utilizing this scale, daily (24 hour) hydrographs were scaled down, creating four different, four and a half hour long hydrographs, outlined in Table 4.2. Each hydrograph experiment was run three times for a total of 12 experimental runs (Table 4.2). Hydrograph experiment runs will be referred to as the hydrograph (A-E) and run number (1-12). Hydrograph experiment D was designed to model a peak of 3.08 ls^{-1} (19 m^3s^{-1}) but it was discovered during the first experimental run of hydrograph experiment C that this would not be possible. The highest discharge attainable in the flume was 2.74 ls^{-1} (17 m^3s^{-1}) and so Hydrograph experiment C was adjusted and Hydrograph experiment D was replaced with a lower peak hydrograph. Hydrograph D occurred on the last day in the flow sequence of replicated hydrographs but to achieve a lower peak, the hydrograph the day prior to hydrograph experiment A in the field was selected to be replicated. The sequence of hydrographs run in the field can be seen in Figure 4.4 occurring from August 2-7, 2012. Due to the replacement of Hydrograph experiment D, runs were done in the sequence on Aug. 3-6 (Hydrographs A, B, C) followed by Aug. 2 (Hydrograph E) with this sequence of runs completed three times.

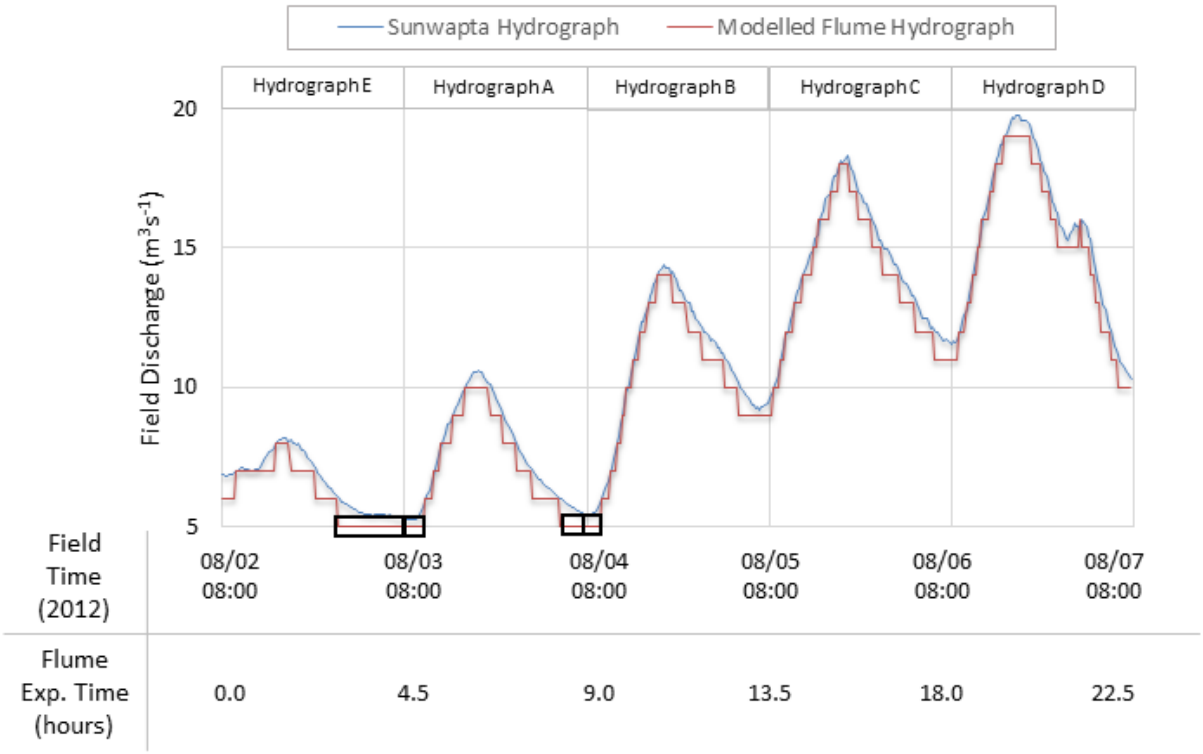

Figure 4.4: Selected representative Sunwapta hydrographs with the intended replicated scaled flume experimental hydrographs. The shortened length of hydrographs A, B and E is highlighted in the black boxes.

Hydrographs A, B and E were shortened to cover only those discharges that had the potential to produce any planimetric change in the field. A previous analysis of the field time-lapse imagery, completed in 2015 found that the river planform did not change at all below a discharge of 7 m^3s^{-1}. Previous hydrograph experiments conducted on the same bed found no bedload transport to occur below a discharge of 1.14 ls^{-1} (7 m^3s^{-1}). Daily hydrographs, A, B and E, had discharges at the beginning and/or end of the daily hydrograph between 5-5.99 m^3s^{-1} and were shortened to reduce the total experimental time and reflect previous research related to planform change and bedload transport (Figure 4.4). The field analysis also showed that planform changes occurred over a limited time each day in relation to the peak discharge, even at the highest flows, with the beginning of the rising and falling limb seen to produce very little planimetric change. The adjusted hydrograph experiment outlines can be seen in Table 4.2.

Table 4.2: The summary of the experimental conditions and time of the four different hydrograph experimental runs, designed to replicate Sunwapta hydrographs.

Hydrograph:		**A**	**B**	**C**	**E**
# of Exp. Runs		**3 (Exp. 1, 5, 9)**	**3 (Exp. 2, 6, 10)**	**3 (Exp. 3, 7, 11)**	**3 (Exp. 4, 8, 12)**
Min Q	**Field (m^3s^{-1})**	6	6	9	6
	Flume (ls^{-1})	0.98	0.98	1.4	0.98
Peak Q	**Field (m^3s^{-1})**	10	14	18	8
	Flume (ls^{-1})	1.6	2.22	2.89	1.29
# of Diff. Hydrograph Stages		5	9	10	3
Rising Limb Exp. Time Removed (hours)		0.50	0.38	0	0.0
Falling Limb Exp. Time Removed (hours)		0.57	0	0	1.50
Total Time Removed (hours)		1.10	0.38	0	1.50
Range of Q Removed		5.22-5.96	5.22-5.96	0	5.28-5.96
Total Exp. Time (hours)		3.43	4.13	4.50	3.00

Experiments were conducted on a previously formed bed, from another, different hydrograph experimental run, with peak discharges of 2.1 ls^{-1}. These previous hydrograph experiments began on a flat bed with a single carved channel, initial dimensions of 50 x 2.5 cm at 1.5% slope. A stable braided morphology was achieved by running a constant discharge of 2.1 ls^{-1} for 24 hours to allow the model to self-form a fully braided channel.

4.3 Experimental Data Collection

A comparable data set was required to examine the relationship between channel pattern change and discharge in the field and over modelled hydrographs run in the field prototype. This relationship was then extended with the acquisition of topographic measurements made possible in the controlled setting of a physical model. The experimental data consisted of time-lapse imagery, photogrammetric data, bedload measurements, and observations made throughout all experimental runs, explained below. These surveys were completed at a hydrograph stage at the beginning of the rising and falling limb to allow comparable images to be created for planform measurement. Additional photo surveys of the wetted surface were completed when time was available, with a large amount of data recorded on the end of the falling limb due to the longer time period of hydrograph stages (Figure 4.5). At every hydrograph stage an observation and measurement were collected of the number of active channels and total number of channels giving an indication of the Active Braiding Index (ABI) and Braiding Index (BI), discussed further below. A corresponding bedload transport sample was collected after the ABI/BI recording, ~2m downstream at each hydrograph stage during all experimental runs (Figure 4.5). Between each experimental run the dry-bed was surveyed to allow accurate DEM and DEMs of Difference (DoDs) to be generated to determine morphological changes and the volume of change through each hydrograph experimental run.

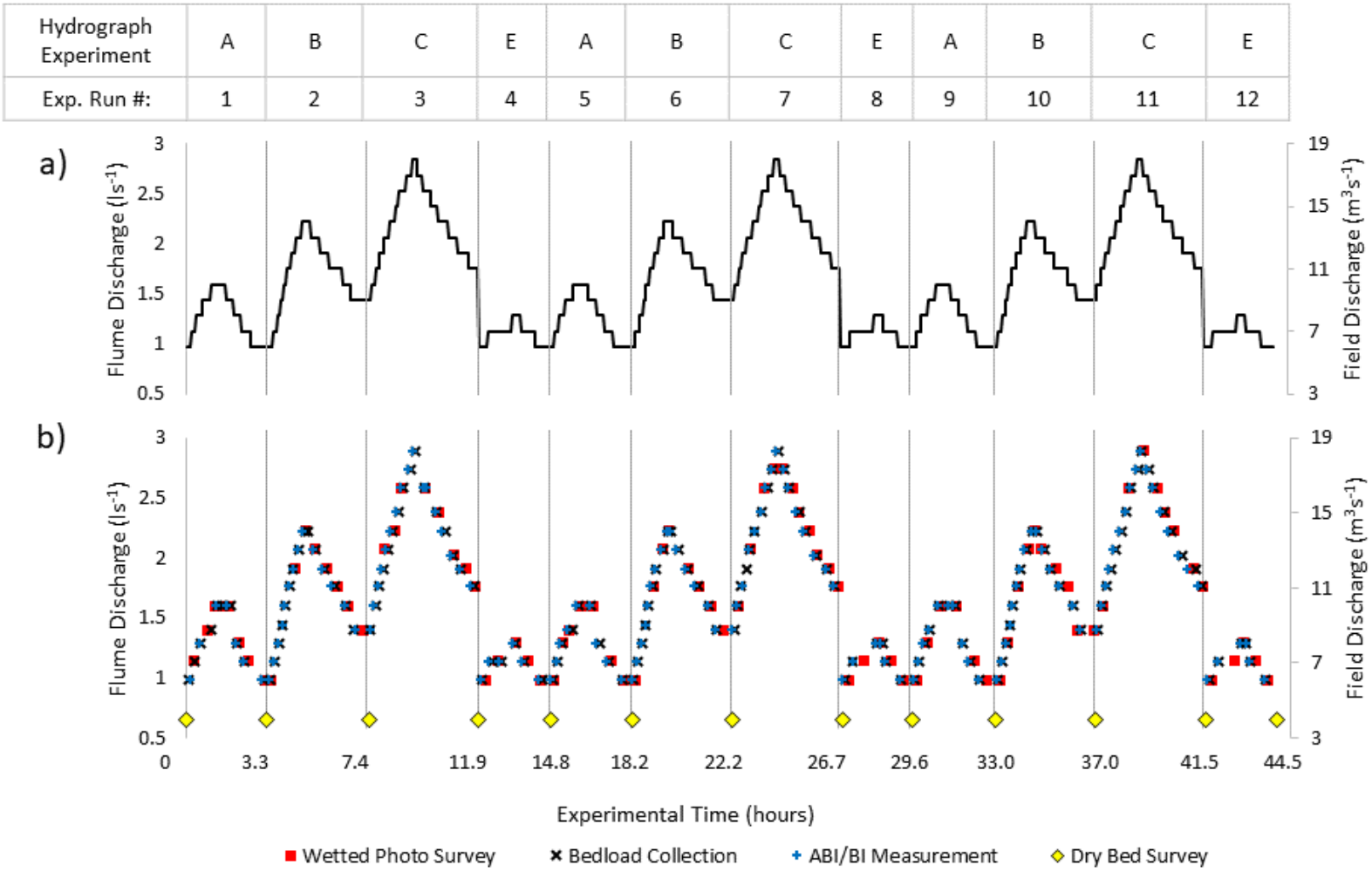

Figure 4.5: Flume hydrograph experimental runs outlined in (a) with the data collected during and between runs seen in (b).

4.3.1 Time-lapse imagery

Two Olympus C5060 cameras with wide angle lenses, located in a fixed position 3m vertically above the axis of the flume were used to give high frequency (1 minute) time lapse record of each experiment. The two cameras covered different areas of the length of the flume with a short (~ 1m) overlap.

4.3.2 Photogrammetry

In addition to the two Olympus cameras, two Canon T5i cameras with a 20mm lens located on a moveable trolley, 2.9m above the flume were used to obtain high resolution imagery for photogrammetry which was used to extract high resolution DEMs of the river at the beginning and end of each hydrograph experiment as well as stitched orthoimages of the wetted surface during runs for planform and wetted area measurement. Positioned to have convergent viewpoints, the cameras had an approximate overlap across the flume of 80% to provide better precision for structure-from-motion photogrammetry compared to a vertical viewpoint (Westoby et al. 2012; Micheletti et al. 2015a; Smith et al. 2016). The cameras were flown down the flume on the trolley and images were taken at 0.3-0.5m intervals along the flume to provide the image collection for photogrammetry. Both cameras were connected to a computer and images were collected and stored using remote camera triggers using DigiCamControl software program.

Photo surveys of the dry river bed were done at the beginning and end of each hydrograph experiment to provide a DEM before and after the hydrograph and from which a DoD (DEM of Difference) could be extracted to measure areas and volumes of topographic change during each hydrograph. The photogrammetric software also generated a stitched ortho-mosaic of the dry river-bed.

Photo surveys were done at select discharges over various hydrograph stages while the flow was running. These surveys were used to map the extent of the wetted channel at each flow stage and to map the areas of planform change over a hydrograph period. 92 wetted surfaces were documented covering ~10m of the flume over all discharges and on both the rising and falling limb of hydrographs. Details of the photogrammetry processing are given below.

4.3.3 Width and Depth Measurements

Width and depth measurements were collected from the same position at every hydrograph stage during experimental runs. These measurements were taken from the bridge, which was positioned in the same location at the downstream end in every experiment, with a measured meter tape stretched across the width of the flume directly in front of the bridge. This allowed the channel dimensions to be measured as well as, if they were active (had bedload), the size of particles moving as bedload, along with observations on how the morphology and planform were altered during each hydrograph experiment.

4.3.4 Bedload Samples

At the downstream end of the flume, located above the tail tank are five sediment baskets, spreading the entire width allowing direct bedload samples to be measured. A one-minute sample was collected at each hydrograph stage. These samples were then each individually dried, weighed and sieved to obtain bedload transport rates and particle size distributions of bedload. These samples, collected in coordination with the width and depth measurement, observations of activity, and images taken of planform provide a snapshot of how the relationship between planform, morphology and bedload develop and evolve throughout a modelled daily hydrograph and a check on the extent to which bedload transport may occur independent of measured planform or topographic change.

4.4 Experimental Data Processing

The wet and dry bed photo surveys were processed using Agisoft Photoscan 1.0.0.1 software package to produce orthoimages and DEMs. Agisoft Photoscan is the most widely used commercially available software package for this type of photogrammetry (Smith et al. 2014; Woodget et al. 2015; Smith et al. 2016). This allowed quality orthophotos and DEMs to be developed using a set of survey images, taken over the same surface. This also allowed high resolution DEMs to be generated similar to previous photogrammetry applications in the flume (± 1mm). The built-in target detection of Agisoft allowed comparable DEMs to be generated much easier and faster compared to traditional photogrammetric methods.

To develop the high-resolution topography photo surveys were completed which included the surveyed targets, located in the flume discussed in Section 4.1.2. These ground control targets

generated a coordinate system and scale for DEM generation and allowed ortho images to be rectified and stitched together (Agisoft, 2016). The surveyed targets were downloaded and printed from Agisoft Photoscan and then attached to either side of the flume walls, 9 on either side located ~2m apart.

Images collected during the photo surveys of the dry bed were input into Agisoft which generated and orthoimage and a DEM of the flume surface with 1.5mm pixels. To correct systematic errors between DEMs a series of steps was performed using an automated script developed by Dr. Pauline Leduc. These steps included:

1) Removal of high frequency noise using a running averaged filter on height
2) Vertical correction using the metal overflow weir with known elevation at the downstream end of the flume

Further details can be found in Peirce, 2017.

An estimate of the error on the DEM data was determined by creating a mask from the last DEM surface of experimental hydrograph runs to determine the standard deviation of the non-moving areas across all corrected-detrended DEMs with a standard deviation of 2.9 mm found (Figure 4.6).

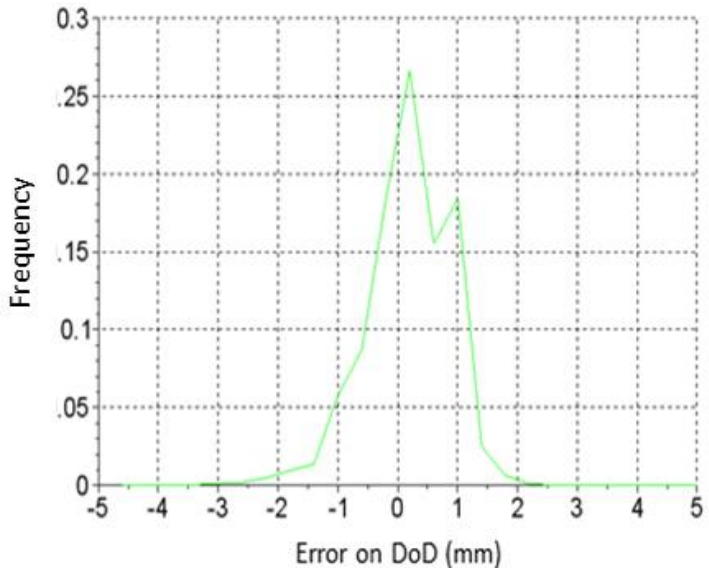

Figure 4.6: The frequency distribution of elevation error on DEMs of Difference, determined by measuring the elevation of non-moving areas across all hydrograph experiments. The standard deviation is 2.9mm.

DoDs were created using two different methods: 1. the simple threshold method involving the removal of all values less than a certain threshold and 2. the application of a dilation filter based on a binary mask. The simple threshold method was run three times at 1σ, 2σ and 3σ, summarized in Table 4.3 below. The dilation filter extended the simple threshold method by taking into account if surrounding cells recorded change or no change. This method was selected as it reduced noise and increased the continuity between areas of change. This involved the creation of a DoD between subsequent surfaces in which no absolute threshold was applied. This DoD was then used to create a binary mask based on 3σ absolute threshold of change where areas of '1' and '0' representing all areas above and below the threshold respectively. A dilation filter was then applied, converting neighbouring areas found within a certain radius of one another. A circle with a radius of 15 cells was chosen based on the area of a small channel in the flume, corresponding to a radius of ~3.3 cm.

Table 4.3: The absolute threshold values applied to DoDs for removal of points based on the first, second and third standard deviation.

1 σ	2σ	3σ
2.9 mm	4.8mm	8.7mm

4.5 Measurements

Replicating daily hydrographs from the Sunwapta River allowed comparable measurements of planform change to be made between the field and the field prototype. Similar to the field, each experimental hydrograph was analyzed as an individual, daily flow event, with the amount of planform change related to the peak discharge and total discharge of the hydrograph. The laboratory setting allowed the analysis daily hydrographs to be extended through the collection of measurements of morphological change and bedload transport rates.

4.5.1 Planform Change Measurement

To determine planform change during each experimental hydrograph, the orthophotos at the lowest recorded comparable discharge were selected for the rising and falling limb of each hydrograph. This is equivalent to the procedure used for field images and hydrographs. Like field images, these orthoimages had a grid placed on allowing for easier visual planform measurements and were all batch cropped to include the same area of 9.5 x 3m of the flume, equivalent to almost three times

the equivalent length in the field. Due to the high resolution and size of these ortho-images problems occurred when trying to apply a grid. Original images had a ground resolution of 1.5mm/pixel and these were compressed to 3mm/pixel to increase processing time. The contrast was increased in all images to enhance the difference between submerged river bed and emerged wet bed (Figure 4.7).

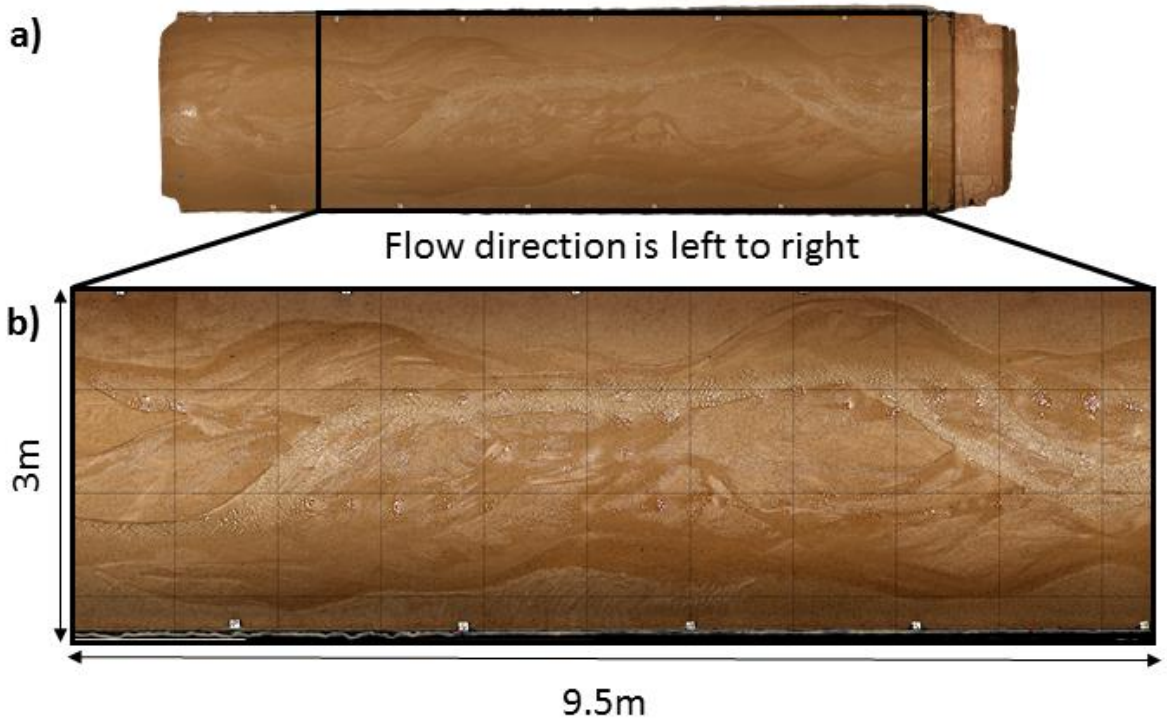

Figure 4.7: An example of (a) a flume stitched orthophoto and (b) the equivalent image with a grid applied, contrast increased and images cropped to the same areas.

Areas of planform change were visually determined using the same approach as field images and measured as individual polygons. The area of the polygon was determined by the known pixel-meter (distance) relationship from the flume (1mm=0.333pixels). The area of individual polygons was then accumulated to determine the total area of planform change.

Measurement of Wetted Width

These cropped ortho-images were divided into one meter wide sub sections, except for the upstream and downstream subsections which were 0.75m with calculations adjusted to account for this difference. The wetted width was visually determined to be any area of the river bed that was

inundated with water, including both stagnant and flowing areas (Figure 4.8). Individual wetted width measurements were added together and multiplied by the width of the subsection to determine the wetted area of each subsection. The total wetted area was then determined by cumulating the area of each subsection.

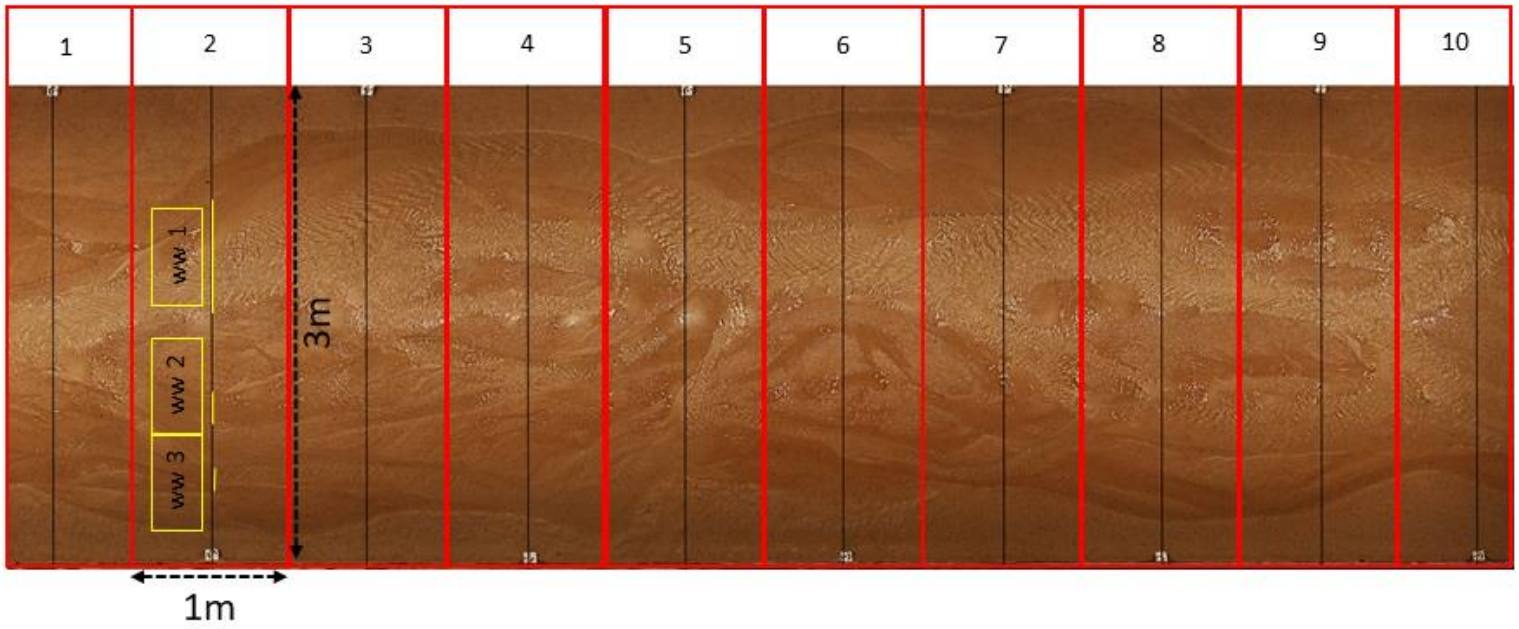

Figure 4.8: An example of a cropped ortho-image from the flume with the 1m sub sections outlined in red with the wetted width measurement made from the cross section outlined in black.

4.5.2 Measurement of Morphological Change

DEM plots from the beginning and end of each hydrograph experiment were used to determine the morphological change produced throughout an entire daily hydrograph experimental run. DEMs were subtracted from one another to determine areas of erosion and deposition, providing an estimate of the total volume of morphological change (Figure 4.9). The generation of DoD plots also allowed areas of erosion and deposition to be related to known areas of planform change.

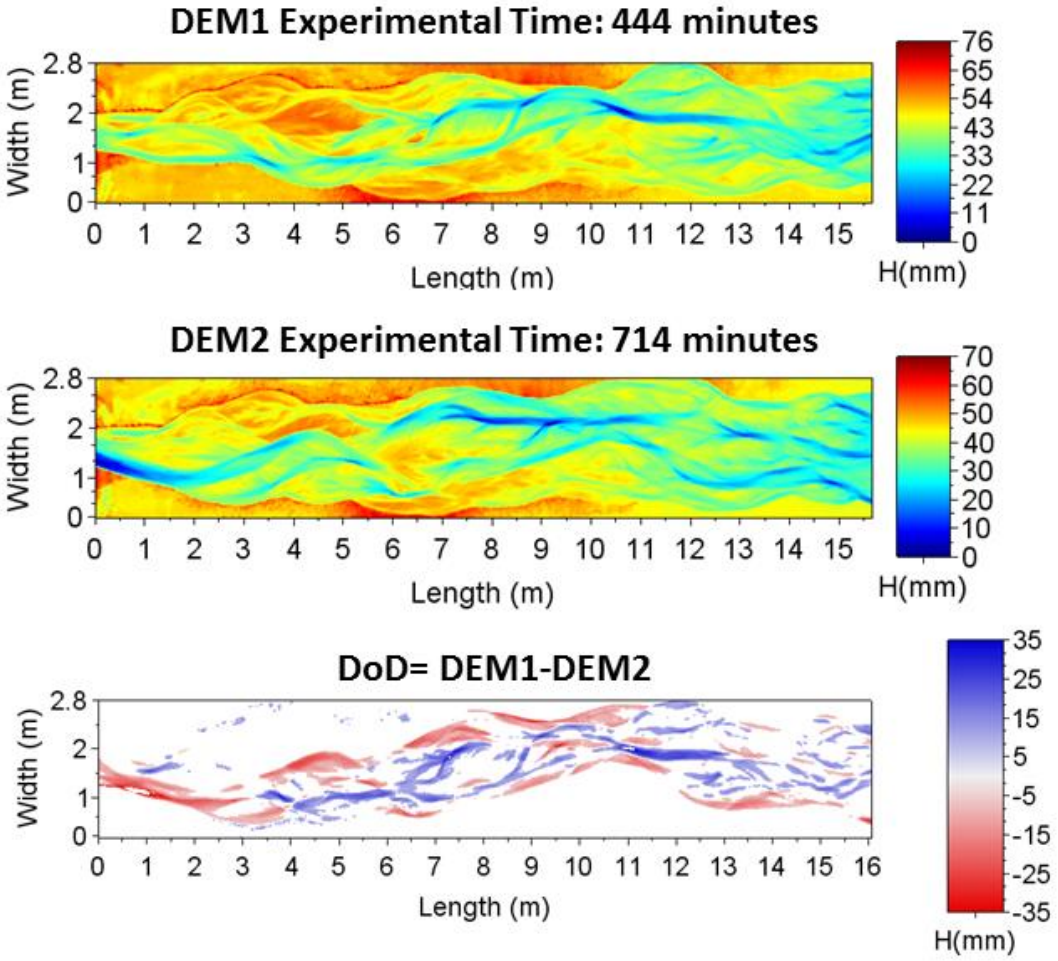

Figure 4.9: An example of a DEM and DoD generated from hydrograph experiment runs with the dry bed at the beginning and end of hydrograph experiment 3 seen in DEM1 and DEM2 respectively. The subtraction of these two subsequent DEMs produces a DoD, showing morphological change in the areas of erosion (red) and deposition (blue).

4.5.3 Measurement of Bedload Transport

Bedload samples were stored and later dried after completion of the experiments. These dried samples were then all weighed and sieved to determine the weight and particle size distribution. Samples were sieved using a mesh size of 0.25mm to 5.6mm (intervals of 0.5 phi). Results were plotted and analyzed using the open-source grain-size distribution software program GRADISTAT to show the full size distribution and determine particle size for the D_{10}, D_{50} and D_{90} percentiles.

Chapter 5

5 Field Results

5.1 Description of Data

Data was collected throughout the entire summer melt-water periods of 2012 and 2013 to ensure a full range of discharges and a complete record of all channel planform changes. Time-lapse images were analyzed to determine the amount of channel planform change the river experienced over different flow periods and the discharges above which channel planform change began. 15-minute discharge values during this time ranged from 1.1 m^3s^{-1} to over 21 m^3s^{-1}.

5.2 Analysis of Sunwapta River Discharge

The discharge record of the Sunwapta River was analyzed in Middleton (2015) to establish the representativeness of the years 2012 and 2013, to show the similarity between the two years and to determine the relationship between total and maximum daily flow. The WSC gauge has historical data dating back to 1948 with 60 years of record available, a gap exists from 1997-2005 when the gauge was not operating. The discharge record is seasonal, covering May to October and is the longest discharge record of a proglacial river in Canada. The annual instantaneous maximum discharge from 1948-2012 shows a median value of 11 m^3s^{-1} equal to approximately 18 m^3s^{-1} at the study reach (Figure 5.1). 2012 and 2013 are both representative years of the known historical flows on the Sunwapta with annual instantaneous maximum discharges at the study reach of 21 m^3s^{-1} in 2012 and 19 m^3s^{-1} in 2013. Previous research found that while the mean annual flow from June to September increased significantly from 1951 to 1996, there was no significant trend in the daily peak discharge values (Haines, 2012). The increase in the total volume of flow is likely due to the increased contribution of glacial meltwater, increasing the potential for the number of days that can produce planimetric change. While the number of days with planform change may have increased through the historical record, the peak discharge values capable of producing change on a daily hydrograph period have remained relatively the same.

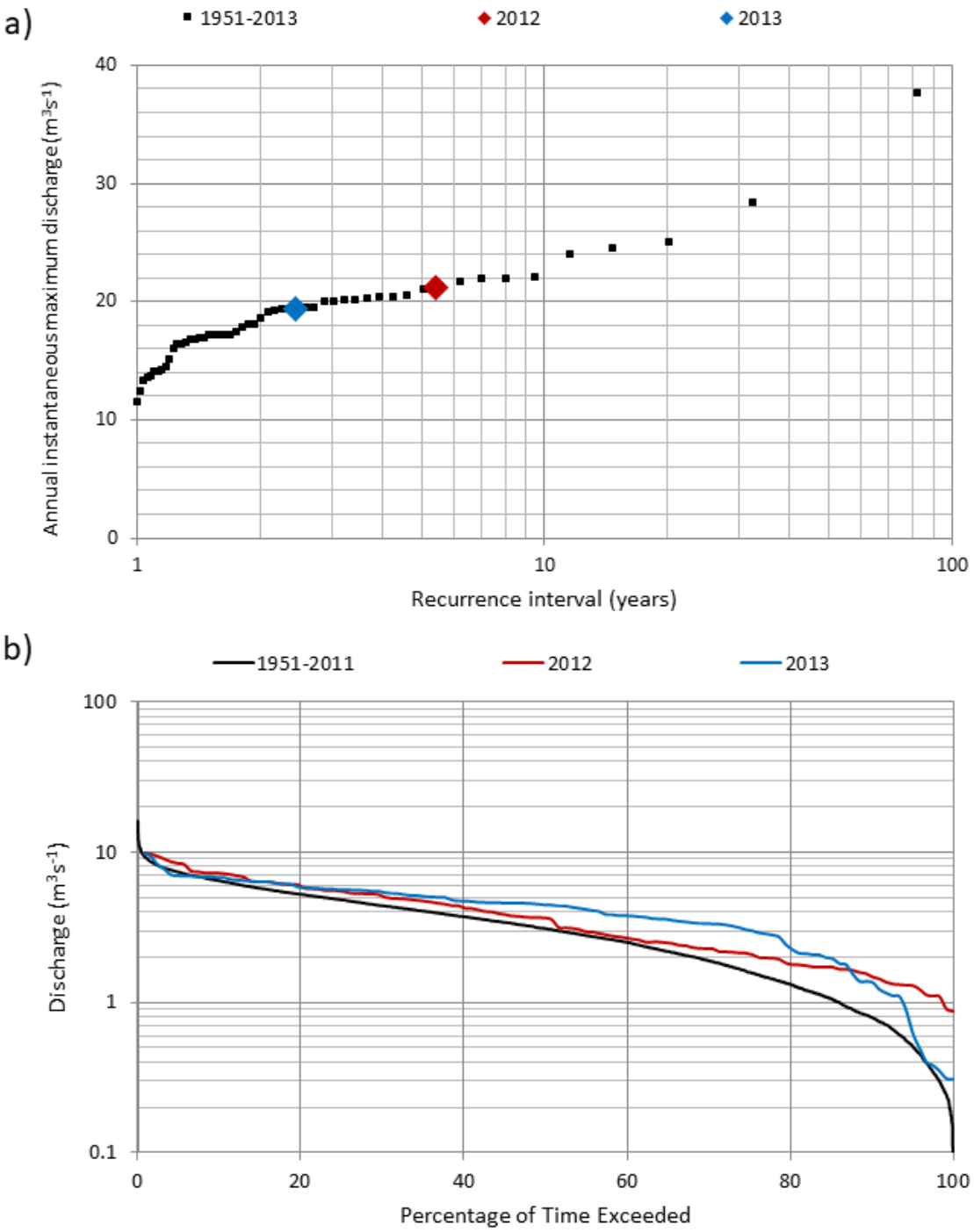

Figure 5.1: The analysis of Sunwapta discharge, (a) the recurrence interval of historical peak discharges at the WSC gauge and (b) the historical flow duration curve.

2012 and 2013 discharges appear to be above average overall compared to historical data, seen mainly in the increase in moderate flows. This may be due to the increased contribution of glacial

water but these moderate flows are seen to carry out little planimetric change (see below). The maximum discharges which produce channel planform change are very typical of an average flow year on the Sunwapta, lying below the historical maximum flows and in line with the average peak flows.

Both 2012 and 2013 also cover the full range of discharges, ranging from 1.1 m^3s^{-1} to over 21 m^3s^{-1} with some differences in timing of the highest flows during meltwater season (Figure 5.2). These stage differences are evident in time-lapse images as the river bed becomes increasingly inundated at higher discharges, discussed further below in the analysis of planform change in relation to the wetted area. Overall 2012 recorded more of the highest peak flow days, with nine days exceeding 17 m^3s^{-1} and with only three recorded in 2013. In 2013 all three high flow days were in the first week of July. In 2012 the highest peak flow days occurred at the beginning of August. 2012 also recorded slightly higher maximum discharges with the highest peak recorded exceeding 21 m^3s^{-1} compared to 19.4 m^3s^{-1} in 2013. 2012 saw flows greatly reduce in September while 2013 had flows sustained until the last week on record in late September. The time of occurrence and number of days capable of producing change differed between years but the range of flows was similar.

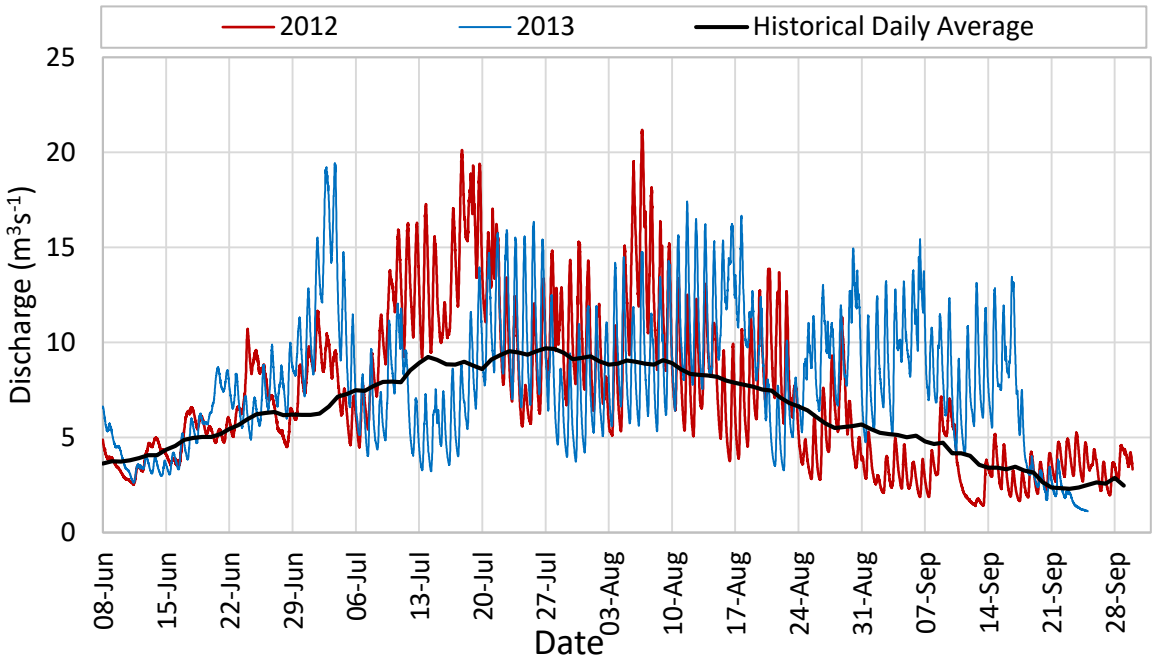

Figure 5.2: 15-minute discharge readings for the study periods of 2012 and 2013 in relation to the daily average historical values.

For a given slope, discharge is an index of the amount of total stream power (rate of energy expenditure) available to drive bedload transport and channel planform change. Two different measures of discharge were used to correlate with rates of channel pattern change. 1.maximum discharge that occurred during a daily hydrograph, 2. flow volume for a 24-hour hydrograph (total energy expended) (Figure 5.3). The two different measures allowed rates of planform change to be related to the magnitude of flow as well as the quantity of flow over a hydrograph period (Haschenburger, 2013; Papangelakis & Hassan, 2016). In a proglacial river daily hydrographs all have a similar shape and time base (Figure 5.4) and consequently peak discharge and total discharge are strongly correlated. Daily hydrographs in these rivers are seen to fluctuate with changes in air temperature with previous research showing this relationship for the Sunwapta River during the study period (Figure 5.5) (Middleton, 2015). Median time of minimum and maximum flows is found to occur at 08:30 and 17:30 respectively.

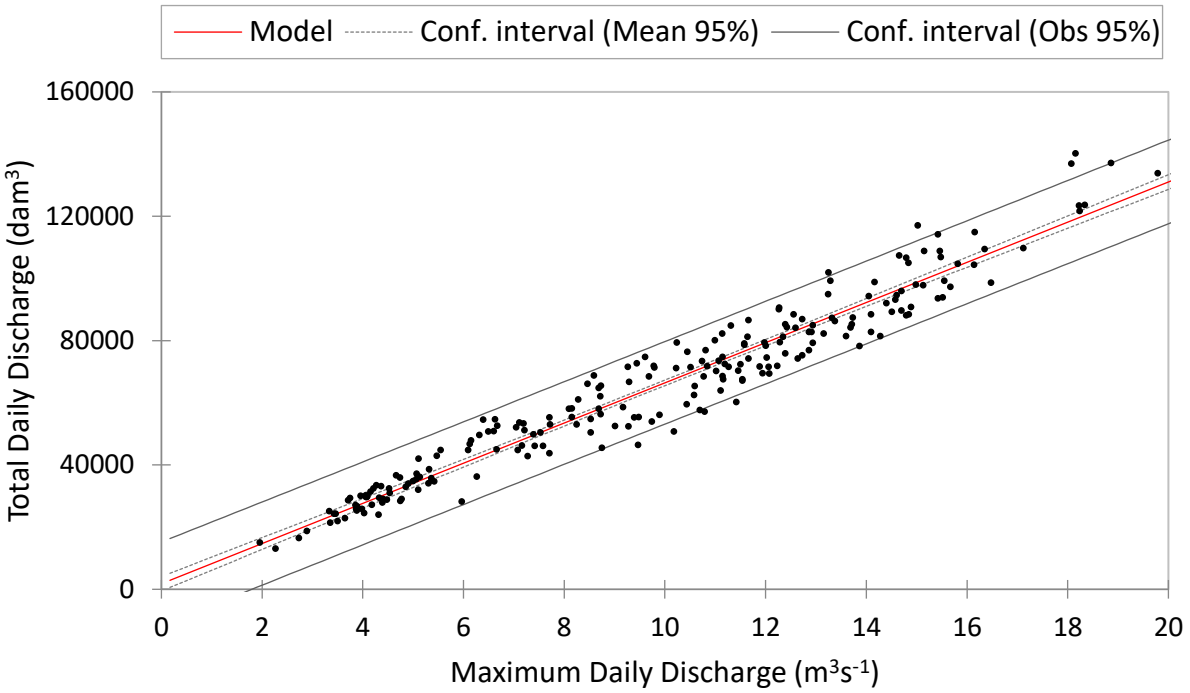

Figure 5.3: The relationship between the maximum and total discharge values for June to September 2012 and 2013.

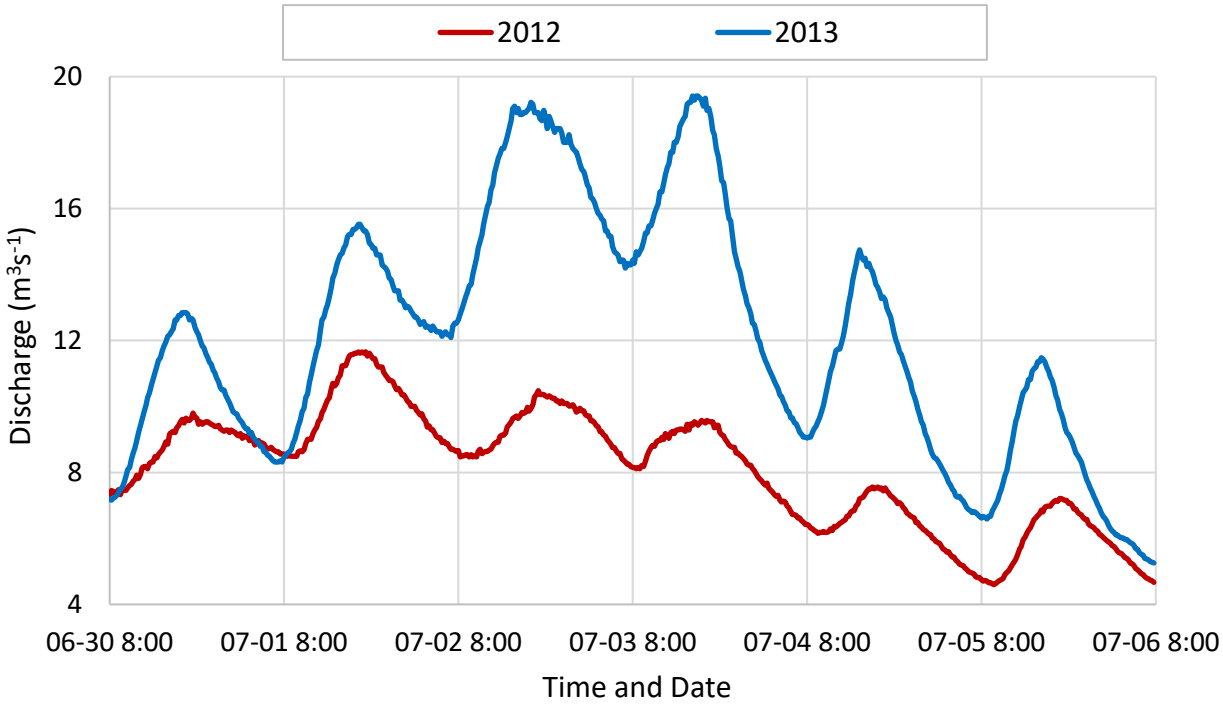

Figure 5.4: An example of a sequence of typical daily hydrographs.

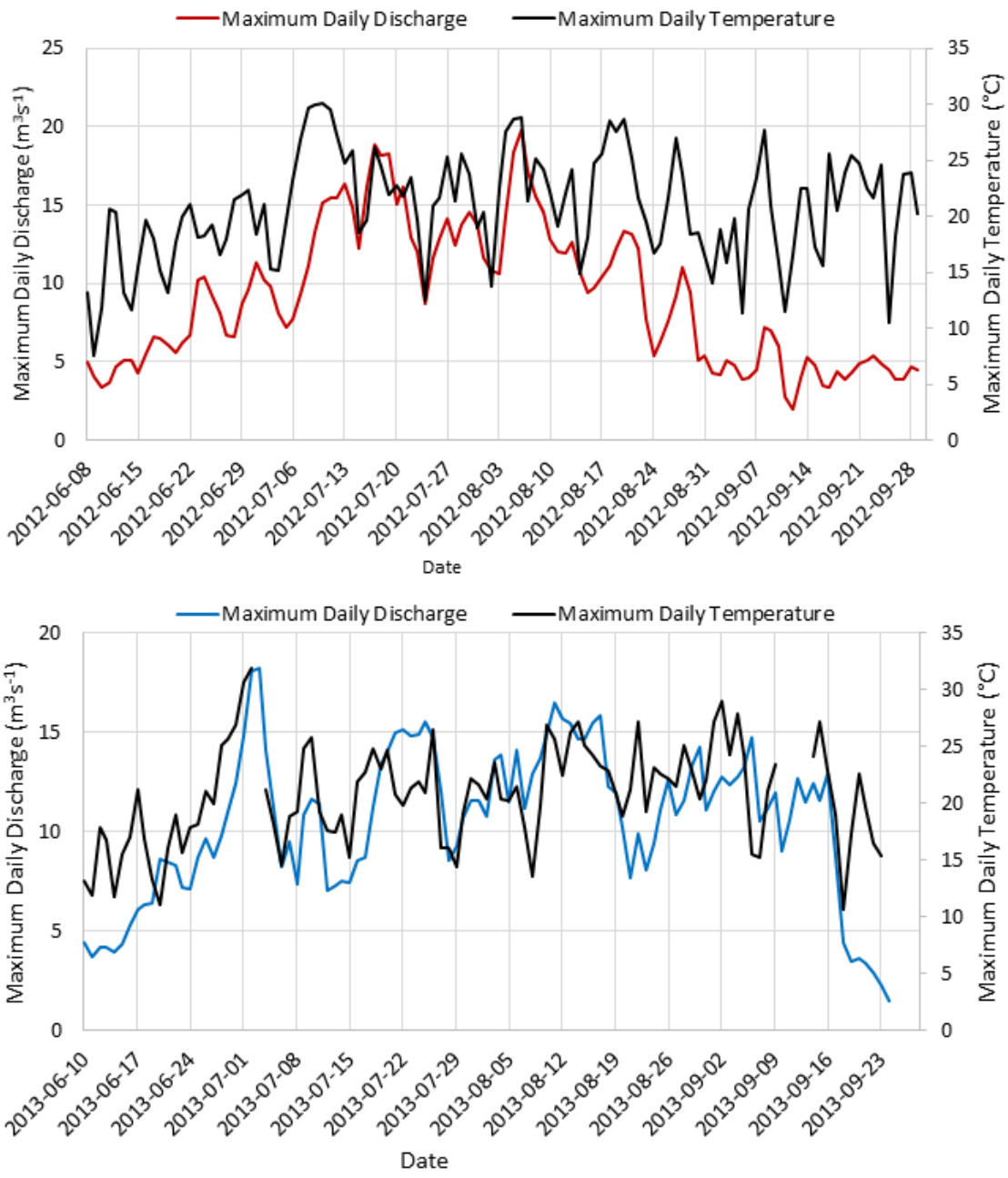

Figure 5.5: The relationship between discharge and temperature for the 2012 and 2013 study periods with air temperature measured at the Nordegg Climate Station.

5.3 Analysis of Sunwapta River Channel Planform Change

Previous research (Middleton, 2015) analyzed changes in the river planform over the same daily hydrograph periods. This analysis measured area of change by counting the number of grid squares showing differences between successive daily low flow times. Change was identified as a change from water to gravel, or from gravel to water, within the gird square. The grid square count was recorded as a proportion of the total bed area covered by the measurement grid. This gave an index of relative area of change but did not give an accurate area of change. The analysis showed that no extensive planform change occurred below 11 m^3s^{-1} and that above this discharge the daily area of change increased but with great variability including days of no change occurring (Figure 5.6b, 5.7b). Consistent planform change was recorded at peak discharges that exceeded 16 m^3s^{-1} but was still found to be variable.

Each daily hydrograph was reanalyzed for this study, for a total of 216 daily measurements of planform change completed to better-estimate the days of no change and provide a more accurate and precise measurement of the total area of change. In general, the reanalysis resulted in fewer days with measurable planform change and lower values of area of planform change when it did occur (Figure 5.6, 5.7). This was especially true for 2013 where small amounts of change were recorded on multiple days with lower discharges during the 2015 analysis (Figure 5.6 b). This difference is partly because re-examination of the images resulted in several days in which changes that had been recorded in the grid analysis were not changes in planform (bed erosion/deposition) but apparent changes caused by slight differences in water stage and flow distribution between days (Figure 5.6c) which could be attributed to stage differences and were recorded as zero change days when reanalyzed (Figure 5.6c). Both methods used to analyze changes throughout the entire season recorded the highest rate of planform change in the first high flow period the river experienced each year (Figure 5.6, 5.7). In 2012 the planform was altered once more following this, in August, while in 2013 only small areas of change were recorded after the first high flow period in July.

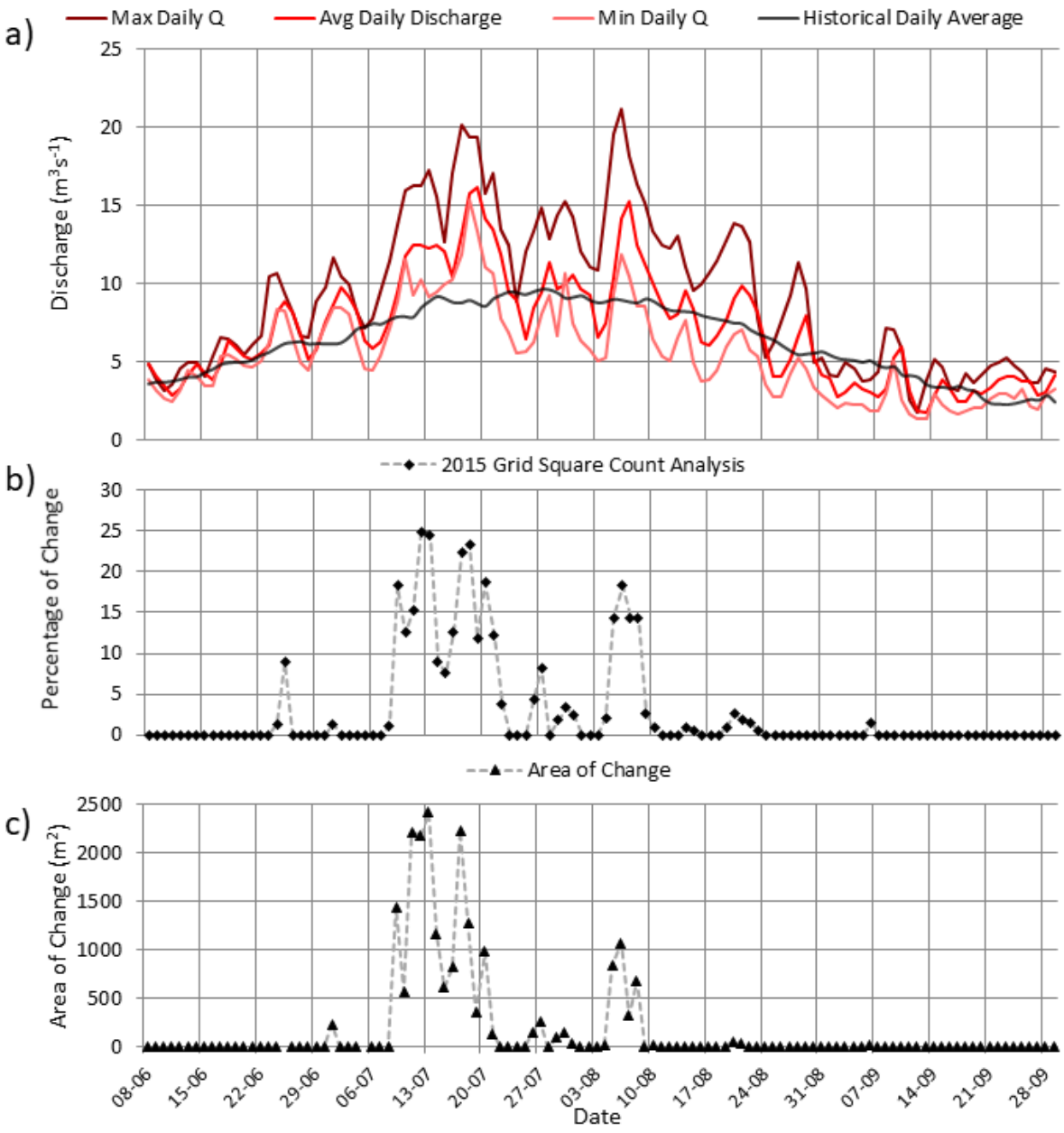

Figure 5.6: The (a) minimum, average, maximum and historical discharge values for 2012 in relation to the measurements of planform change, (b) 2015 grid square analysis of planform change, and (c) the revised and re-analyzed measurements of the area of planform change.

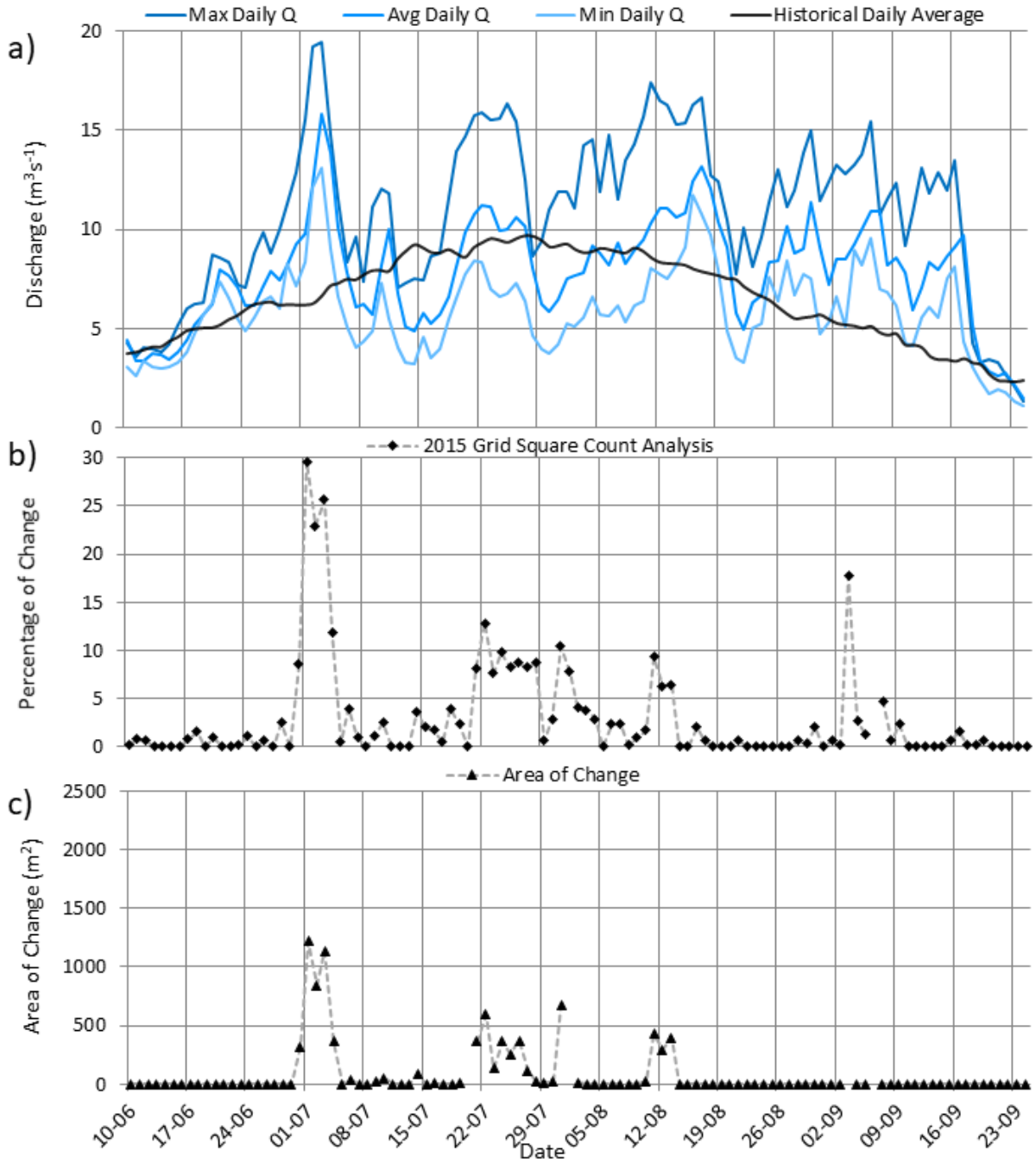

Figure 5.7: The (a) minimum, average, maximum and historical discharge values for 2013 in relation to the measurements of planform change, (b) 2015 grid square analysis of planform change, and (c) the revised and re-analyzed measurements of the area of planform change.

The reanalysis of daily planform changes increased the accuracy of measurements of planform change but the overall relationship with discharge was similar to the results of the previous grid square analysis (Middleton, 2015) (Figure 5.8). The increased accuracy of measurements was most evident at lower peak discharges where peak discharges of $11m^3s^{-1}$ and less were found to produce limited areas of planform change, with the majority of days having no observable areas of planform change (Figure 5.9a). These lower measurements (n=117) were found to be significantly correlated with a slope of zero, showing the high probability of planform change not occurring (Pearson's Correlation: 1) with the summary statistics provided in Appendix E. Discharges exceeding 11 m^3s^{-1} showed an increased ability to produce areas of planform change but this relationship was very variable and not found to be significant (Figure 5.9b).

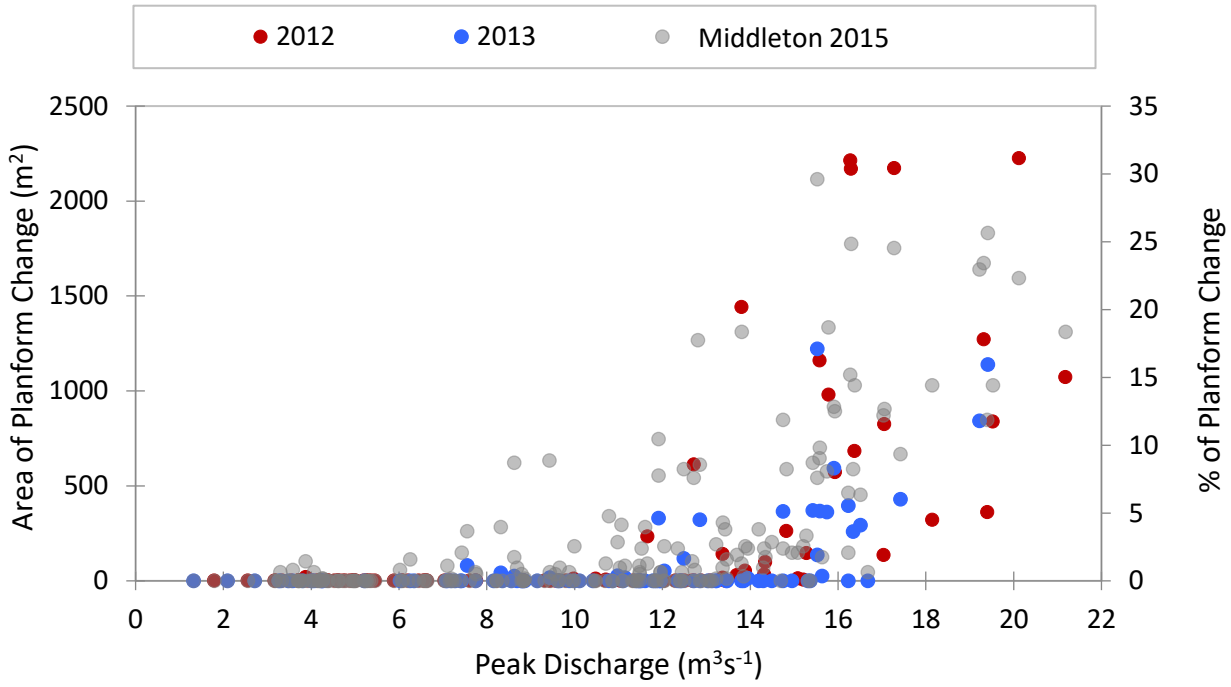

Figure 5.8: The relationship between planform change and discharge produced using the manual image analysis method and results from Middleton, 2015.

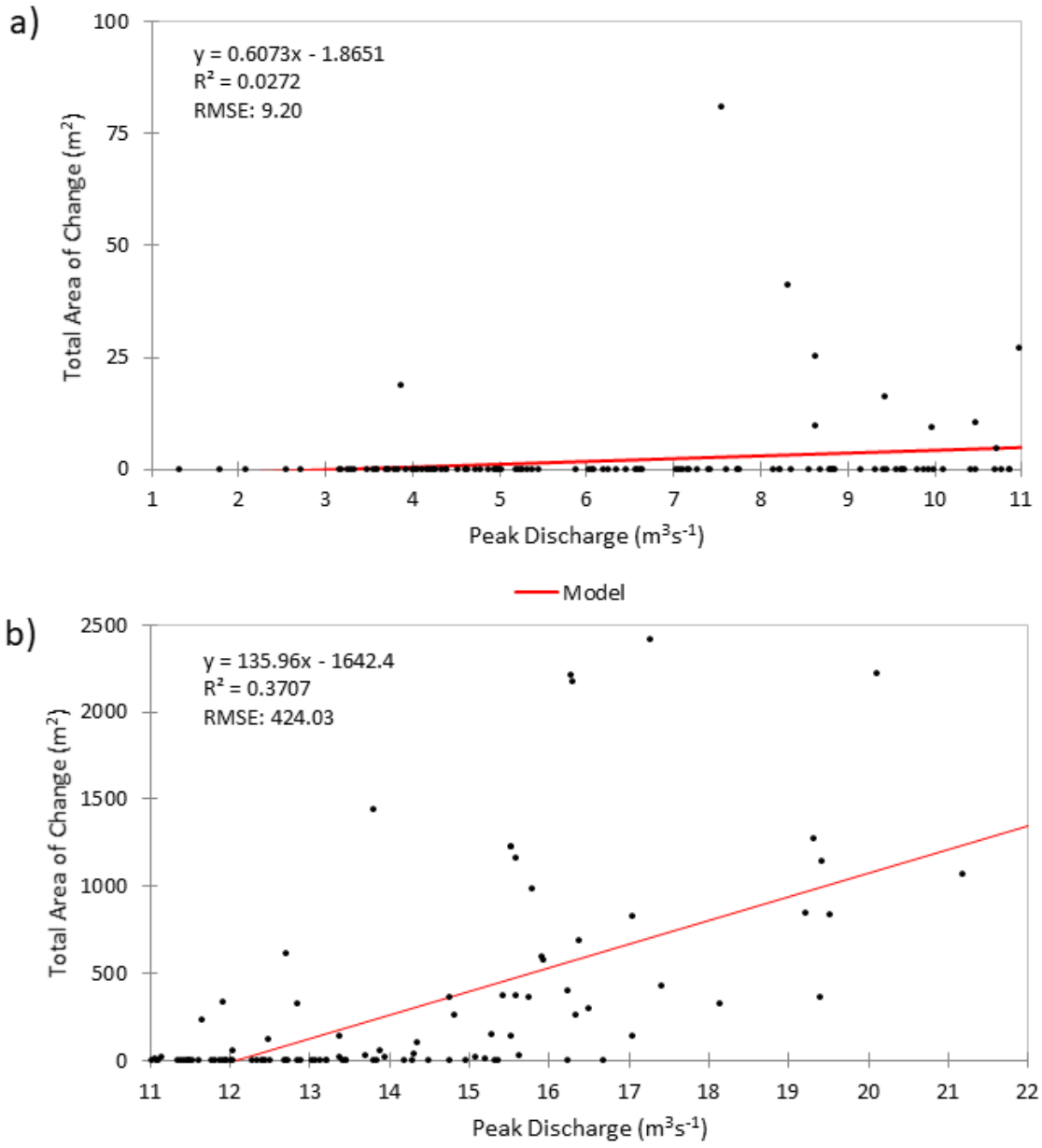

Figure 5.9: The relationship between two discharge groups, (a) 11m^{3}s^{-1} and less and (b) greater than 11m^{3}s^{-1}with a linear function fitted as an initial description of trends.

The styles of planform change experienced during this study period are discussed fully in Middleton (2015). Only minor changes were recorded in the channel planform at peak discharges below 14 m^{3}s^{-1} (Figure 5.10). Minor changes included small areas of bar and bank erosion (Figure 5.10) potentially leading to the lateral migration of the channel in areas (Figure 5.11). These minor changes were recorded at higher daily peak discharges as well but were the lowest amount of change recorded with the large alterations in the river planform also recorded (Figure 5.12). Large

changes were recorded when the planform was altered across the entire width surveyed, seen through channel avulsion, confluence shifting, channel expansion and migration, and large areas of bar erosion and deposition (Figure 5.12).

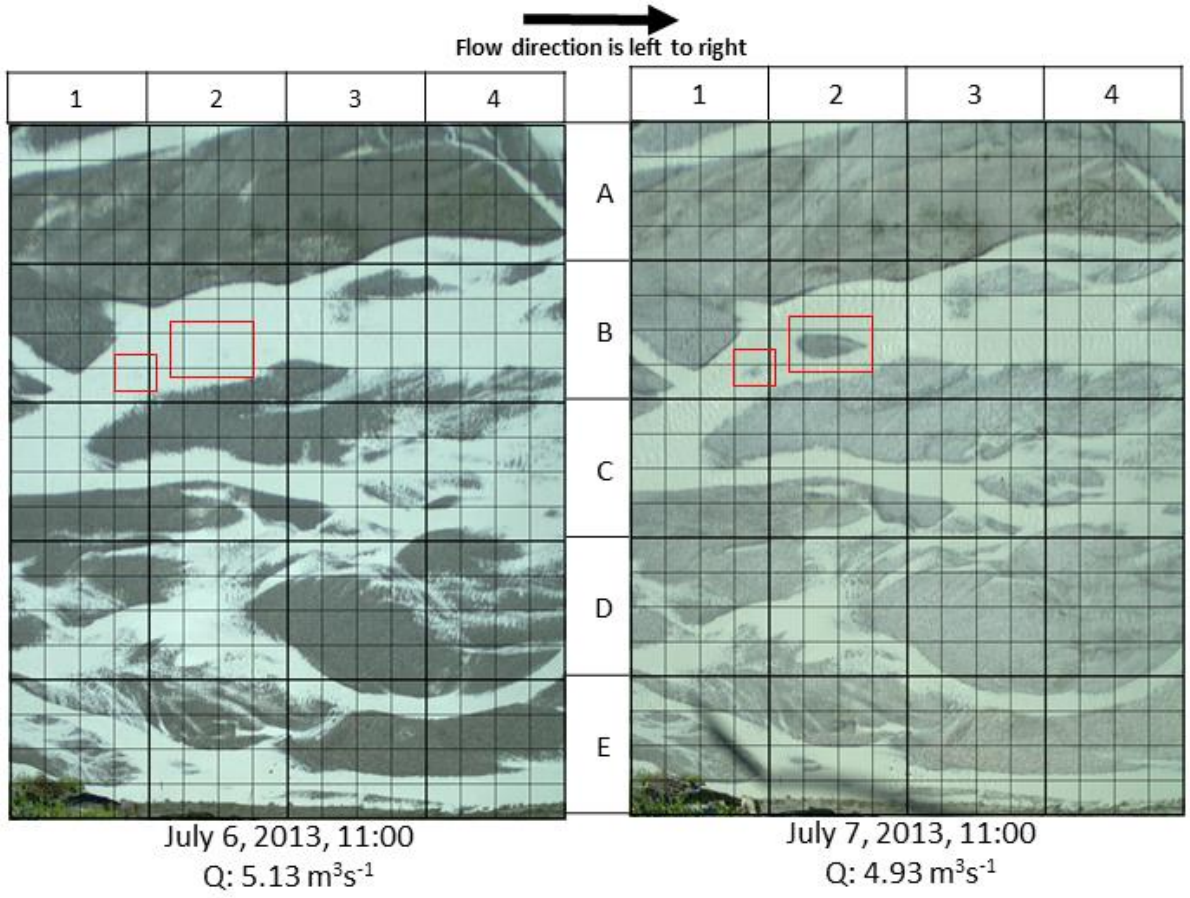

Figure 5.10: An example of small area of planform change recorded at a lower discharge analyzed, maximum discharge is 8.32 m^3s^{-1}. The small amount of change is indicated in the two red boxes where the deposition of sediment is evident, beginning a new braid bar.

Figure 5.11 documents the area of planform change observed on July 22-23 2013 in relation to a peak discharge of almost 16 m^3s^{-1}. Only the primary channel underwent a planform change, outlined in red with the lateral migration of the two channels seen. This is due to the deposition of material on the braid bar, adjusting the position of the channels flowing around the bar.

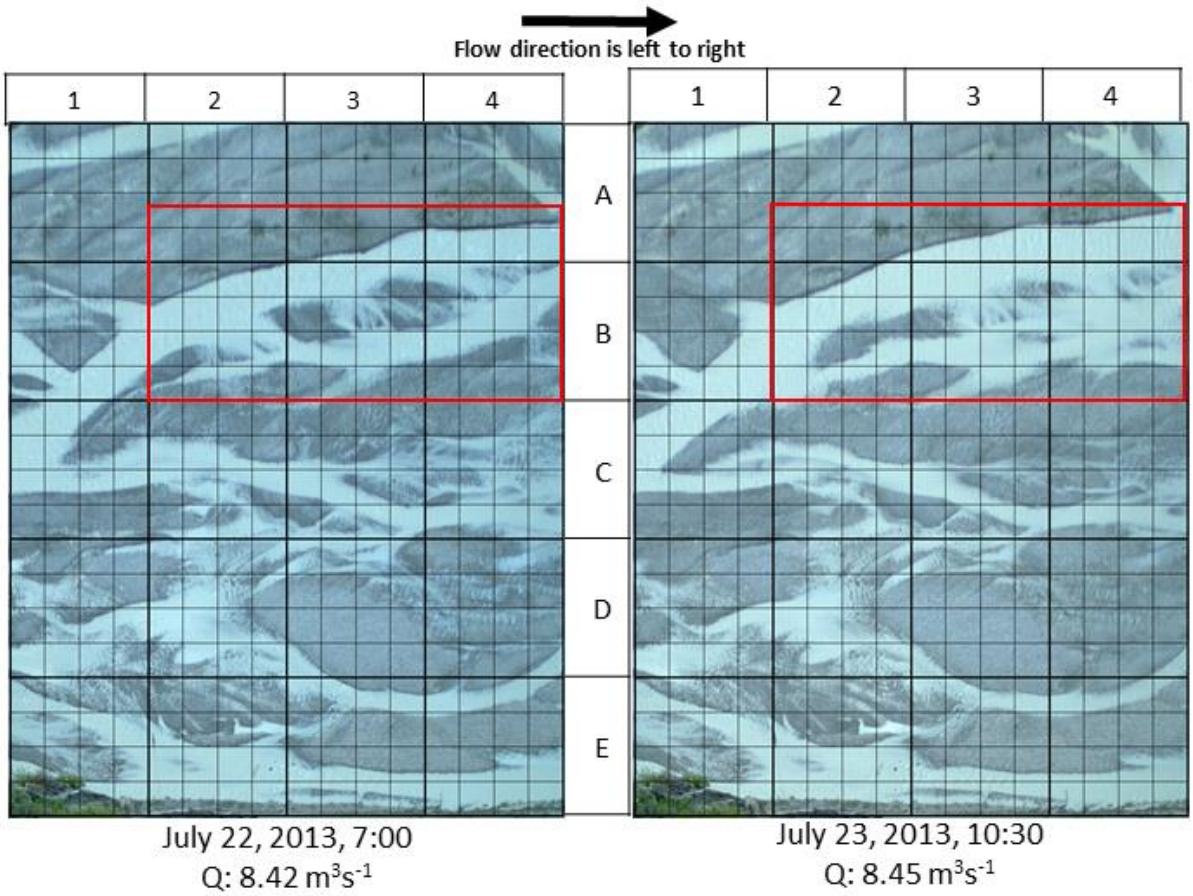

Figure 5.11: An example of small area of planform change recorded at a higher peak discharge analyzed (15.91 m^3s^{-1}).

Figure 5.12 shows the highest rates of planform change recorded during the 2013 melt water period, from July 1-2 documenting the potential for higher discharges to completely alter the overall planform configuration. The primary channel outlined in red underwent extensive planform change, with parts of a head and tail end of a braid bar seen in B-C 4 and 1 respectively, partially eroded. Between these two features the channel has altered position and greatly widened. Flow appears to be more concentrated on July 1 compared to a lower stage on July 2.

Other planform changes are also evident in the secondary channel where changes upstream have led to the increase of flow in the secondary channel, highlighted in yellow.

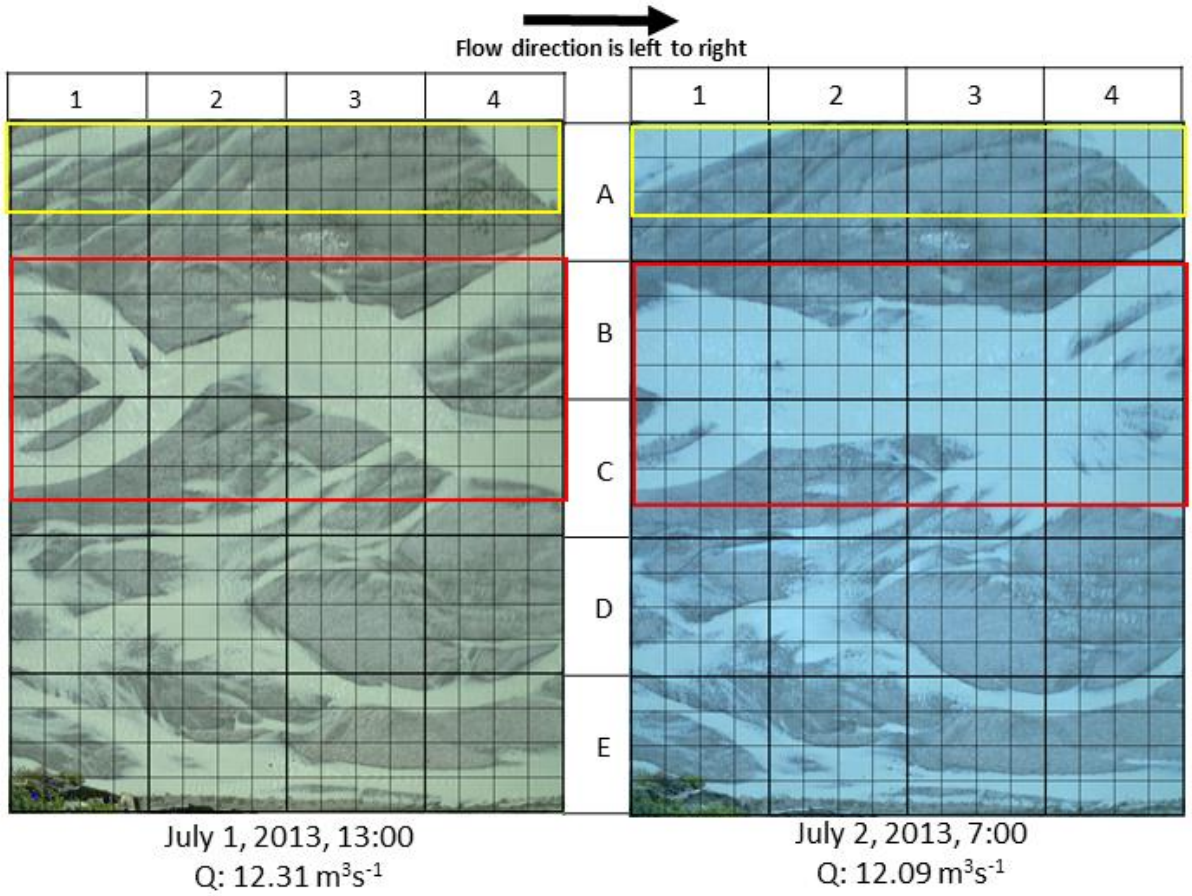

Figure 5.12: An example of a high peak (15.51 m^3s^{-1}) that resulted in large areas of planform change. This is mainly seen in the large changes in the primary channel, highlighted across the entire width in red. Smaller changes are also seen to the secondary channel.

5.4 Automated Image Analysis

The automated image analysis measurement of planform change was completed for all daily hydrographs found to have planform change from the manual analysis, as discussed in section 3.3.4. 52 measurements of daily planform change were made in total, 26 each in 2012 and 2013. Rates of planform change were found to increase (with variability) as peak discharges increased, as found in the manual measurement. The area of change measured, however, was much larger, with measurements recorded exceeding an area of 3100 m^2 (Figure 5.13) This was due to inherent

differences of field time-lapse imagery and the differences in automatic detection, discussed below. Days in which there were very small planform changes documented using manual analysis (less than 10 m^2) yielded much higher areas using automated analysis (greater than 500 m^2) (Figure 5.14).

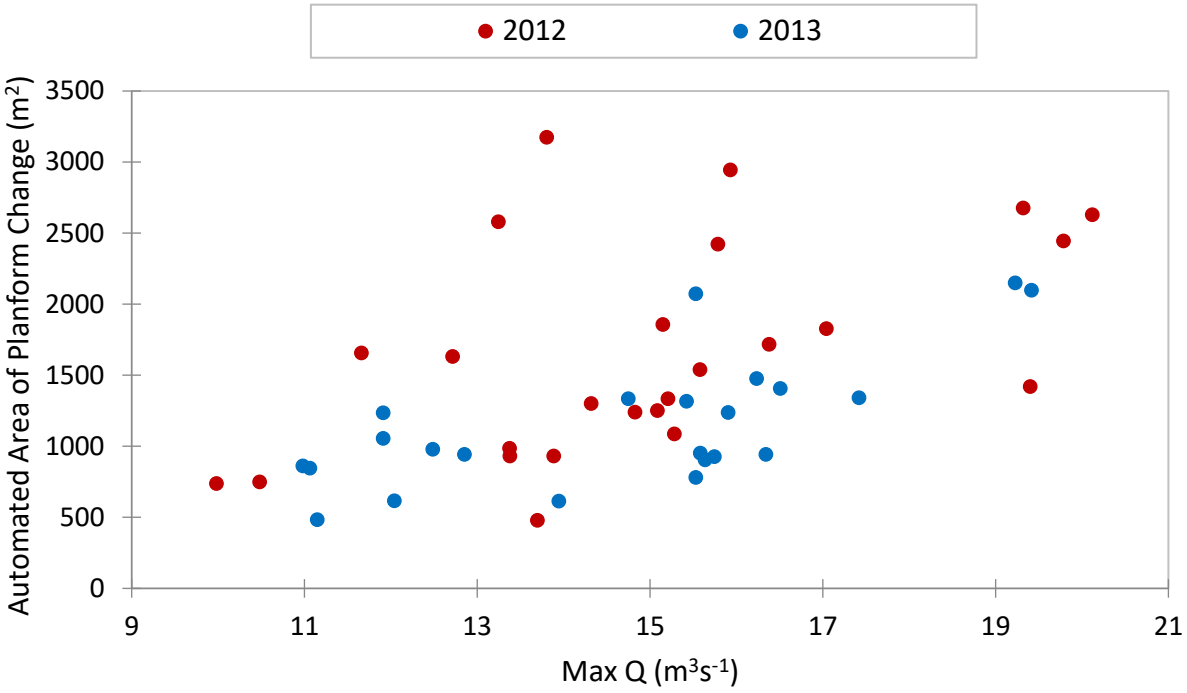

Figure 5.13: The relationship found between peak daily discharge and area of planform change using automated image analysis.

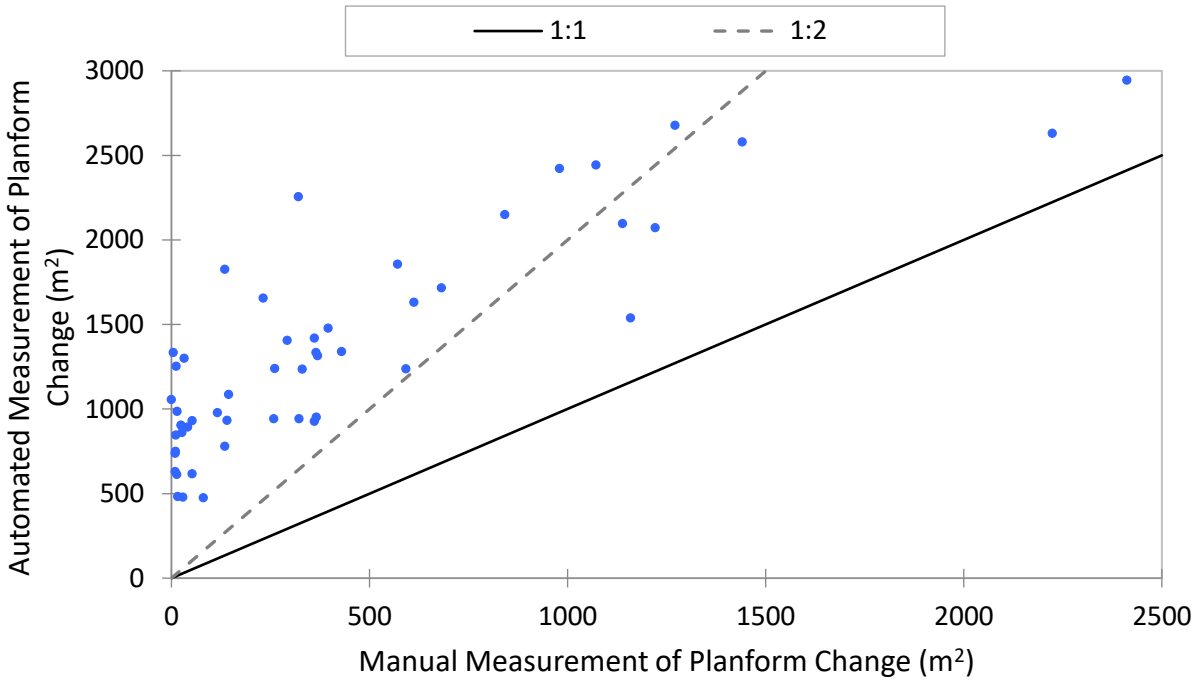

Figure 5.14: The relationship between areas of planform change documented using automated analysis and manual analysis methods.

The automated image analysis method was tested as a way of reducing the subjectivity associated with the manual analysis method. Due to the differences of lighting in a field setting and the dynamic nature of braided rivers the automated detection of areas of gravel and water was very difficult. The areas of water surface automatically detected were visually accurate but the errors occurred when subtracting two different images, leading to the large overestimation of areas of change, which were due to differences in lighting, reflections and shadows between images. The automated method was based on identifying shifts between water and gravel between subsequent images. This therefore also picked up differences in stage and the distribution of flow without any actual morphological change to the river bed, with this effect also seen in the results from Middleton (2015) (Figure 5.15). These differences in stage and distribution of flow could be assessed using the manual method, which produced a more reliable measurement (Figure 5.16). Overestimates were also seen when planimetric changes upstream altered flow to areas of the channel downstream without altering the planform position (Figure 5.17). This was observed when channel avulsion cut off flow to other channels, but there were no observable changes to the channel or bar topography. Flow was often reconnected in a short period of time as the channel

position altered again. The automated detection was useful in determining the total wetted area at different discharges and planform configuration but was not reliable in subtracting images and determining planform changes between the two images and therefore the manual analysis method preferred.

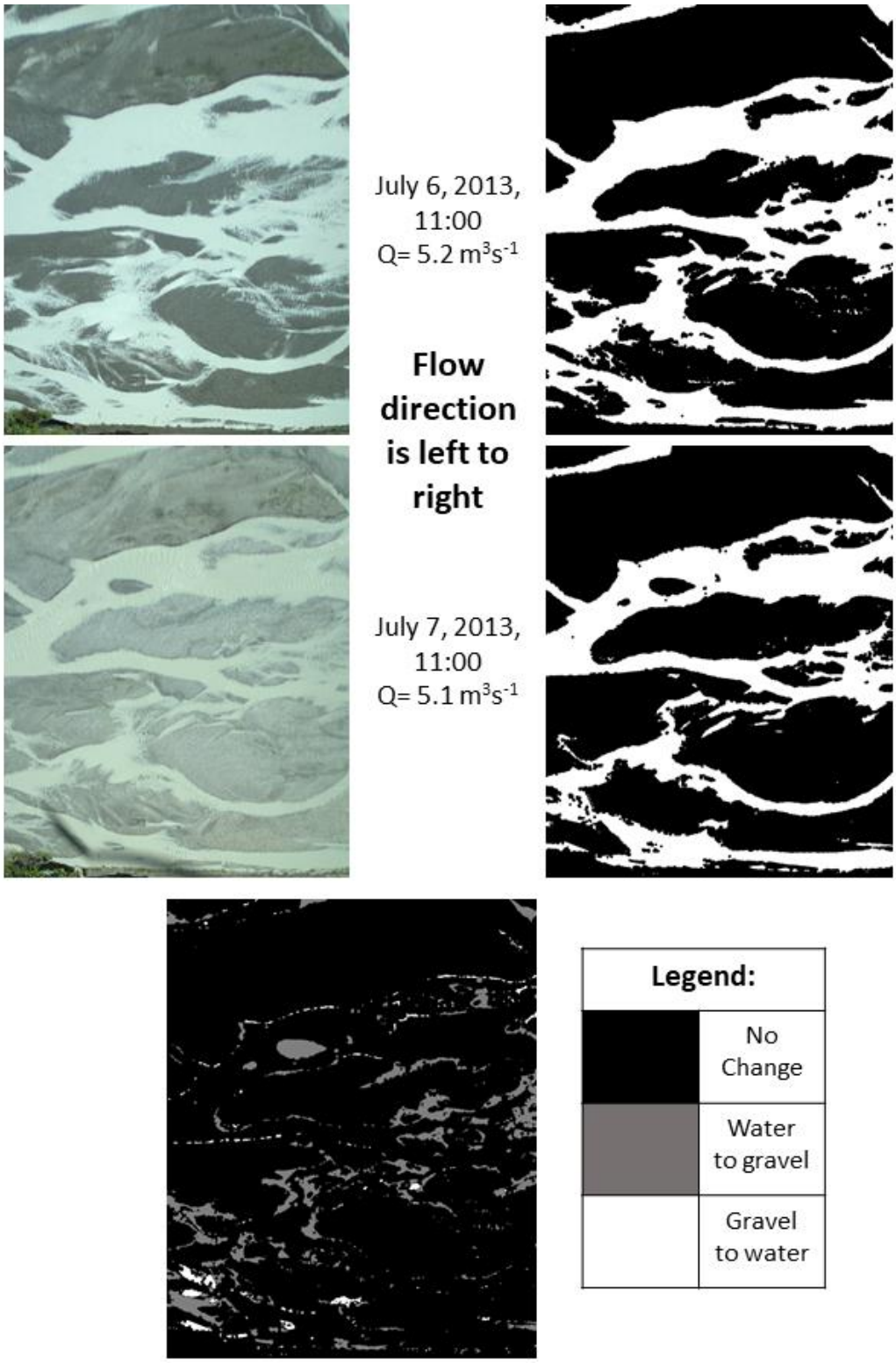

Figure 5.15: Measurement of planimetric change using automated image analysis and the different detection produced due to inherent differences in time lapse imagery.

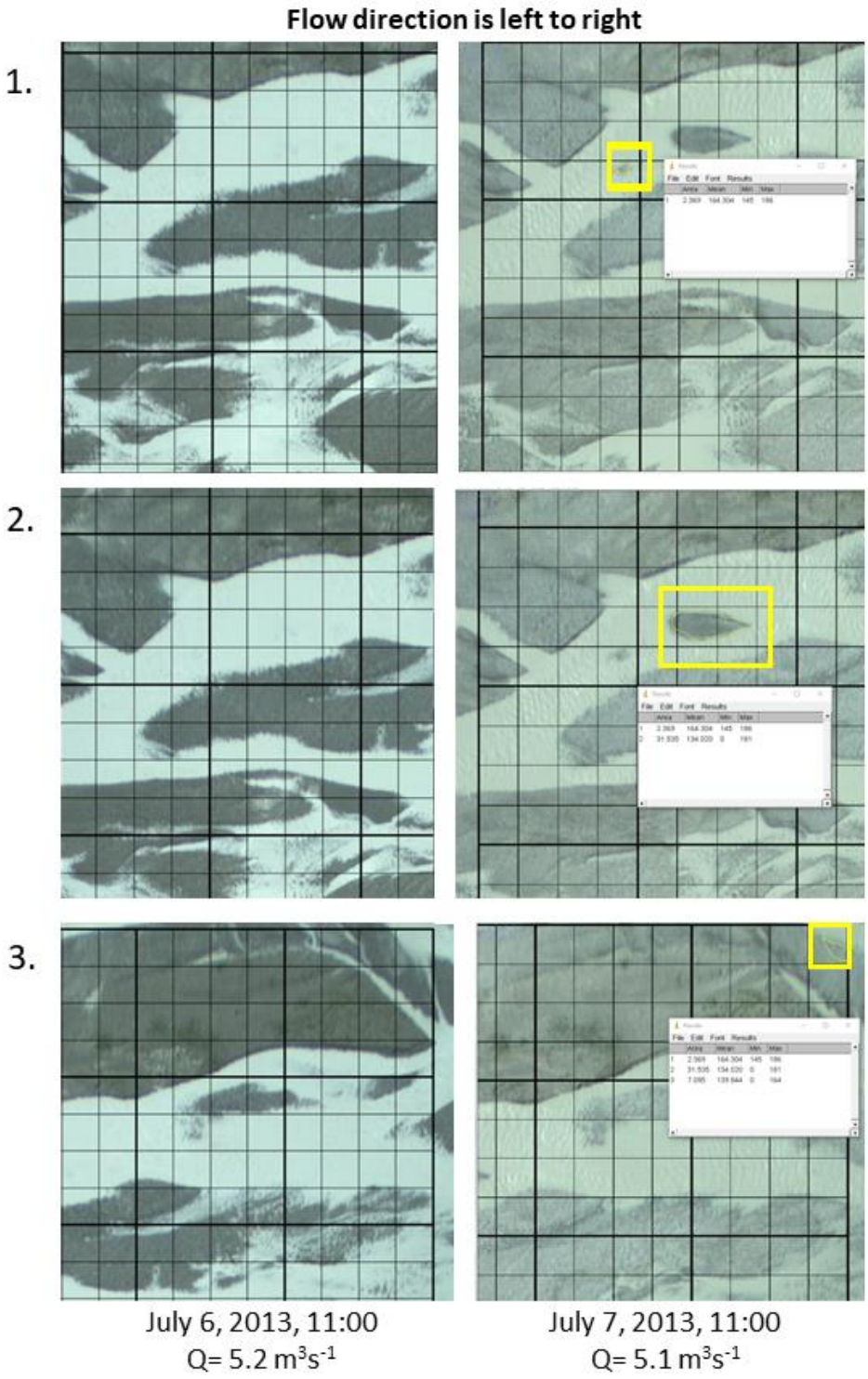

Figure 5.16: Measurement of planimetric change using manual image analysis over the same daily comparison period as the automated assessment above in Figure 5.15, with the three individual polygons digitized seen, outlined in yellow.

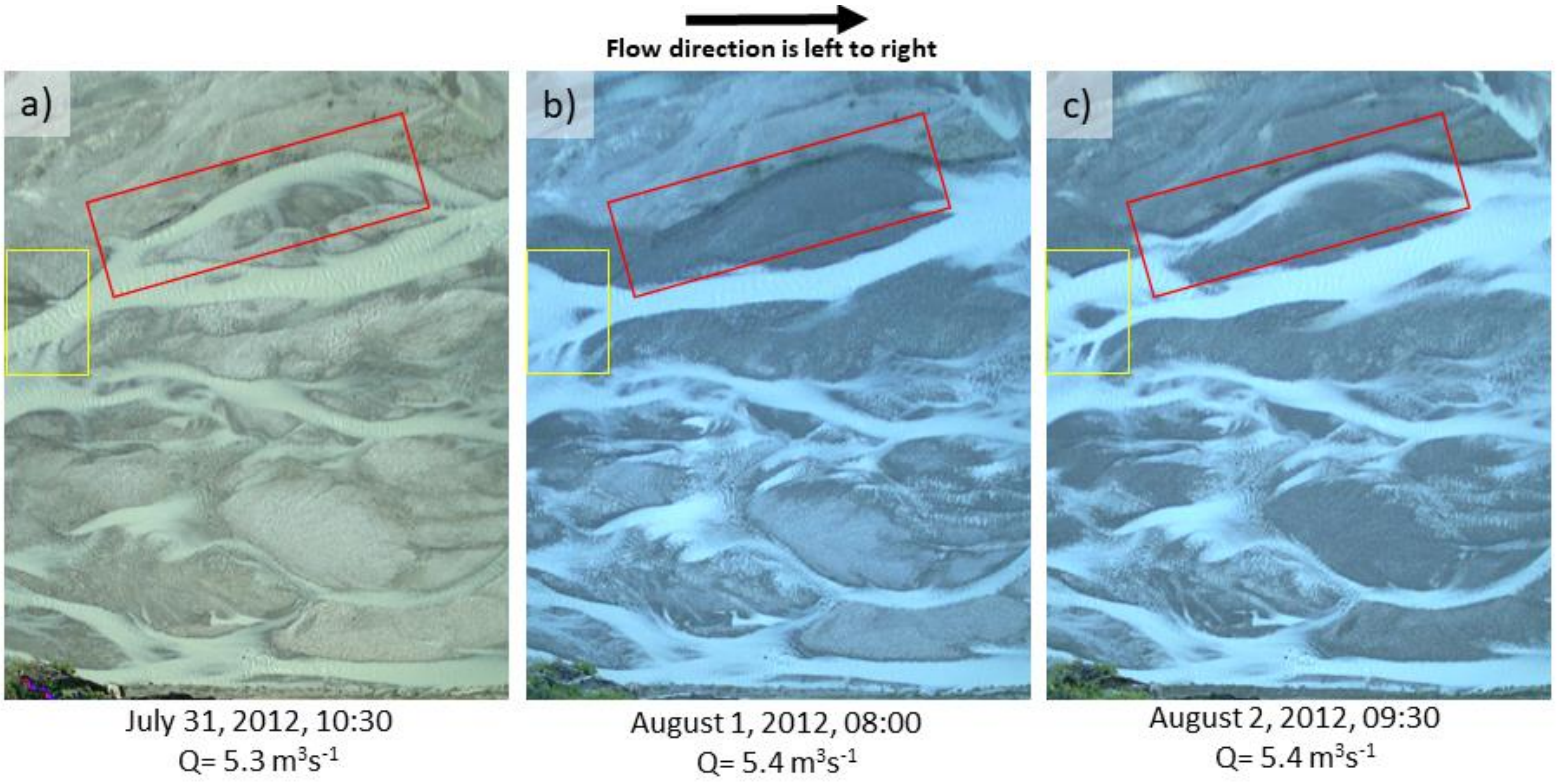

Figure 5.17: An example of channel avulsion which occurred over a daily hydrograph seen from (a) to (b) outlined in red with it reconnected in (c). A change in planform outlined in yellow lead to this channel being abandoned and reconnected within a 48-hour period.

5.5 Planform Change and Wetted Area

The wetted area was measured for peak flow for all daily hydrographs that recorded rates of planform change. Scaling area of planform change by wetted width allowed comparison with flume data as well as the potential for subsequent analyses of rivers of different sizes. 66 daily hydrograph peaks were measured, 33 in 2012 and 33 in 2013, showing that while variable the wetted area increased with discharge (Figure 5.18). 46 additional wetted area measurements were added, measured at the minimum flow for the original daily planform measurement analysis. The increase in wetted areas was obvious in images as the river bed became inundated at higher discharges (Figure 5.19).

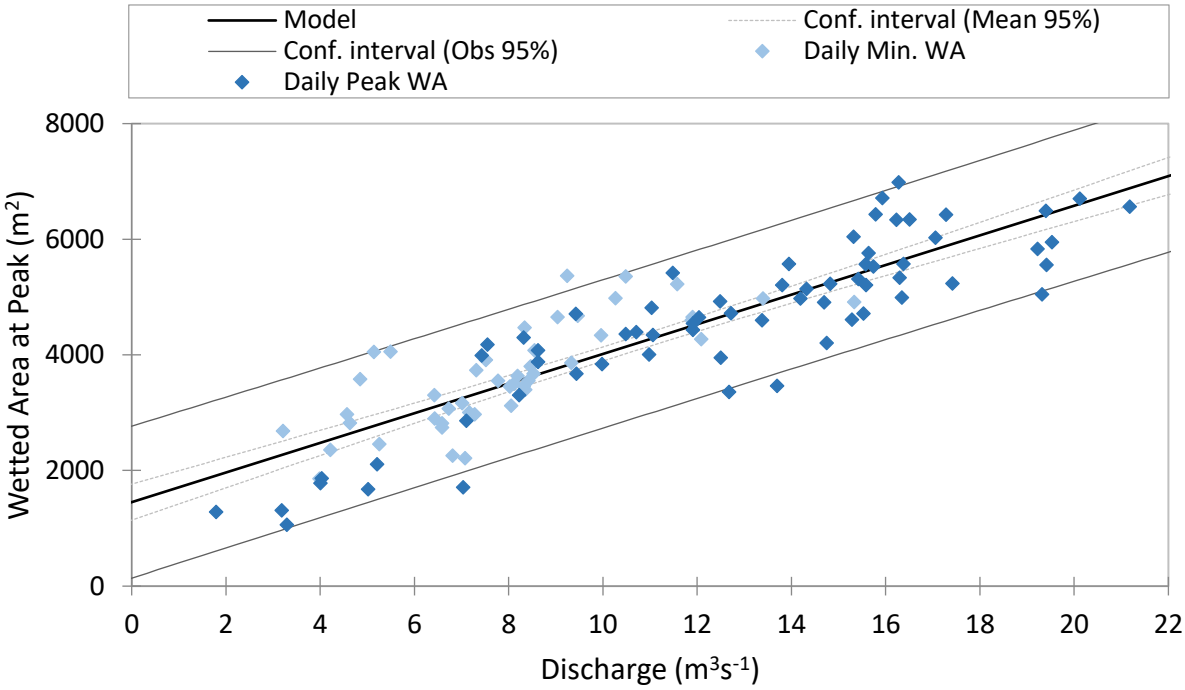

Figure 5.18: The relationship between the wetted area and discharge at the daily hydrograph peak and minimum discharges.

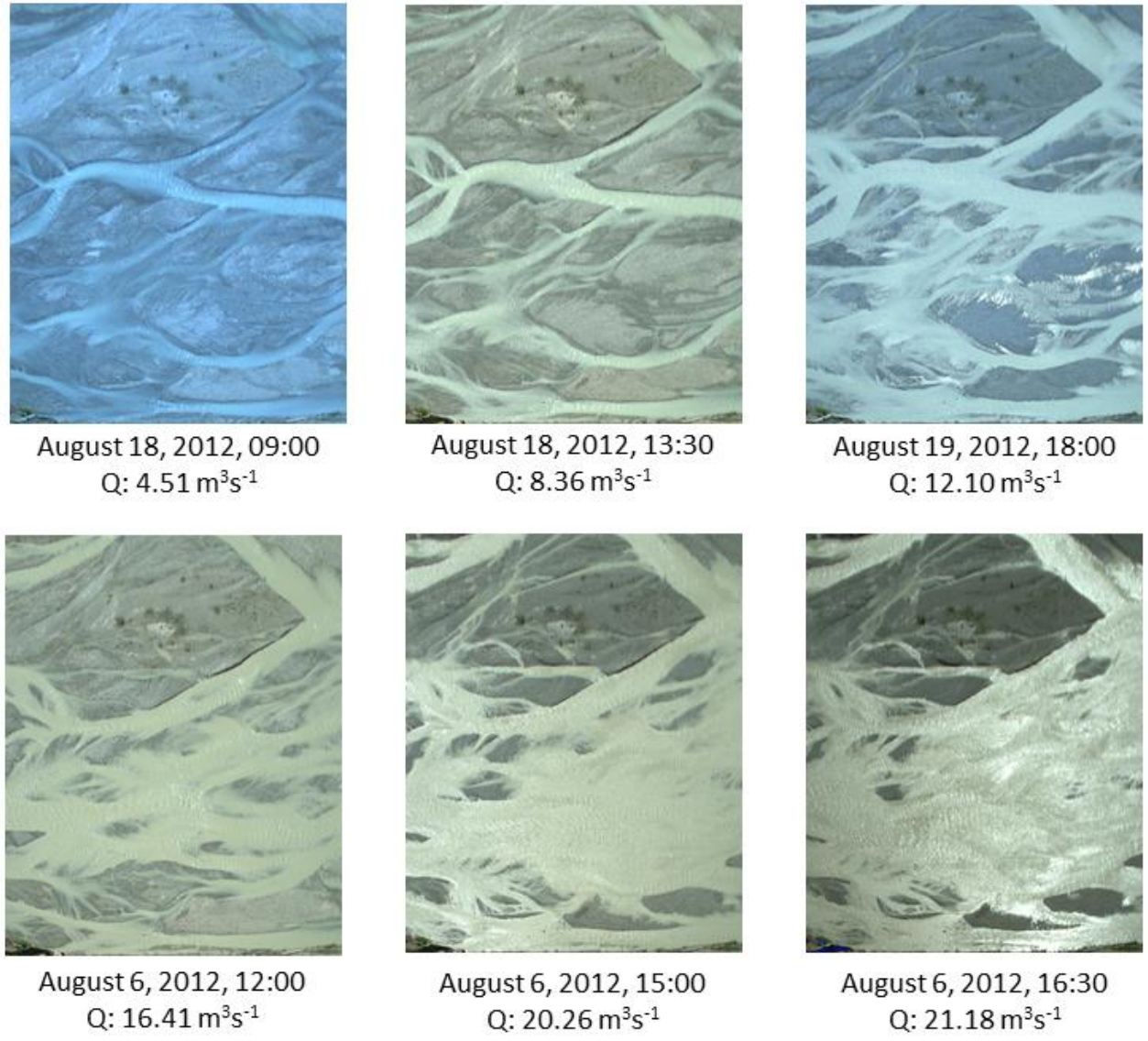

Figure 5.19: Examples of images at different stages, highlighting the increase in wetted area as discharge increases.

Area of planform change (using the manual method) as a proportion of wetted area shows considerable scatter but, visually there is an increase with increasing discharge with a maximum of 0.45 (Figure 5.20). All daily hydrographs with a peak of 14 m^3s^{-1} or less, except one, had active areas of less than 15% of the wetted area. This highlights the limited area of river bed that experiences planform change, even at the highest peak discharges and is consistent with known values of Active Braiding Intensity (ABI) which are generally low (Egozi & Ashmore 2009).

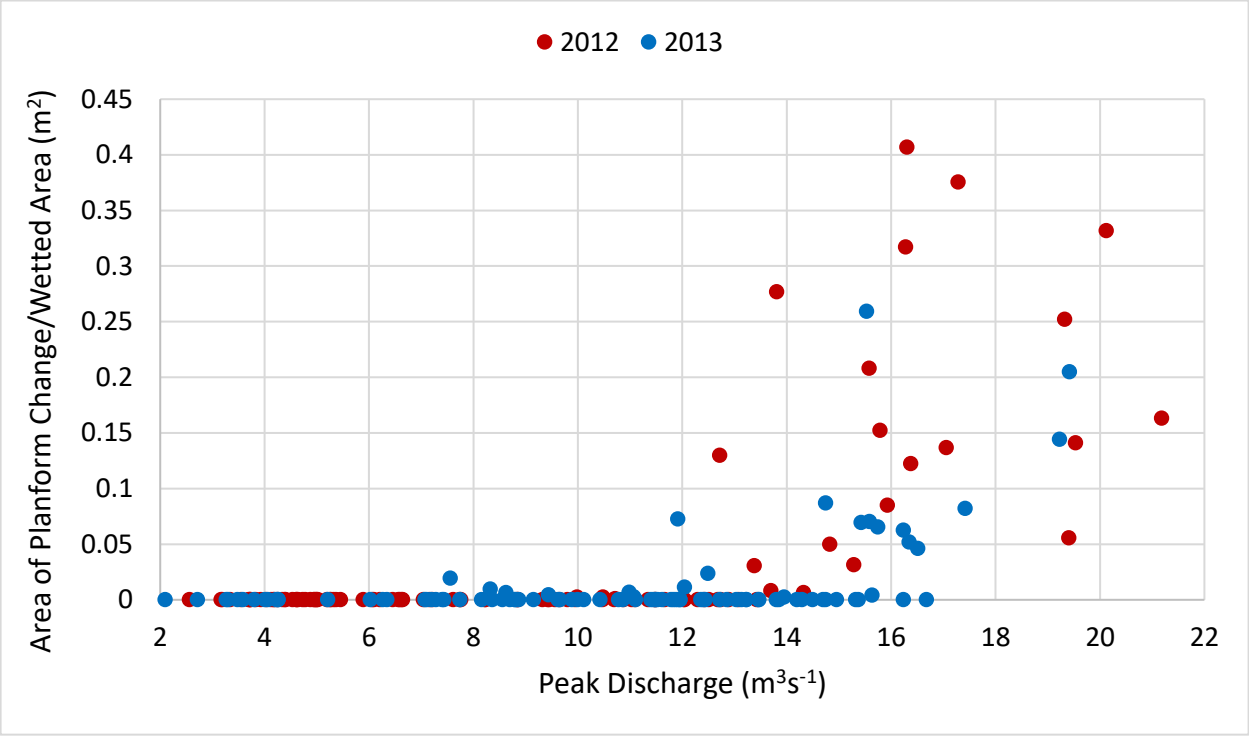

Figure 5.20: The relationship between peak discharge and the normalized area of planform change.

5.6 Field Results Summary

The reanalysis of daily hydrographs in the field using the manual method changed the results relative to the grid square analysis done previously by Middleton (2015) on the same image set. The polygon method used here eliminated some of the apparent changes due to flow stage and distribution picked up in the grid square method and gave more precise measurements. The result is a similar trend in planform change with increasing discharge, but fewer days with planform change at lower discharges, and lower overall areas of change. Results showed that areas of planform change increased in relation to an increase in discharge at discharges greater than 11 m^3s^{-}

[1], approximately consistent with Middleton (2015). Larger areas of channel planform change were recorded at all daily hydrographs with peak discharges greater than 17 m^3s^{-1}. The area of change increased, with scatter, in relation to discharge, with select high flow days producing areas of change greater than 2000 m^2. Below peak daily discharge of 11 m^3s^{-1} only 10 of 117 daily hydrographs showed any observable planform change and those showing change had areas of < 80 m^2, which is less than 1% of the wetted river area. Some peak daily discharge events between 11-17 m^3s^{-1} show large areas of planform change but rates are variable, with 60% of these days having no measurable planform change. The automated analysis was completed in an attempt to decrease the subjectivity of the manual analysis but results showed that it overestimated areas of planform change, especially at low discharges, and further refinement is needed for this method to be reliable.

Field results provided a wide base of planform measurements across a range of different discharge conditions. This allowed the relationship between planform change and discharge in the field setting to be fully understood, capturing the inherent variability and complicated nature of planform dynamics in braided rivers.

Chapter 6

6 Laboratory Results

6.1 Description of Data

Flume experiments were run as models of particular Sunwapta daily hydrograph events, chosen to represent the range of daily peak flows observed during the period of field image analysis. The intent of the hydrograph experiments was to replicate Sunwapta hydrographs to allow comparison of rates of planform change and use the physical model to extend the relationship between planform change and discharge to include morphological change and bedload transport. Comparable data and observations to the field were collected in the laboratory allowing for comparison between the two. Equivalent field discharges during experimental runs ranged from 5-17 m^3s^{-1}.

6.2 Analysis of Flume Discharge

Four daily hydrographs from the Sunwapta River were replicated as experimental runs. A series of four successive days was selected with varying peak discharges, covering a range of conditions representative of the Sunwapta River (Figure 6.1). Each of the four, daily hydrographs was run three times (see Chapter Four).

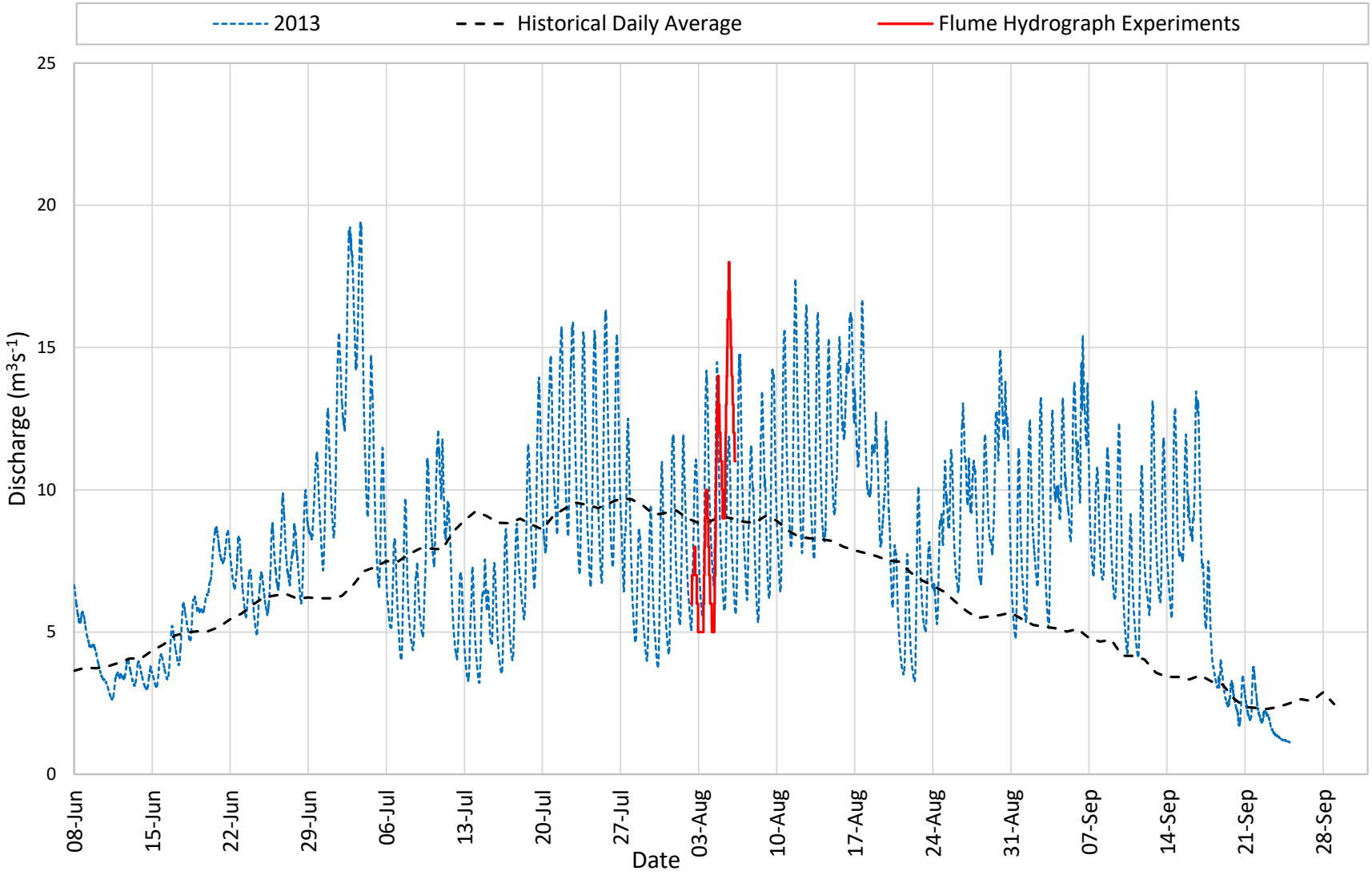

Figure 6.1: The range of discharges in Sunwapta River for both 2012 and 2013 with the representative hydrographs selected shown in red.

6.3 Measurements

6.3.1 Planimetric Measurements

Planform measurements were made of daily hydrograph experimental runs using the manual method used in the field daily hydrograph analysis. Images were selected of the wetted surface at the minimum stage at the beginning of the rising and end of the falling limb of each hydrograph experimental run, for a total of 12 hydrographs measurements. Planform change measurements covered a total flume area of 28.5 m^2 (9.5 x 3 m). Areas of planform change ranged from zero to almost 7 m^2, equivalent to 24% of the total measured river area (Figure 6.2). The rates of planform change increased with peak discharges, with a large increase between hydrographs with at peak discharges of 1.4 and 2.22 ls^{-1} (equivalent to 10 and 14 m^3s^{-1} in the field). Peak discharges of 1.4 ls^{-1} and less (10 m^3s^{-1}) showed limited planform changes, with change areas of less than $1m^2$. These small areas of change are similar changes at the equivalent discharge in the field, with minor isolated areas of bank or bar erosion along the primary channel with both locations having areas of change less than 5% of the total surveyed area. At peak discharges of 2.22 ls^{-1} and greater (14 m^3s^{-1}) these areas were seen to increase and occur across the entire length and width surveyed, connecting all areas of change. This is similar to the field observations. Laboratory analysis extended the total area surveyed, measuring planform changes over a river length of almost three times the comparable area in the field from which it can be inferred that types and rates of change are similar at a given discharge within a longer reach and the shorter reach observed in the field. The comparison between planform changes in the physical model and field prototype is discussed further in Chapter 7.

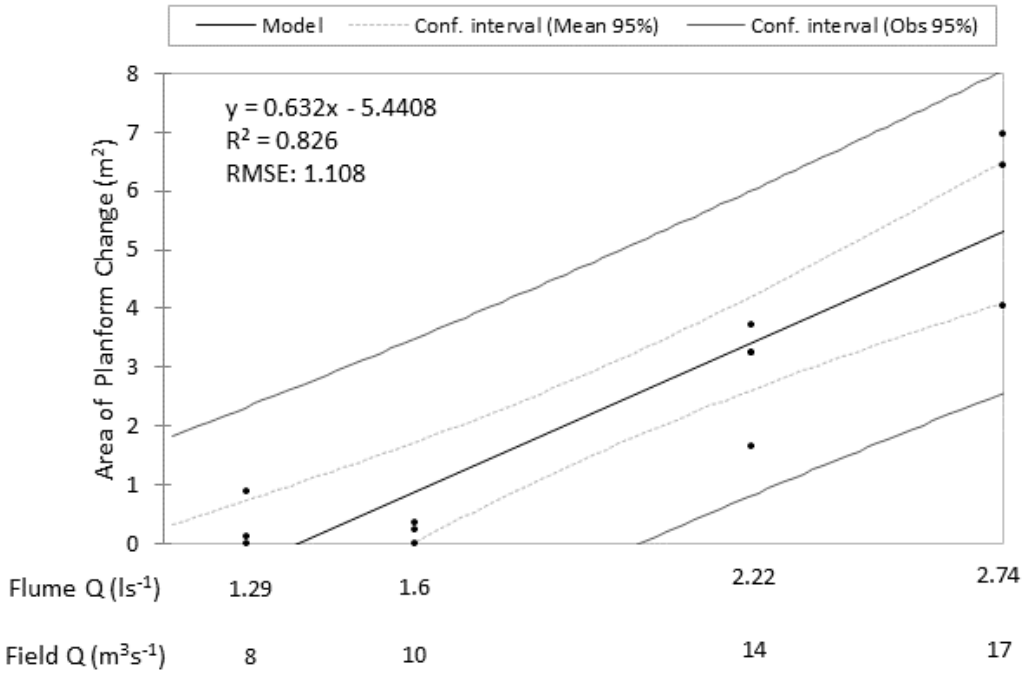

Figure 6.2: The relationship between planform change and peak discharge in the flume.

6.3.1.1 Potential Area for Planform Change Measurement

The wetted area was measured at the peak of each hydrograph. Except in experimental run 12, peak discharges of 10 m^3s^{-1} and lower did not exceed an area of planform change of 10% of peak wetted area. All hydrographs with peaks higher than 10 m^3s^{-1} had areas of planform change at least 15% of the peak flow wetted area (Figure 6.3). Overall the area of change/wetted area relationship was stronger in the flume than in the field although the general trend is the same in both. The same relationship was shown as the area of change/wetted area increased in relation to peak discharge but a larger potential area of change was recorded in the flume.

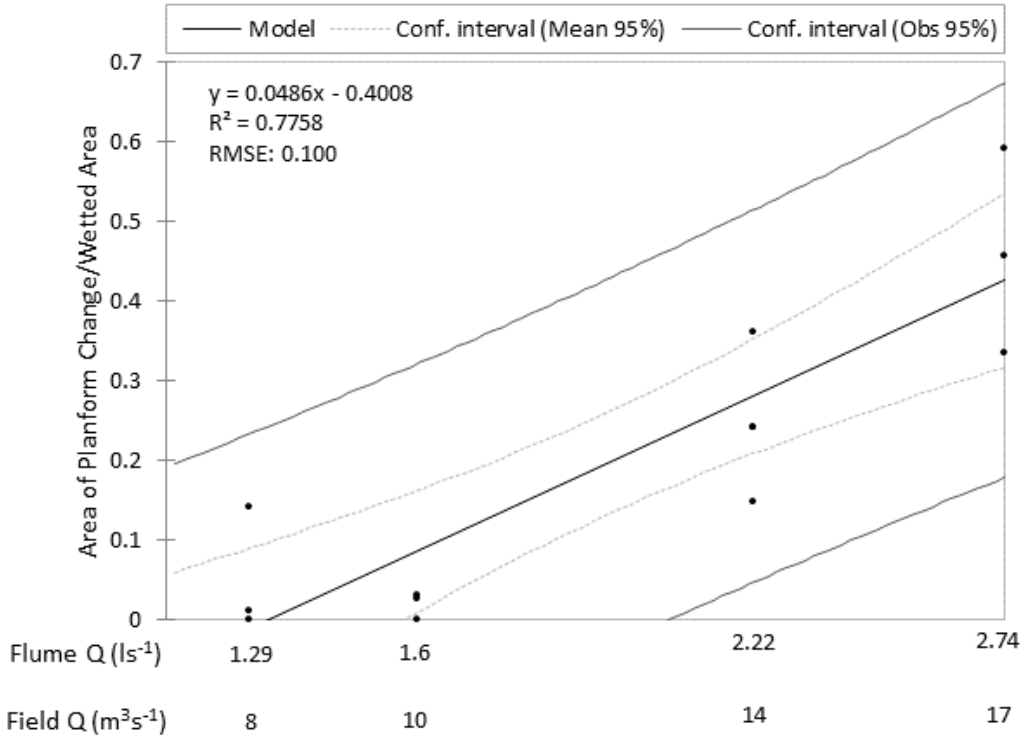

Figure 6.3: The relationship between peak discharge and the area of change as a proportion of peak flow wetted area.

6.3.2 Morphological Measurements

Morphological measurements were made on each of the 12 hydrograph experimental runs to determine the net area, depth and volume of erosion and deposition. These measurements were made using digital photogrammetry on dry-bed photo surveyed images at the beginning and end of each hydrograph experimental run. The DEMs at the beginning and end of each hydrograph were differenced to produce a DEM of Difference (DoD) from which the data were extracted (see section 4.3.5).

The areas of morphological change increased in relation to an increase in peak hydrograph discharge (Figure 6.4). DEMs of Difference showed that the areas of erosion and deposition both increase at higher peak discharge as these areas became connected throughout the channel. Each hydrograph run had measurable volumes of change but not all had observable areas of planform change. The measurement of areas of planform change is missing some volumetric changes, especially at lower flows. Experimental run 9 showed no areas of planform change but did have a

very small area of erosion and deposition, with erosion depths not exceeding 12mm (Figure 6.5). Hydrographs with peaks of 1.6 ls^{-1} (10 m^3s^{-1}) and lower produced smaller areas of morphological change that were localized and did not connect to one another along the length of the channel. This was observed in all cases except for experimental run 12 (Figure 6.5). As discharges increased, areas of morphological change increased and were connected, spanning the length of the flume. At the highest peak hydrographs, morphological change occurred across the length and width of the river bed. The depth/height of erosional and depositional features also increased in relation to an increase in discharge, with the depth of erosion/deposition exceeding 30mm at peaks of 2.22 ls^{-1} (14 m^3s^{-1}) and greater. The total volumes of change (sum of erosion and deposition) ranged from 0.01 to 0.21 m^3, with rates increasing with peak discharge (Figure 6.6). Similar to rates of planform change, total volume of change was variable between repeat hydrographs.

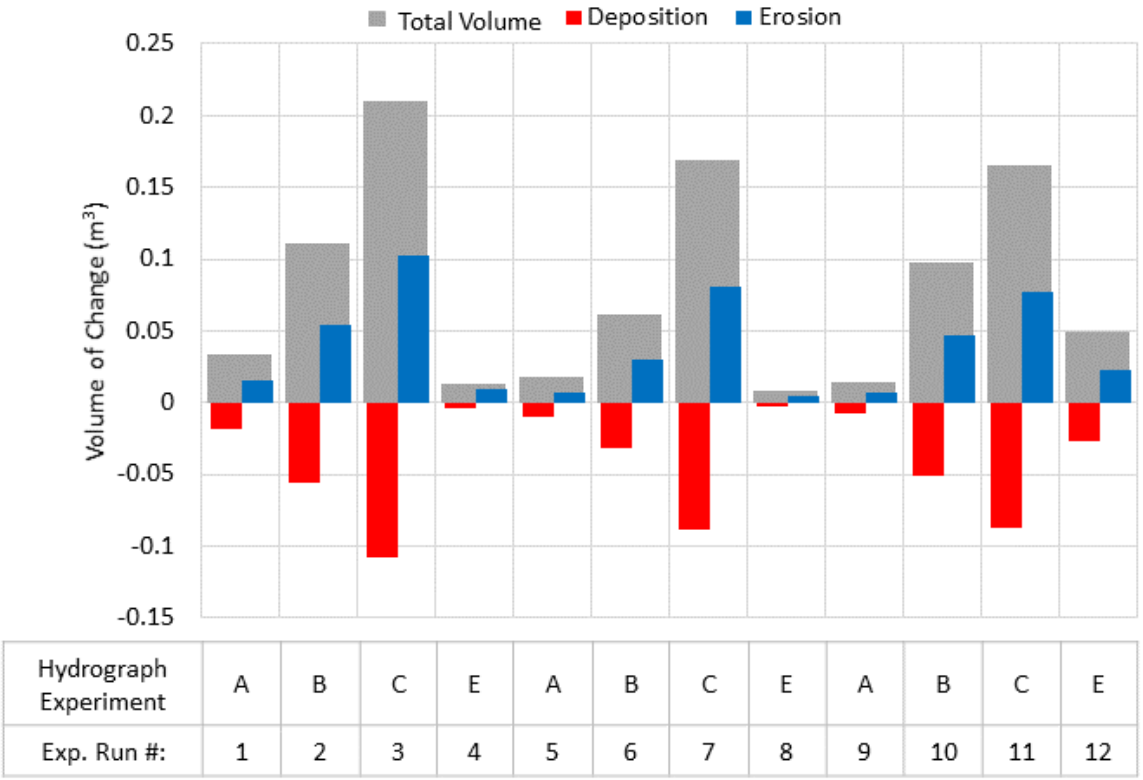

Figure 6.4: The volumes of erosion, deposition, and the sum of the two shown in relation to the sequence of hydrograph experiments.

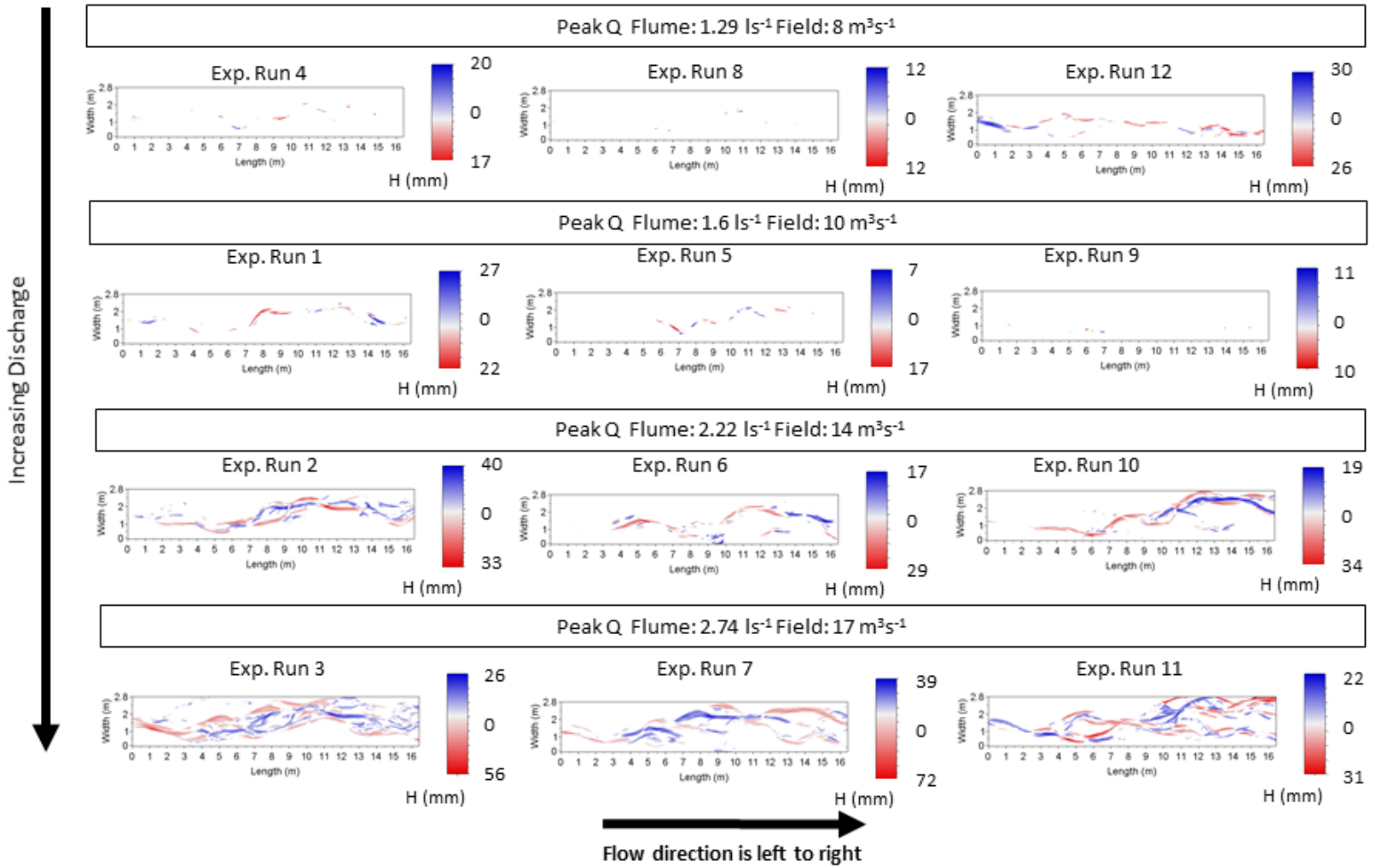

Figure 6.5: DEMs of Difference for each hydrograph experiment showing the increase in areas of erosion (red) and deposition (blue) and the increase in the depth (intensity of red/blue) of these features as discharge increases.

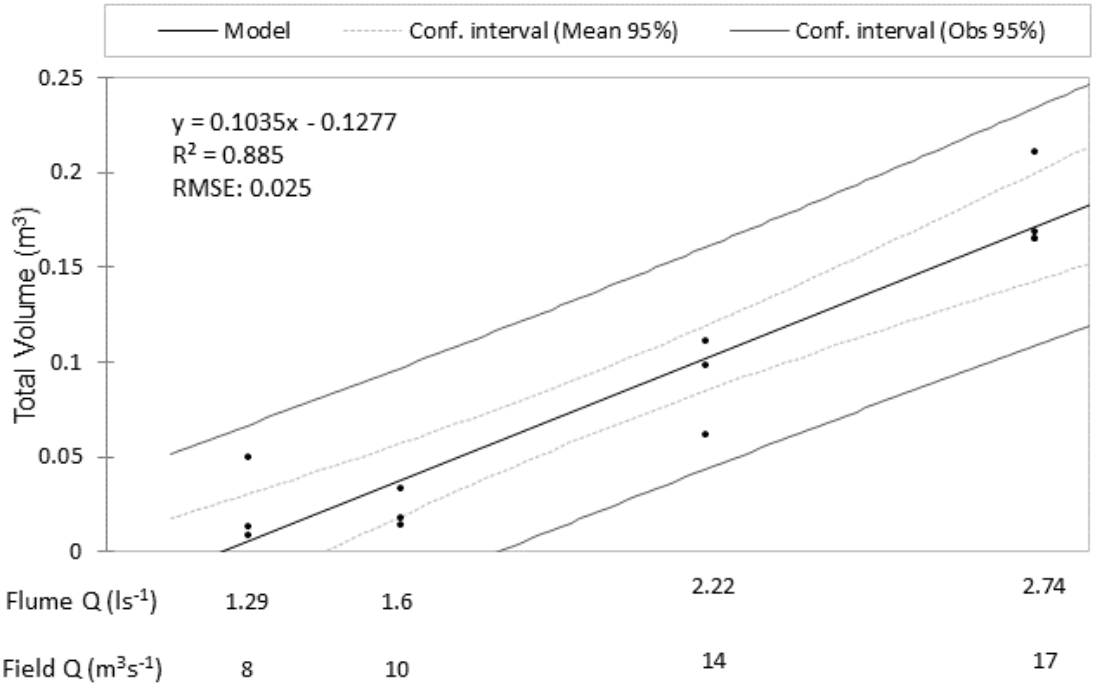

Figure 6.6: The total volume of erosion and deposition in relation to the peak discharge.

6.3.2.1Morphological versus Planform Change

These morphological changes aligned with observed areas of planform change. A Pearson's correlation computed found a significant positive relationship between the two variables (0.928, n=12), with more information provided in Appendix E (Figure 6.7). There is a slight offset related to the lower hydrographs in which the small volumes of change in DEMs occur without measurable planform change. At lower discharges planform change alone may therefore slightly underestimate volumetric changes. This may be due to planform changes being recorded over a wet bed, with inundated areas masking small areas of morphological change where erosion/deposition occurred within the channel. High-resolution surveys possible over a dry bed are able to show these localized areas of morphological change not visible from wetted planform measurements.

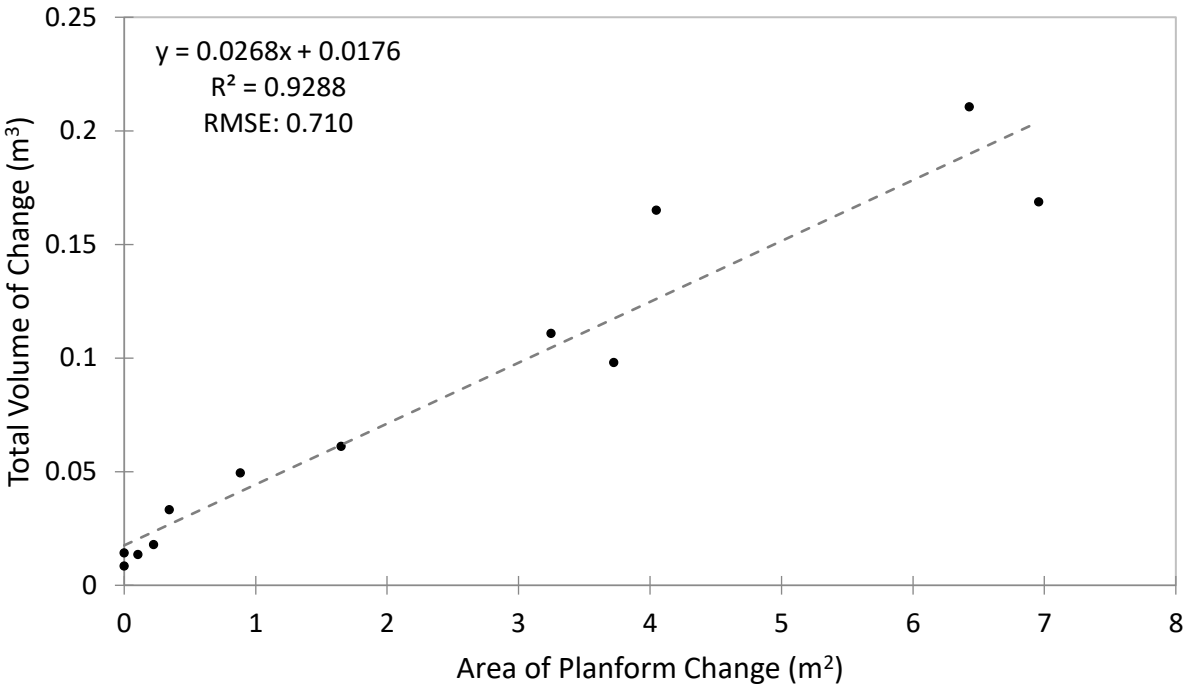

Figure 6.7: The relationship between planform and morphological change from measurements made during experimental runs of hydrograph experiments.

Areas of planform change mapped were found to coincide spatially with those in the DoD analysis. Lower peaks of 1.6 ls^{-1} (10 m^3s^{-1}) and less, recorded small areas of planform and morphological change seen in localized areas of bank and bar erosion. These were measured as planform changes as the channel laterally migrated eroding sediment, seen in two examples of lower hydrographs with these changes highlighted in red (Figure 6.8, 6.9) and evident in the red area of erosion in the DoD (Figure 6.8c, 6.9c). Other small areas of planform change were evident in changes to the braid bar configurations, highlighted in blue (Figure 6.8, 6.9) as the morphology was altered due to different erosional and depositional events, seen in small areas of both blue and red in the DoD (Figure 6.8c, 6.9c).

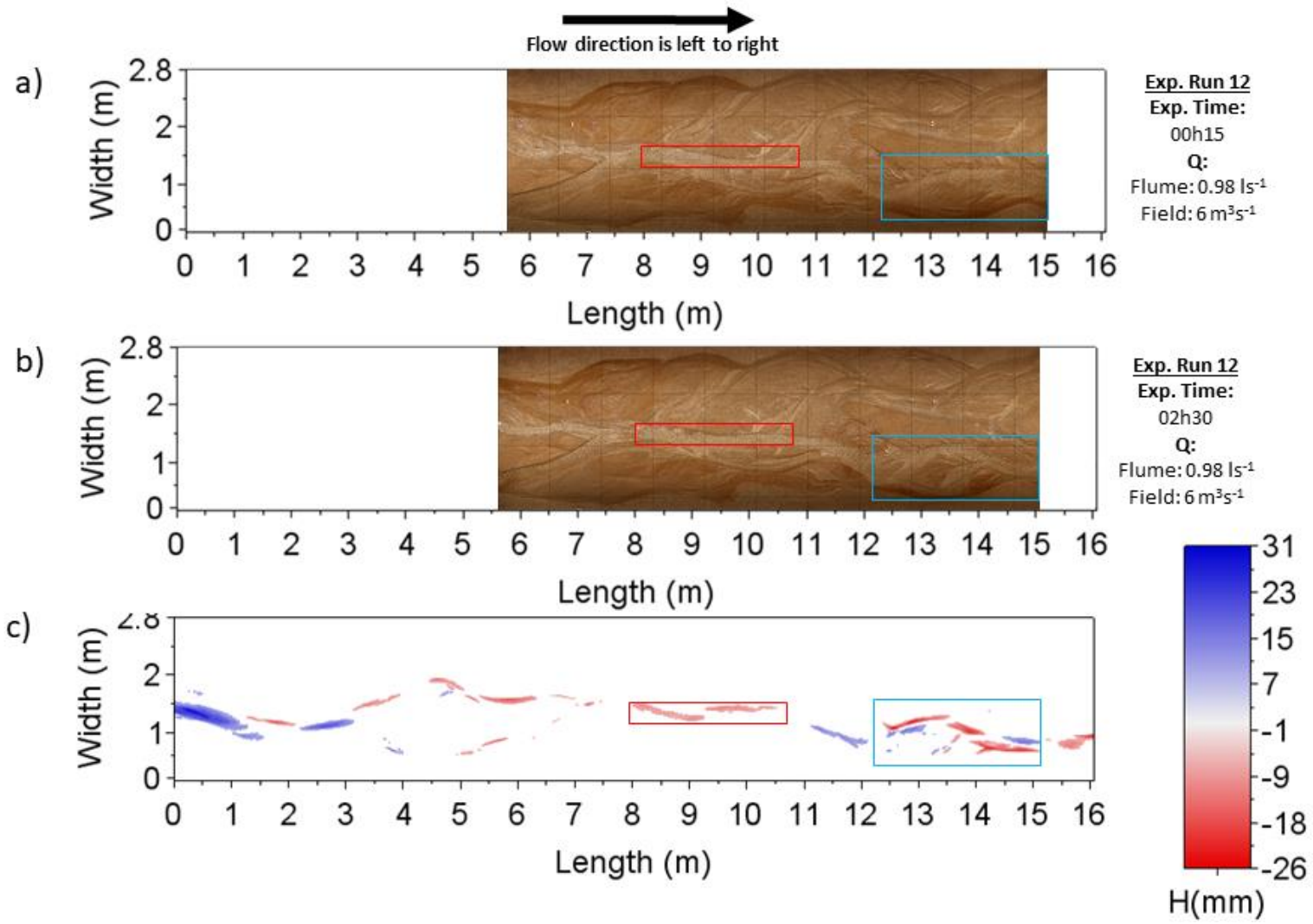

Figure 6.8: An example of small areas of planform and morphological change documented at the lowest peak discharge where changes were limited to small sections of the river bed.

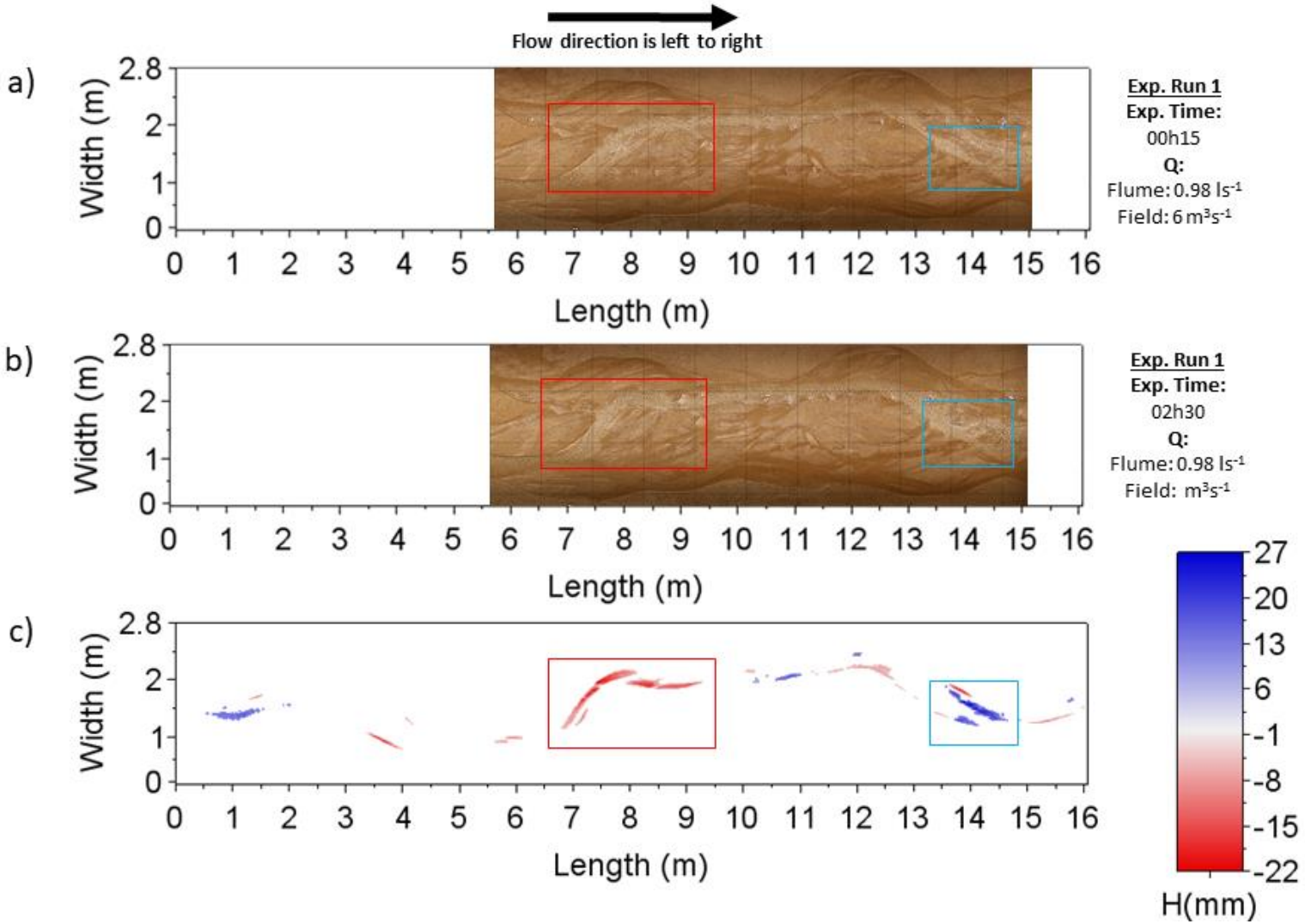

Figure 6.9: An example of small areas of planform and morphological change documented at the second lowest peak discharge where changes were limited to small sections of the river bed.

As peak discharges increased at 2.22 and 2.74 ls^{-1} (14, 17 m^3s^{-1}) larger areas of planform and morphological change were recorded and connected over larger areas. These changes represented large changes in the river planform and created large erosional and depositional features. Large areas of deposition were created as sediment was eroded due to the lateral migration of channels, highlighted in red (Figure 6.10, 6.11) and evident in the red area of erosion in the DoD (Figure 6.10c, 6.11c). Channels laterally migrated as confluences shifted, altering flow as well as the configuration of braid bars, highlighted in blue (Figure 6.10, 6.11) evident in both erosional (red) and depositional (blue) features (Figure 6.10c, 6.11c). These changes were extensive and seen to alter the planform and morphology across the entire length and width of the flume at higher discharges.

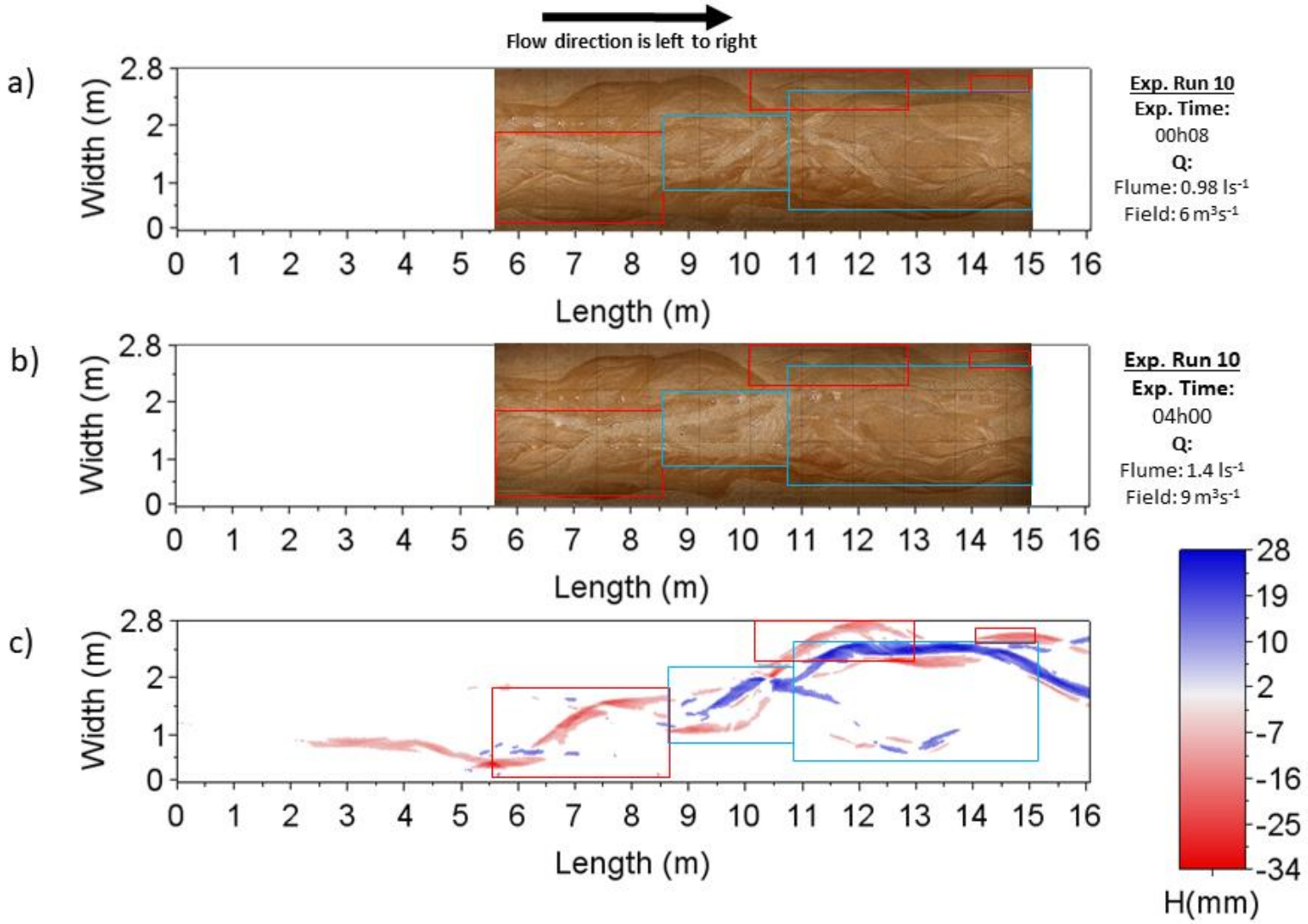

Figure 6.10: An example of large planform and morphological changes documented at the second highest peak discharge where changes were recorded across the entire length and width surveyed.

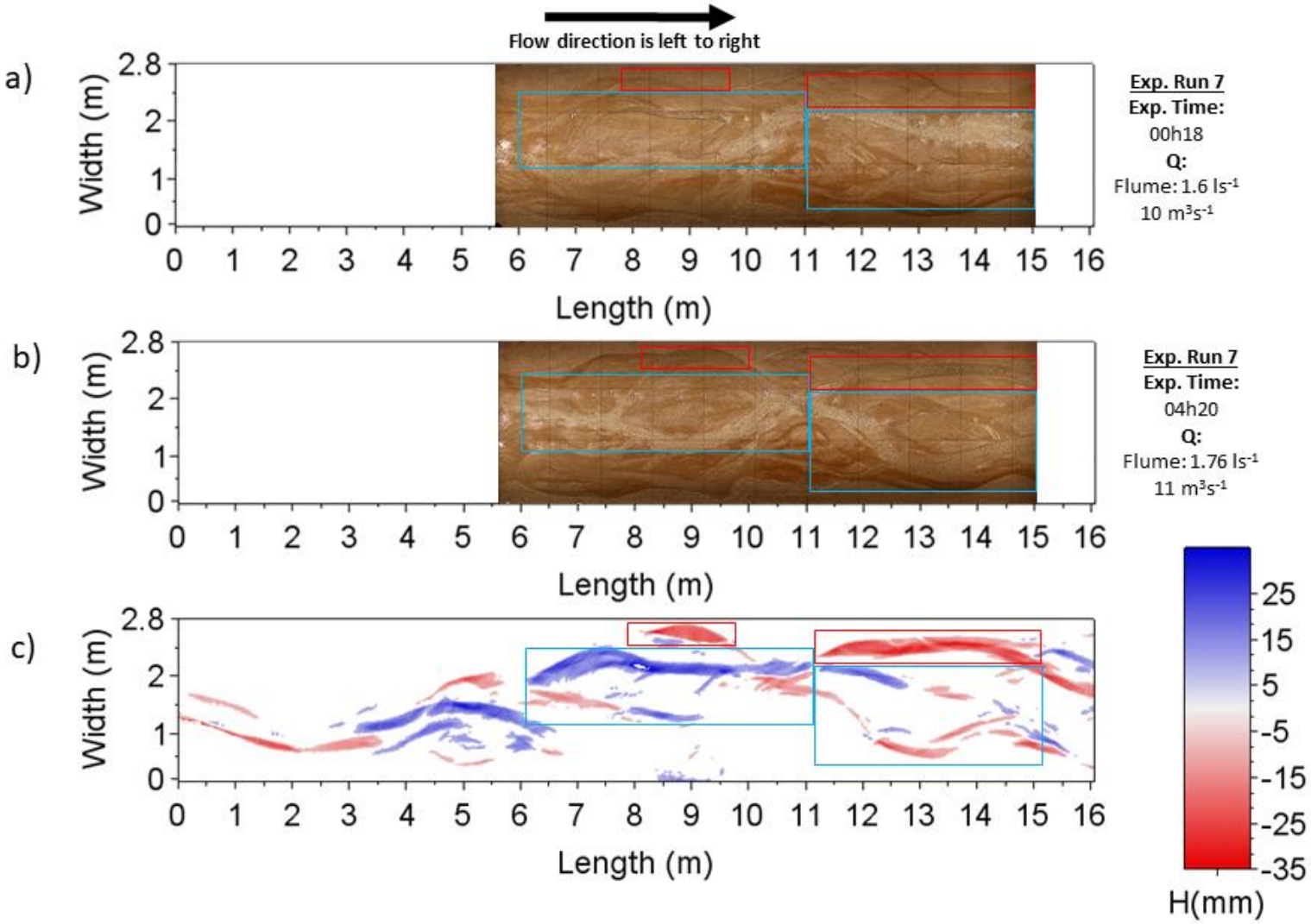

Figure 6.11: An example of large planform and morphological changes documented at the highest peak discharge where changes were recorded across the entire length and width surveyed.

6.3.3 Bedload Measurements

6.3.3.1 Bedload Sample Weights

The weight of individual sediment samples, measured as the total weight transported over the one minute collection period, was also seen to increase in relation to an increase of the hydrograph stage (Figure 6.12). Even at the lowest discharges in the hydrographs some bedload transport occurred but below 1.3 ls^{-1}, rates were negligible, except in the case of run 12, discussed further below. These weights were also considered in relation to the braiding intensity, with the active braiding intensity (ABI) used, based on the definition provided by Egozi and Ashmore 2009, as the number of channels actively transporting bedload. Observations of bedload transport were taken at only one cross-section location and so only provide one small viewpoint of the ABI and cannot be related to other areas of the channel. These observations were recorded at the downstream end, 2m away from the location of sediment sample location and samples collected only a minute apart. This allowed the ABI of the planform configuration of one position to be related to the weights of sediment transported produced over the same discharge conditions and closely related time intervals, discussed further below. Overall as ABI increases the weight of bedload transport was also found to increase, with some variability (Figure 6.13). More information on the box plot and distribution of sediment weights over different ABI can be found in Appendix F. Some of the variability recorded in bedload weights can be related to temporal variations between hydrograph experiments (Figure 6.14).

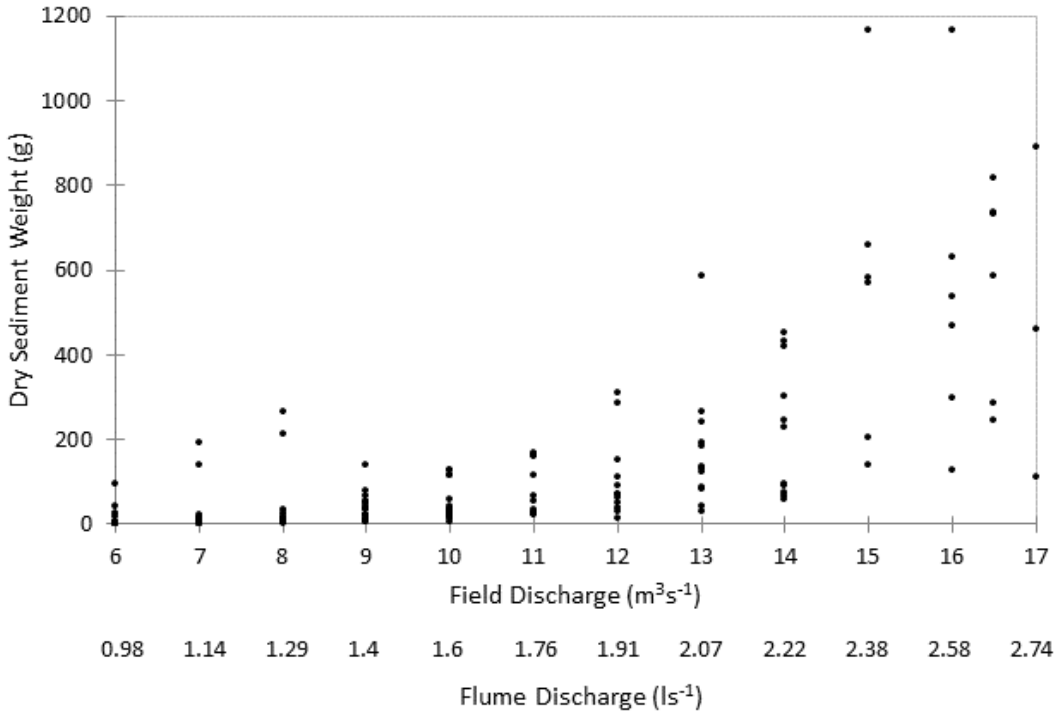

Figure 6.12: The relationship between the bedload transport rate of individual samples and discharge.

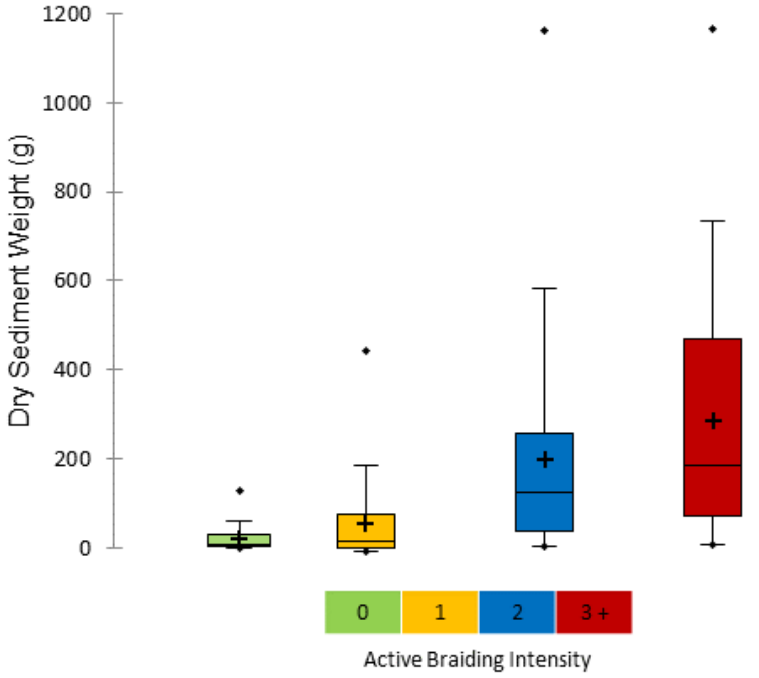

Figure 6.13: The ABI in relation to the bedload sample weight, both measurements collected at the downstream end ~2m apart.

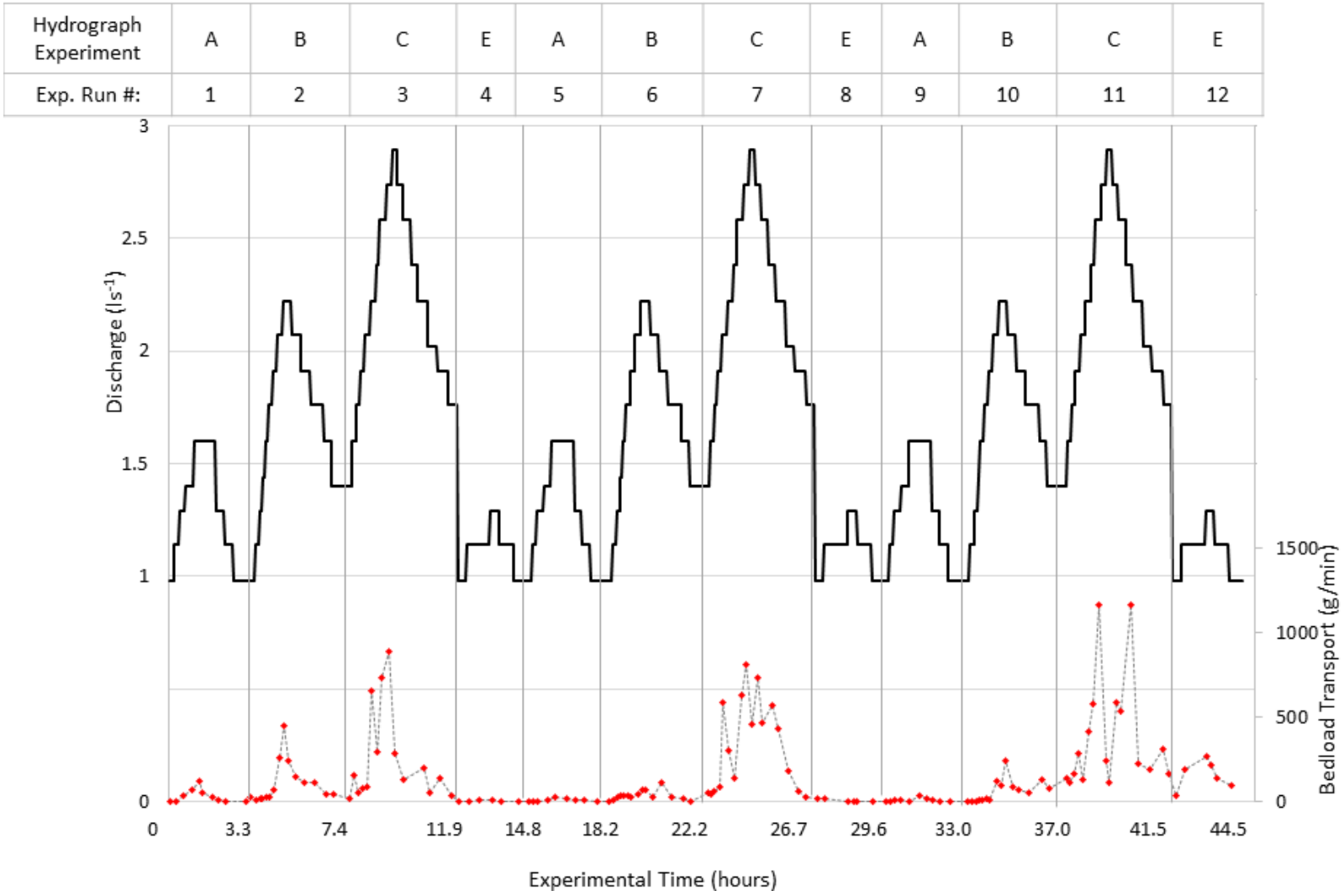

Figure 6.14: The rate of bedload transport in relation to discharge and hydrograph stage.

6.3.3.2Total Bedload Transport

Bedload samples collected over a hydrograph run were calculated into a total bedload transport weight. This allowed the total weight transported over an experimental hydrograph run to be related to areas of planform and morphological change which were measured over the entire hydrograph period. The total bedload weight transported was calculated by inferring that each one-minute sample was representative of the total time at the hydrograph stage it was collected. Bedload samples were therefore multiplied by the number of minutes of the hydrograph at the stage the sample was collected at and then summed to produce a total transport rate over each hydrograph run.

Overall, the total bedload transport weight was found to increase with increasing discharge, with greater variability at higher transport rates (Figure 6.15). The average bedload weight (average of sediment weights collected at each stage during experimental runs) showed a large increase above a peak discharge of 2.22 ls^{-1} (14 m^3s^{-1}).

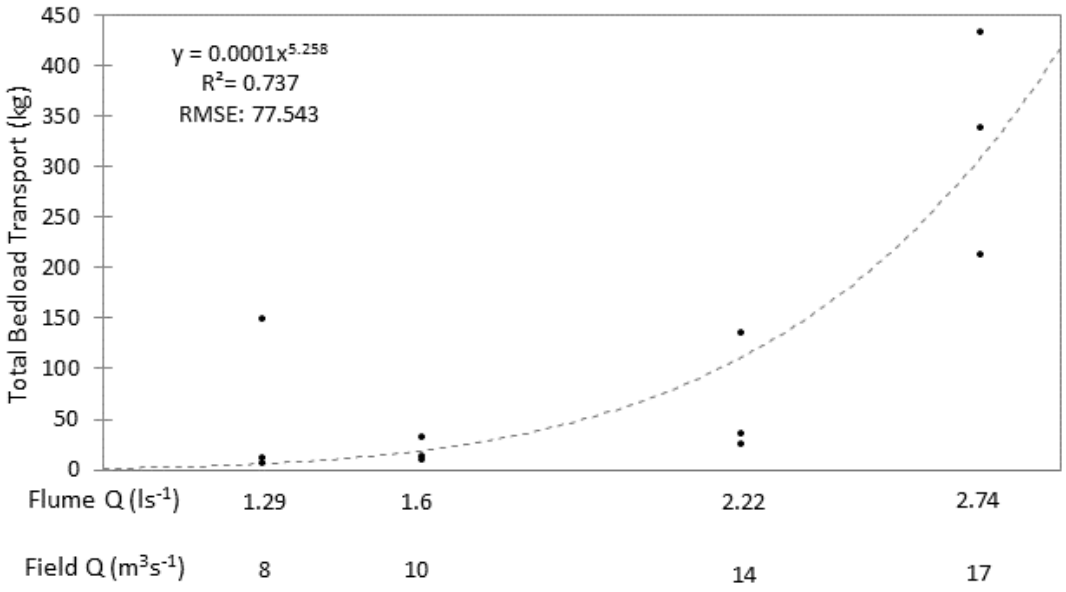

Figure 6.15: The relationship between average sediment weight transported during an experimental run in relation to the peak discharge in the flume.

6.3.3.3 Grain Size Distribution

Particle size analysis of the bedload samples also showed some distinct trends. The summary statistics are given in Table 6.1. In general the D_{10} and D_{50} showed very little change with increasing discharge but the D_{90} shows an upward trend (Figure 6.16). Some samples at low

discharges had higher values of D_{90} but these were mostly cases in which very small quantities of coarse grains were rolling over an immobile bed. Individual particle size samples show a general shift from finer to coarser with increasing discharge (Figure 6.17). The minimum and average of the D_{50} at each discharge were seen to generally increase with an increase in discharge. The maximum D_{90} at each discharge was found to be much more variable than the D_{50} (Figure 6.16). The highest D_{90} was measured at the beginning of the first experimental run of all hydrograph experiments. (Figure 6.16 at top left of plot). The flow had just been turned on, flowing over a very dry-bed due to a break from previous experimental runs. The potential to transport larger particles may have then been greater then, with a burst of sediment transport possible. The first sample was collected during the first five minutes of the experiment and may have captured this influx of larger particle sizes and was only 3.07 grams, indicating it may not be fully representative of the capability to transport at this discharge. The same sample corresponds with the lowest discharge (0.98 ls^{-1}, 6 m^3s^{-1}, lightest shade) to produce the highest sediment distribution, seen to lie below all other distributions (Figure 6.18). The two highest maximum D_{50} values, recorded at 0.98 ls^{-1} (6 m^3s^{-1}) and 1.76 ls^{-1} (11 m^3s^{-1}) had a much larger standard deviation (0.40, 0.27) between the samples collected at these discharges, compared to all other standard deviations which fell below 0.20. As the weight of bedload samples increased no impact was seen on the size of D_{10} and little on the D_{50} while the D_{90} was seen to increase (with variability) as the bedload weight increased (Figure 6.19). No temporal trends were observed in the size of D_{10} or D_{50} through hydrograph experiments but the D_{90} was seen to increase (with large variability) in relation to temporal changes and the increase/decrease of discharge over a hydrograph experiment (Figure 6.20).

Table 6.1: The summary statistics from the individual sediment samples collected at each discharge.

Q (ls^{-1})	Q (m^3s^{-1})	# of Samples	Minimum D_{50} (mm)	Average D_{50} (mm)	Maximum D_{50} (mm)	Standard Deviation
0.98	6	15	0.46	0.89	1.98	0.40
1.14	7	15	0.69	0.93	1.39	0.19
1.29	8	14	0.70	0.94	1.30	0.19
1.4	9	15	0.80	0.99	1.42	0.20
1.6	10	14	0.77	0.95	1.20	0.16
1.76	11	11	0.76	0.99	1.67	0.27
1.91	12	12	0.82	1.02	1.25	0.15
2.07	13	10	0.87	1.12	1.39	0.19
2.22	14	11	0.93	1.11	1.37	0.16
2.38	15	12	0.78	1.11	1.30	0.13
2.58	16	11	0.99	1.26	1.47	0.16
2.65	16.5	9	0.95	1.16	1.47	0.19
2.74	17	5	1.00	1.24	1.34	0.14

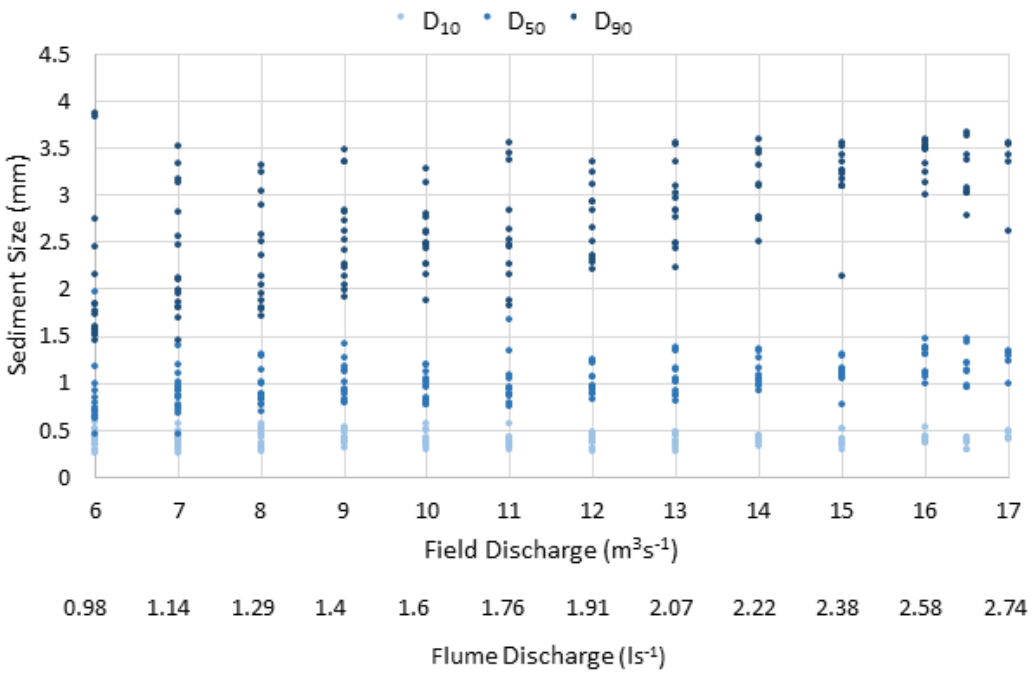

Figure 6.16: The relationship between the D_{10}, D_{50} and D_{90} of individual sediment samples and discharge.

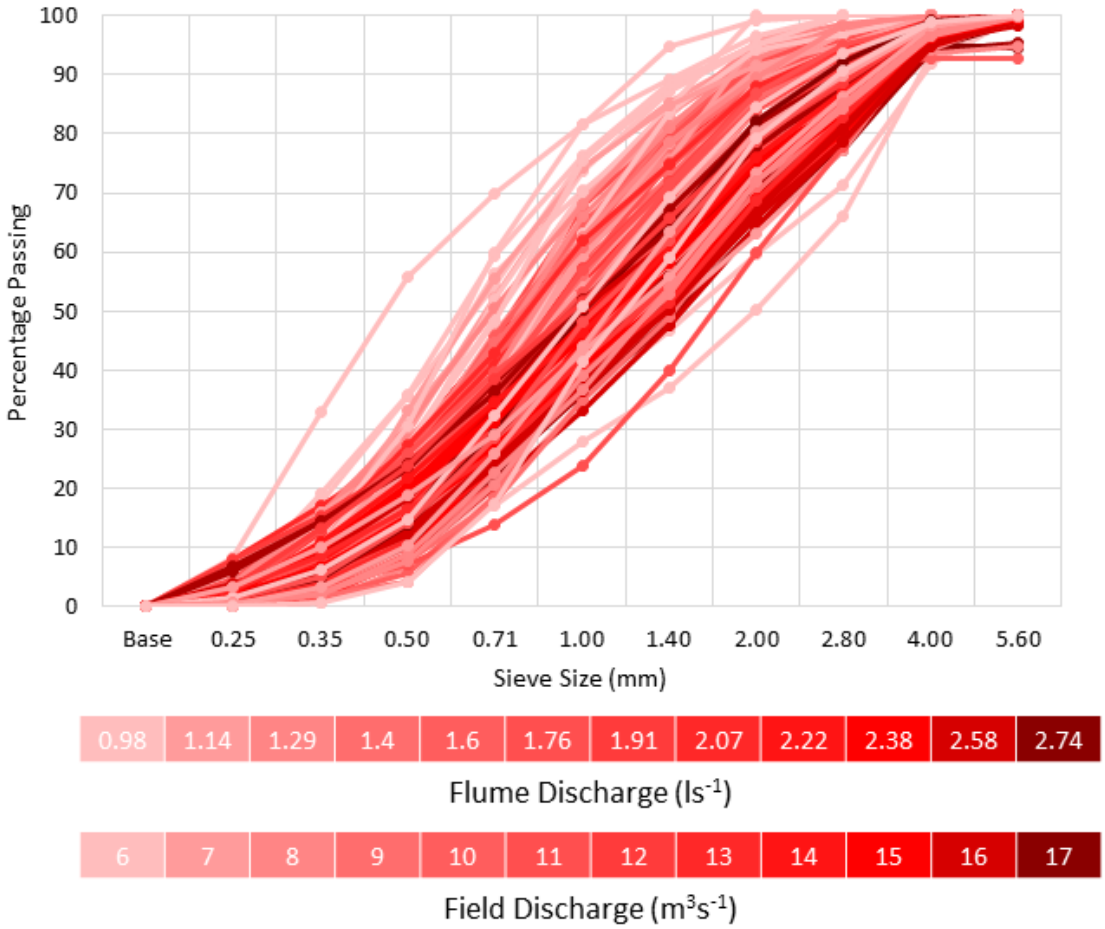

Figure 6.17: The sediment distribution of individual sediment samples sieved with increasing discharge in darker colours.

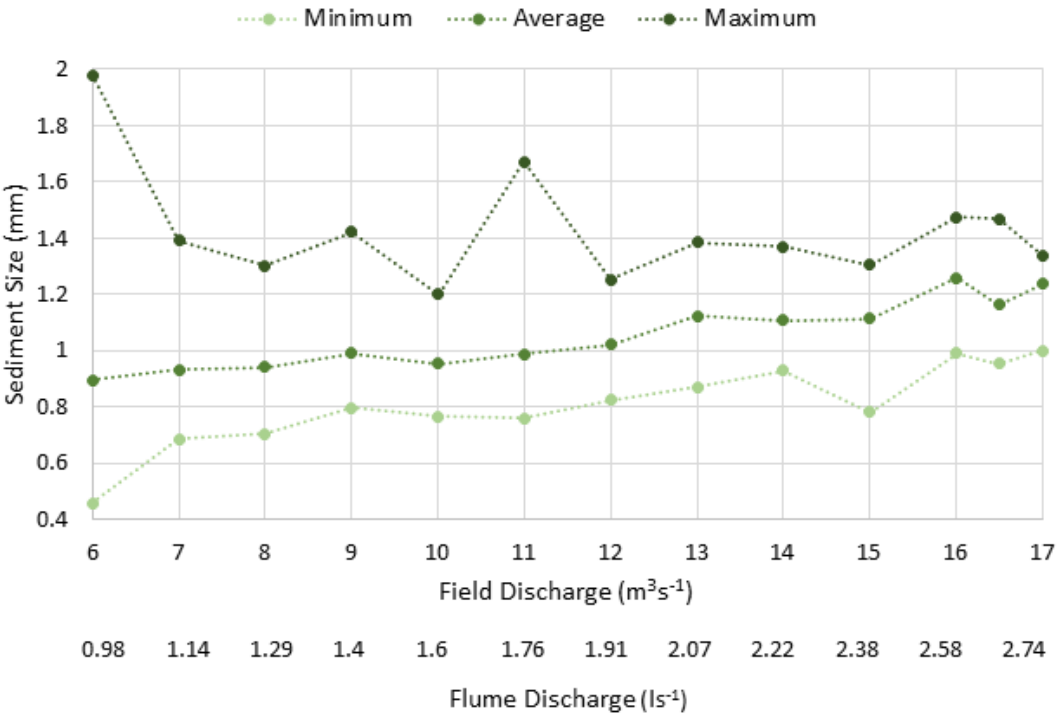

Figure 6.18: The summary statistics of the D_{50} for sediment samples at different discharges.

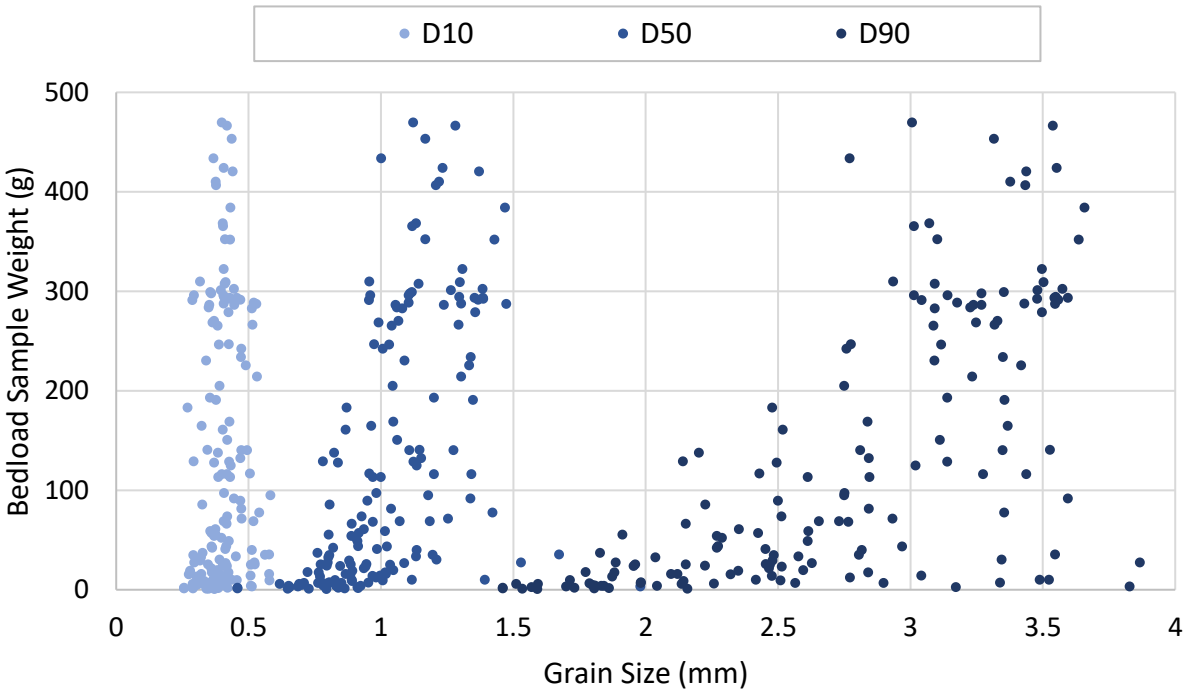

Figure 6.19: The relationship between weight of a bedload sample and the size of D_{10}, D_{50} and D_{90}.

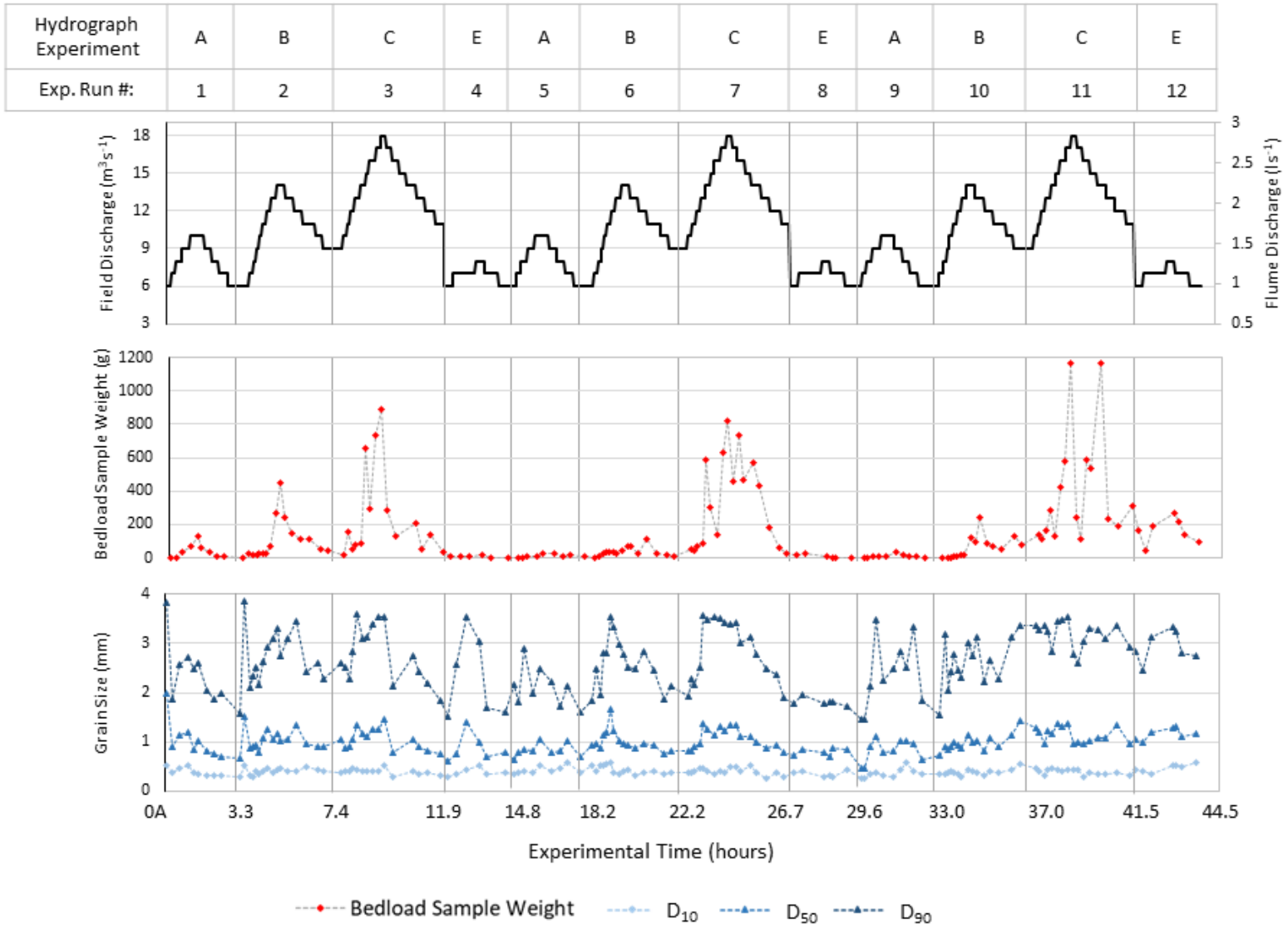

Figure 6.20: The temporal relationship between bedload transport and grain size distribution throughout hydrograph experiments.

In summary, the analysis of grain size distribution shows as the river planform is changing all sizes of the bedload are moving. As both discharges and the weight of sediment samples increased, the grain size distribution showed no trends in D_{10} or D_{50} but the D_{90} increased. This shows that while samples collected at all discharges had the same range of grain size distribution, higher discharges and larger sediment samples had an increased proportion of larger grains and were coarser overall.

6.3.3.4Bedload Transport Rates vs Planform and Morphological Change

Overall, the rate of bedload transport showed a positive, significant relationship with the total area of planform change over the hydrograph experiments (Figure 6.21a). Substantial bedload transport was not found to occur without areas of planform change, with very little transport during hydrographs with a lower peak discharge, which also had limited areas of planform change. Two hydrographs can be seen to have higher bedload transport rates with lower planform change. These are experimental runs 11 and 12 during which the primary braid channel hit the flume wall and increased rates of sediment transport, discussed further below. Without these two measurements, the relationship is more significant, summarized below in Table 6.2 and shown in Figure 6.21b. Additional information is provided in Appendix E.

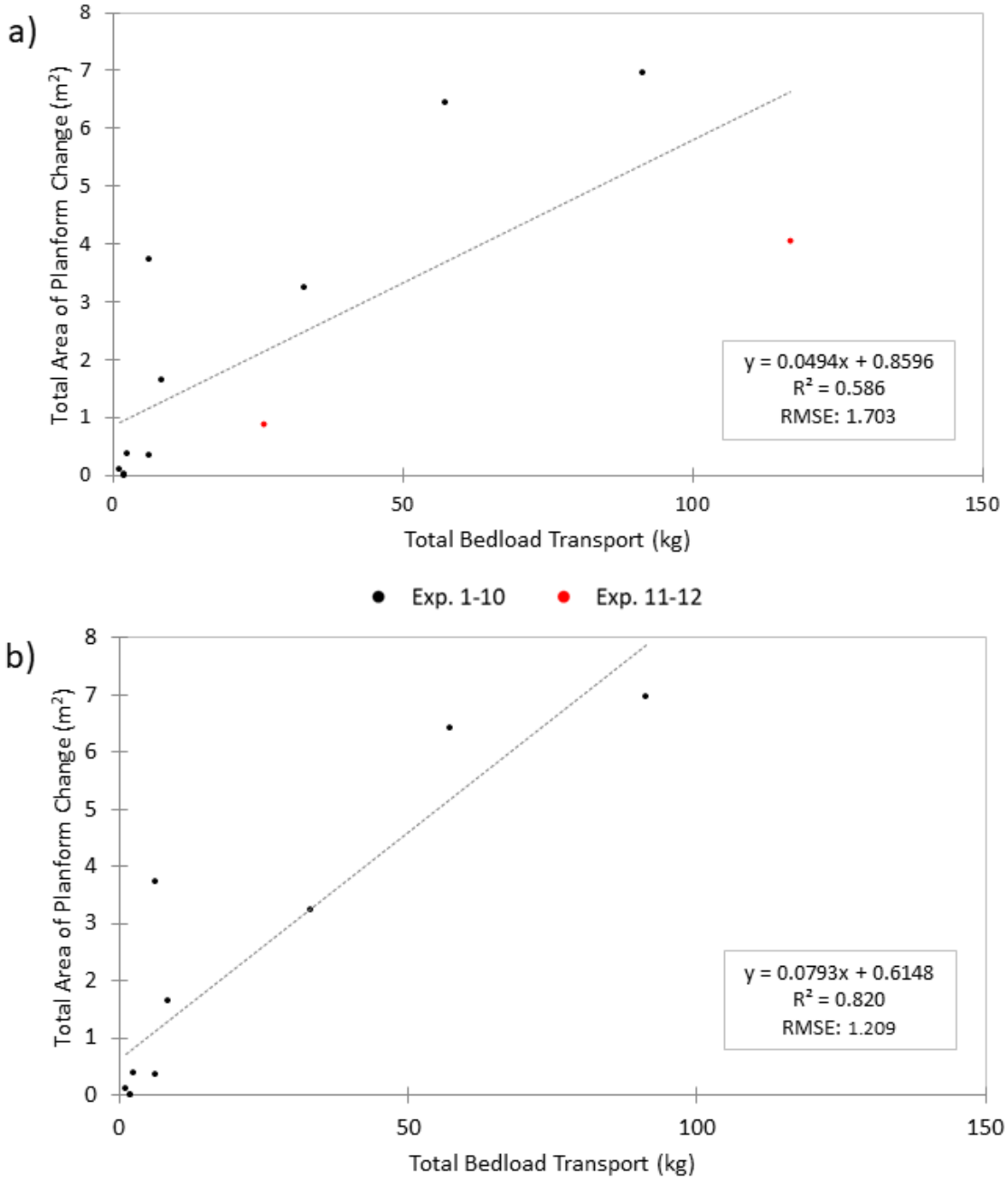

Figure 6.21: The relationship between total bedload transport weight and areas of planform change, with (a) the overall relationship and (b) the relationship plotted without experimental run 11 or 12.

Table 6.2: P-values of the correlation between total bedload transport and areas of planform change for exp. 1-12 and 1-10. n= number of observations.

Pearson's Correlation P-values	Exp. 1-12	Exp. 1-10
	0.0037	0.0003
n	12	10

Bedload transport rates are seen to be greater for Hydrograph experiments 11 and 12 in relation to other hydrographs experiments with the same peak. High rates of bedload transport were produced in relation to a different planform configuration (Figure 6.22). Bedload transport rates were much higher due to the primary channel hitting the flume wall, increasing the velocity of this channel and mobilizing large amounts of sediment, of all sizes into the sediment collection basket, directly downstream (Figure 6.22). This change in planform was also seen to alter the morphology as a scour hole with a depth of over 30mm was created from the erosion of mobilized particles. The planform configuration can therefore impact rates of bedload transport at a given discharge but overall rates of bedload transport were negligible at 1.4 m^3s^{-1} and less, not including Exp. 12.

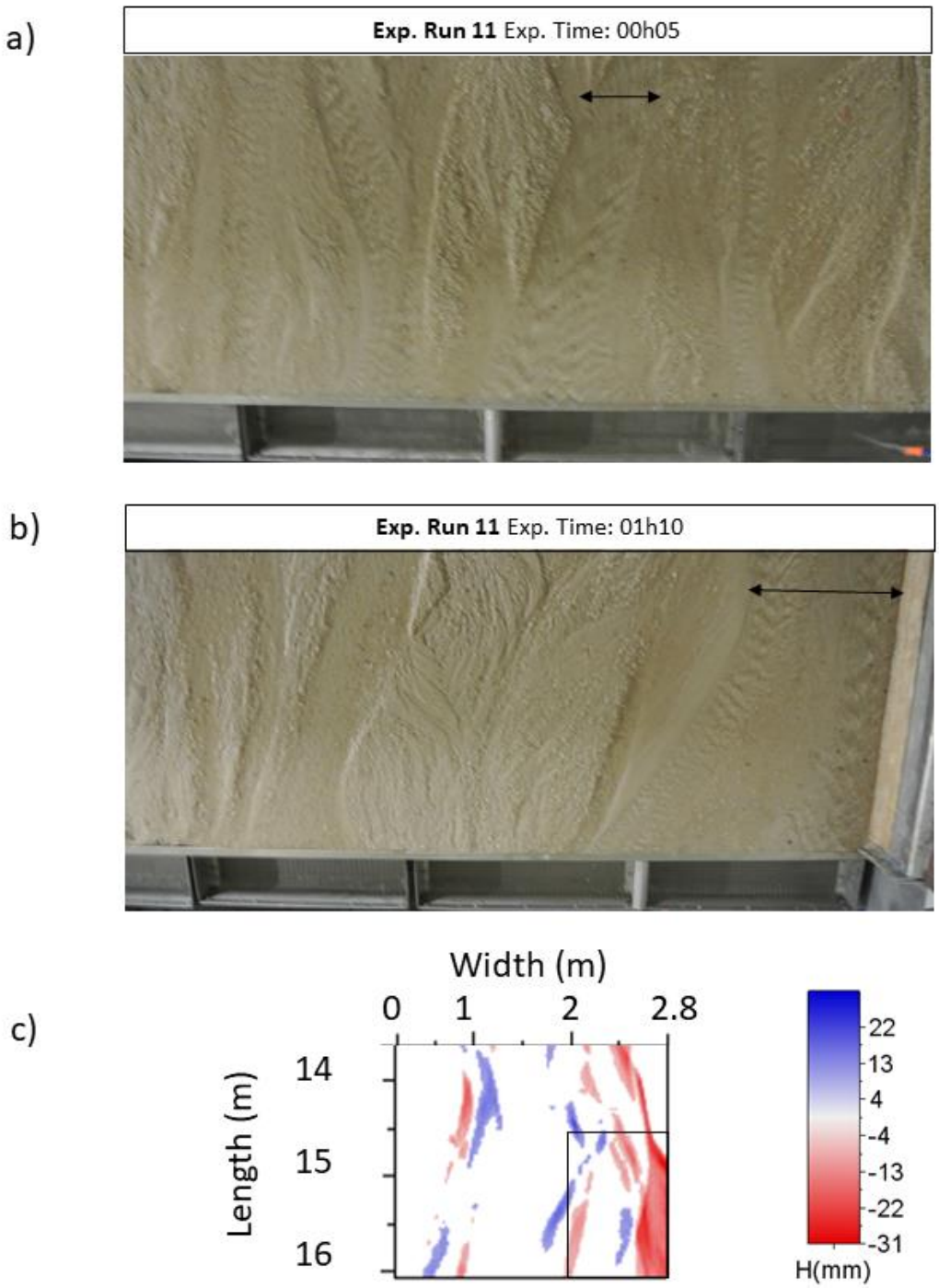

Figure 6.22: An example of run 11 which saw the primary channel laterally migrate from the beginning (a) to middle (b) of the experimental run at the downstream end. This increased rates of sediment transport from experimental time 01h10 forward, into run 12. The increased rates of bedload transport, evident in the area of erosion, over 30mm deep recorded, highlighted in black box (c).

6.3.4 Measurements Summary

The area of planform change, total volume of morphological change and total bedload transport weight increased in relation to discharge over hydrograph experiments. Areas of planform change had a significant correlation with both volume of change and bedload transport weight with the results summarized in Table 6.3 below. Linear regression between the areas of planform change measured, in relation to both volume of morphological change and total bedload transport showed that the measurement of planform change may miss small movement of bedload transport and areas of erosion and deposition.

Table 6.3: The PCC and significance of the relationship between areas of planform change, volumes of morphological change and total bedload transport weight over a hydrograph run.

Variables		**Area of Planform Change (m^2)**	**Volume of Morphological Change (m^3)**	**Total Bedload Transport Weight (kg)**
		Significance (p-value)		
Area of Planform Change (m^2)	***Pearson's Correlation Coefficient (PCC)***		**< 0.0001**	**0.004**
Volume of Morphological Change (m^3)		0.928		**0.001**
Total Bedload Transport Weight (kg)		0.586	0.690	

6.4 Laboratory Results Summary

The replication of Sunwapta hydrographs run as experimental runs in the flume allowed the field data to be extended and assess volumes of morphological change and bedload transport in relation to planform change. Rates of planform change, morphological change and bedload transport were found to increase in relation to an increase in peak discharge and be significantly related to one another. All variables showed a threshold discharge of ~1.6 ls^{-1} (equivalent to 10 m^3s^{-1}) above which the area of planform change, volume of morphological change and total weight of bedload transport were variable but directly related to each other during that hydrograph run. Areas of morphological change and weight of bedload transported are slightly above zero when planform change is zero. This indicates that the measurements of planform change may be missing some

small ‘background’ movement of bedload that are not sufficiently large to appear as measurable planform change. These are generally found to have a finer grain size than bedload distributions at larger planform changes.

Peak discharges equivalent to Sunwapta discharges of 8 and 10 m^3s^{-1} were seen to perform little geomorphic work overall (planform change, bed erosion/deposition or bedload transport). An exception is experimental run 12 which was seen to have higher rates of change, but this may be caused by the primary channel hitting the flume wall, increasing rates of change. Not including this experiment, rates of planform change at these discharges were limited to less than 1.5% of the total area surveyed and rates of morphological change below 0.035 m^3.

Rates of change increased at peak discharges equivalent to 14 m^3s^{-1} and again at peaks of 17m^3s^{-1}. Hydrograph experiment B with a peak of 14 m^3s^{-1} saw areas of planform change to occur over 5.5-13% of the total area surveyed with volumes ranging from 1.6-3.7 m^3. Hydrograph experiment C with a higher peak of 17m^3s^{-1} saw higher areas and volumes of change with areas ranging from 14-25% of the total area surveyed and volumes from 4 to almost 7 m^3.

Chapter 7

7 Discussion

The results of the lab and field analysis helped answer research questions #1 and #2, related to the reanalysis of field daily hydrographs from Middleton (2015) and the comparison between area of planform change measured over a daily hydrograph in the physical model in relation to simultaneous measurements of bedload transport and morphological change.

Field analysis showed that the manual method of measuring planform change improved the accuracy of previous measurements (Middleton, 2015). The automation of the detection of planform changes was not possible however due to the complicated nature of braided rivers and the inherent differences between time-lapse images in a field setting. The analysis of measurements collected in the physical model found that areas of planform change measured over replicated daily hydrographs had a significant correlation with simultaneous measurements of both bedload transport and morphological change. The results from the field and lab analysis showed similarity in the rates of planform change between field and model hydrographs which provides validation of the model, answering research question #3, discussed further below.

7.1 Field and Laboratory Comparison of Planform Change

Areas of planform change over a daily hydrograph period were measured using the same methodology for both the field and physical model. Measured areas of planform change from both locations were then scaled to produce the equivalent areas of change in the field and model. Utilizing the 1:33 Froude-scale, areas of change from the laboratory were scaled to the equivalent area in the field and then multiplied by the ratio of equivalent area in the field to the model (because the model measurements are based on a reach length about 3.2 times the river width whereas field data are for a reach 0.8 times river width).

Results from the field and field prototype both showed areas of planform change to increase in relation to an increase in peak discharge, with increasing variability and covering a similar range in equivalent area (Figure 7.1). Field results showed a wider variability in the rates of planform change in relation to an increase in discharge and while extensive planform changes were measured, it was not observed over all hydrographs at the highest discharges as it was in the physical model, discussed further below.

Peak discharges of 11 m^3s^{-1} and less had limited areas of change in both lab and field, remaining below 5% of the total area measured. This is biased in the lab results by the somewhat anomalous conditions in run 12, without which all areas of change are below 2% of the total river area measured. Both the field and model showed the low probability of planform change occurring at peak discharges below 11 m^3s^{-1}(or model equivalent).

The three hydrograph experimental runs with a peak discharge of 14 m^3s^{-1} (2.22 ls^{-1}) had slightly higher average areas of planform change compared to all field measurements but were within the same range of variability of the equivalent field measurements for hydrographs with peak discharges ranging from 11-17 m^3s^{-1}. Daily hydrographs from the field in this peak discharge range had some cases with large areas of planform change but multiple days also showed no planform change at all. In slight contrast all flume experiments with a peak discharge equivalent to 14 m^3s^{-1} (2.22 ls^{-1}) had areas of planform change.

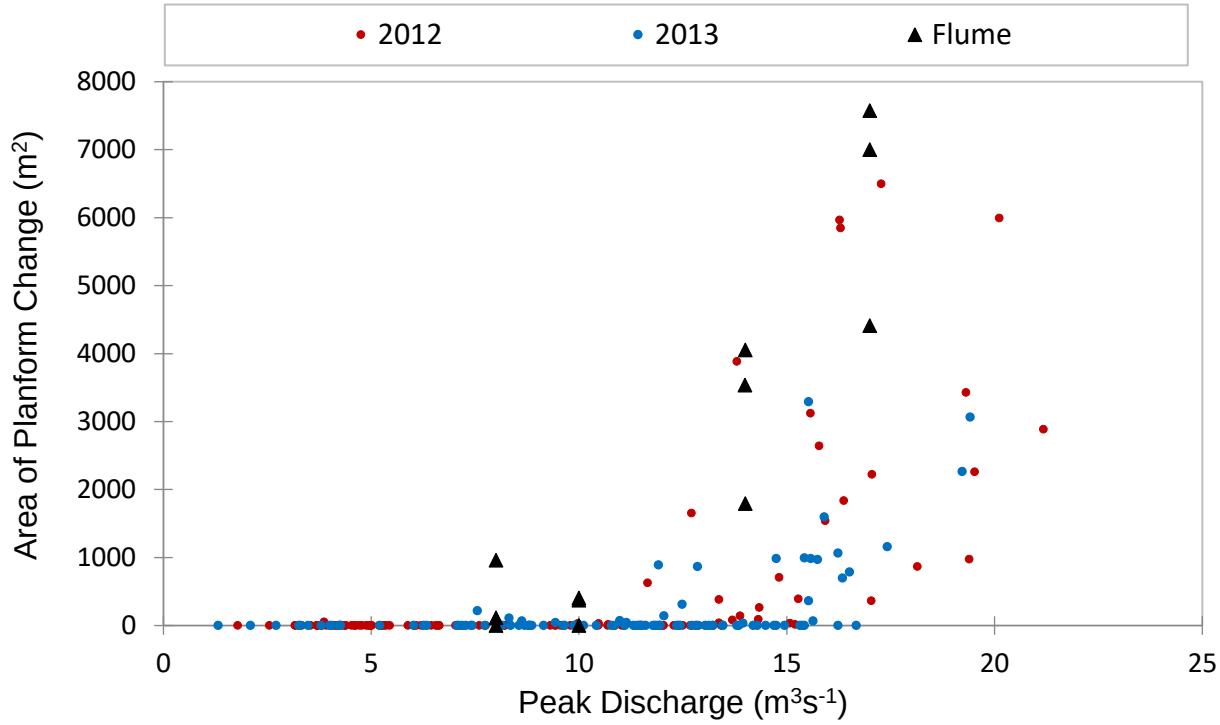

Figure 7.1: The relationship between areas of planform change and peak discharge for equivalent areas of the field and the field prototype (flume).

Higher areas of planform change in both the lab and field were evident as areas of change became connected across the river bed. This showed planform changes were conditional on the overall

channel pattern change and planform configuration. This was found in both the field and physical model but was made more evident when measuring a larger river length in the physical model compared to the field. For example, a change in the channel position upstream can be seen to divert water across a braid bar, highlighted in red in Figure 7.2 a, b. These planform changes are seen to alter the direction of flow and produce subsequent planform changes to a braid bar downstream highlighted in yellow. The highest planform changes measured on hydrographs with a peak between 11-17 m^3s^{-1} had similar areas in both the field and flume. These are shown in Figure 7.3a (area of planform change of 3882 m^2 in the field) and 7.3b (equivalent area of 4050 m^2 in the physical model).

This similarity in areas of change produced makes it reasonable to conclude that the larger equivalent area surveyed in the physical model was the same as results made over a shorter width in the field prototype. The planform area of field measurement is therefore sufficient to capture the dynamics of the braided system.

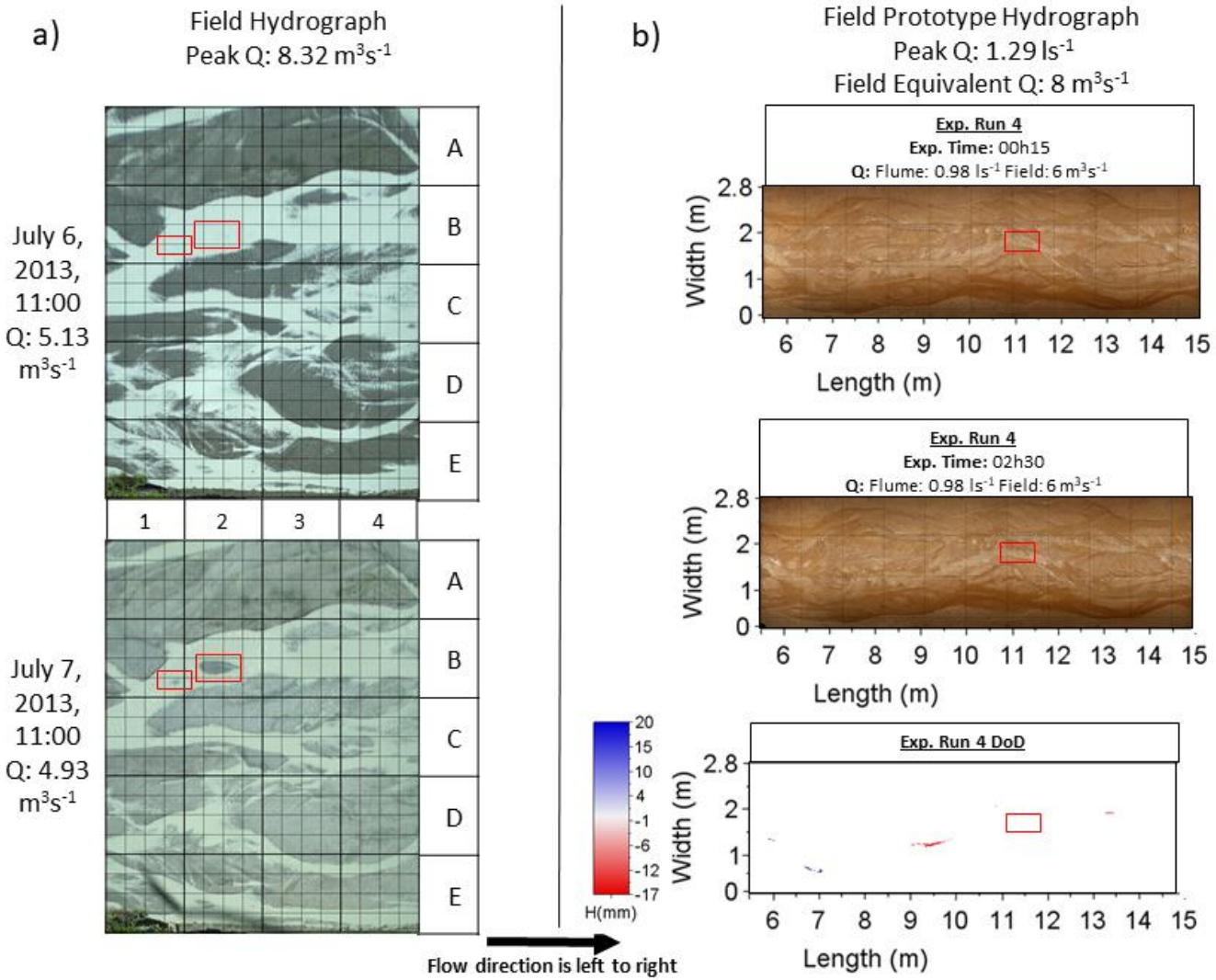

Figure 7.2: An example of planform changes over a daily hydrograph with a peak below 11 m^3s^{-1} in (a) the field and (b) the flume. The field show the deposition of sediment in the development of two unit bars highlighted in red whereas the flume recorded the erosion of sediment and channel incision as a unit bar was eroded.

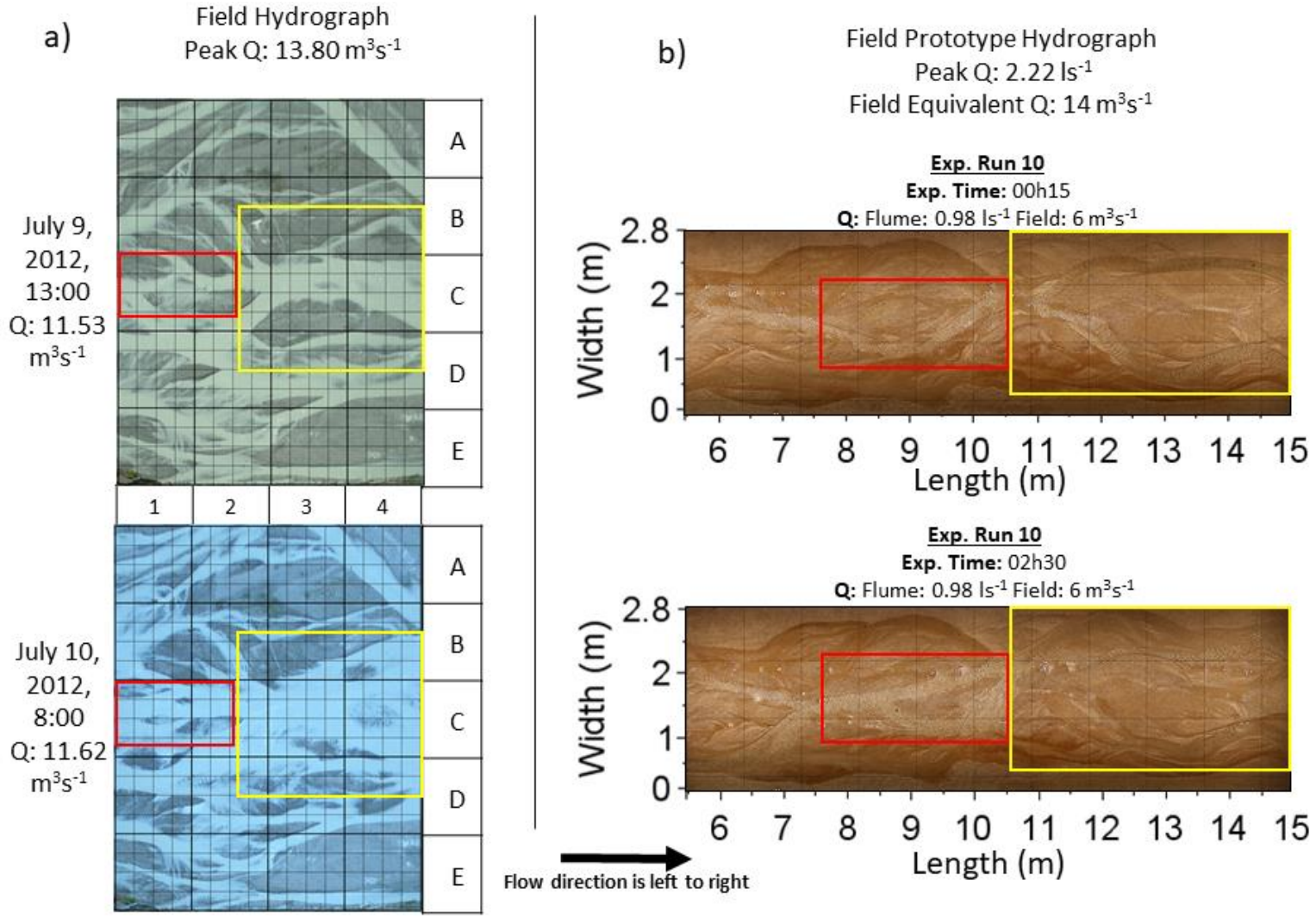

Figure 7.3: An example of planform changes over a daily hydrograph with a peak below 11-17 m^3s^{-1} in (a) the field and (b) the flume. Large planform change was recorded in more continuous areas across the river bed seen as a change in channel position highlighted in red changes the direction of flow and braid bar configuration downstream highlighted in yellow.

Peak discharges of 17 m^3s^{-1} and greater consistently produced areas of planform change in the field and physical model, with variability still recorded among the areas of change. Large changes recorded over daily hydrographs at the highest peak discharges resulted in the entire river planform being reworked, with only small areas of the river unchanged from the previous day. These changes were observed over all experimental runs at the highest peak discharge (2.74 ls^{-1}, equivalent to 17 m^3s^{-1}) but were not consistently observed at the equivalent peak discharges in the field. Areas of change measured in the physical model were slightly higher than those measured in the field at the highest discharges. Experimental run 3 and 7 (shown in Figure 7.4b) measured areas of change greater than 7000 m^2 while the highest area measured in the field was 6497 m^2 (Figure 7.4a).

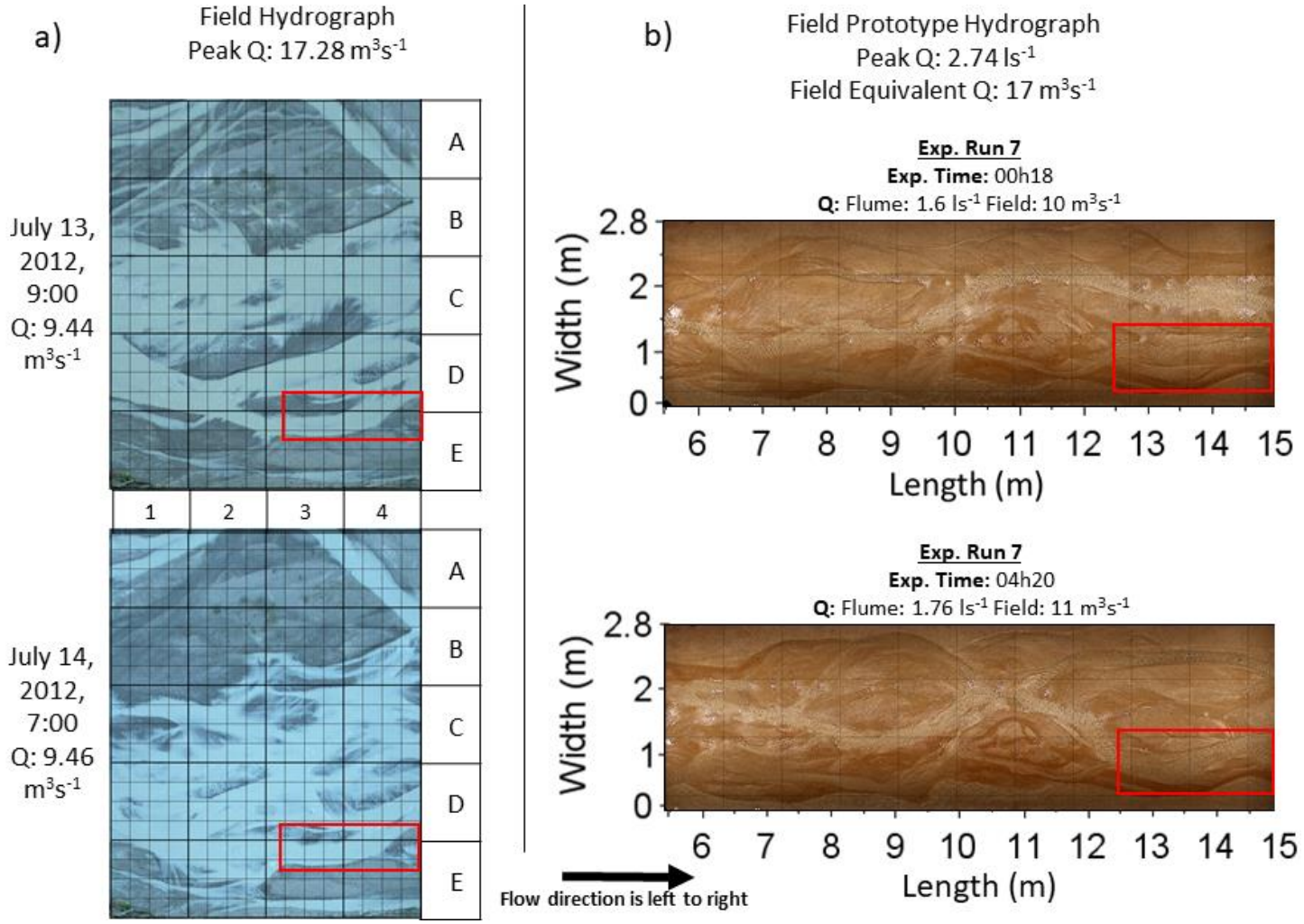

Figure 7.4: An example of planform changes over a daily hydrograph with a peak greater than 17 m^3s^{-1} in (a) the field and (b) the flume. The river planform experienced large changes in both settings with only small areas of the previous channel position remaining, highlighted in red. These sections of channel experienced changes in flow upstream which increased flow in both cases, causing the lateral expansion of the channels but with the planform position remaining the same overall.

Equivalent areas of planform change in relation to the wetted area had higher values for hydrographs replicated in the model compared to the field (Figure 7.5). The total wetted area was determined using automated image analysis for the field images, which was not possible in the flume due to the clear water and similarity between water and sediment in images. The wetted area of flume images was determined by visually measuring the wetted width at multiple cross sections, allowing an estimated area of each cross section, as discussed in section 4.5.1. The difference in methodologies may lead to the slightly smaller wetted areas detected in the flume where shallow flows are not easily seen, increasing the apparent area of planform change/wetted area (Figure 7.5). These shallow areas have a distinct colour in the field making detection much easier.

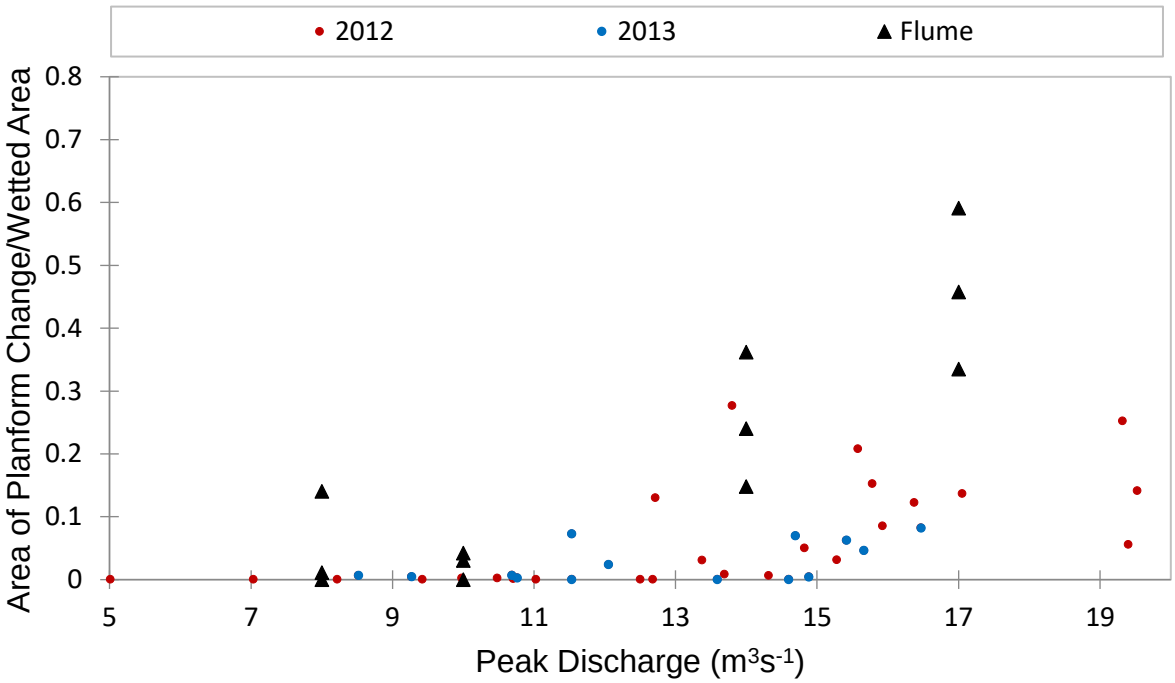

Figure 7.5: The relationship between the area of planform change/wetted area and peak discharge for equivalent areas of the field and physical model (flume).

7.2 Extension of Field Analysis

The laboratory analysis allowed the known relationship between planform change and discharge in the field to be extended, including the collection of morphological and bedload transport samples. The main objectives of the experiments were to confirm planform change rates in relation to hydrograph peak discharge and to determine the relationship between bedload transport,

morphology and planform change in a braided river to assess whether significant bedload transport and/or morphological change occurred independently of rates of planform change. This helped answered research question #4, if the measurement of planform change could be used as a surrogate method measuring bedload transport in a gravel-bed braided river.

Simultaneous measurements of the area of planform change, volumes of morphological change, and total weight of bedload transported over hydrograph experiments had a significant positive correlation. Bedload transport and morphological change were recorded over all hydrograph experiments but areas of planform change were not always observed. This occurred in only one experiment, run 9 (Figure 7.6) and may indicate that in some instances, small rates of bedload transport occur independently of planform change, masked by the inundated channel and involving small amounts of bed erosion or deposition with no discernible change in width, channel migration or bar erosion/deposition. This showed that the measurement of planform change provided comparable measurement of bedload transport except for at lower discharges and small 'background' noise of bedload transport in limited areas of the channel.

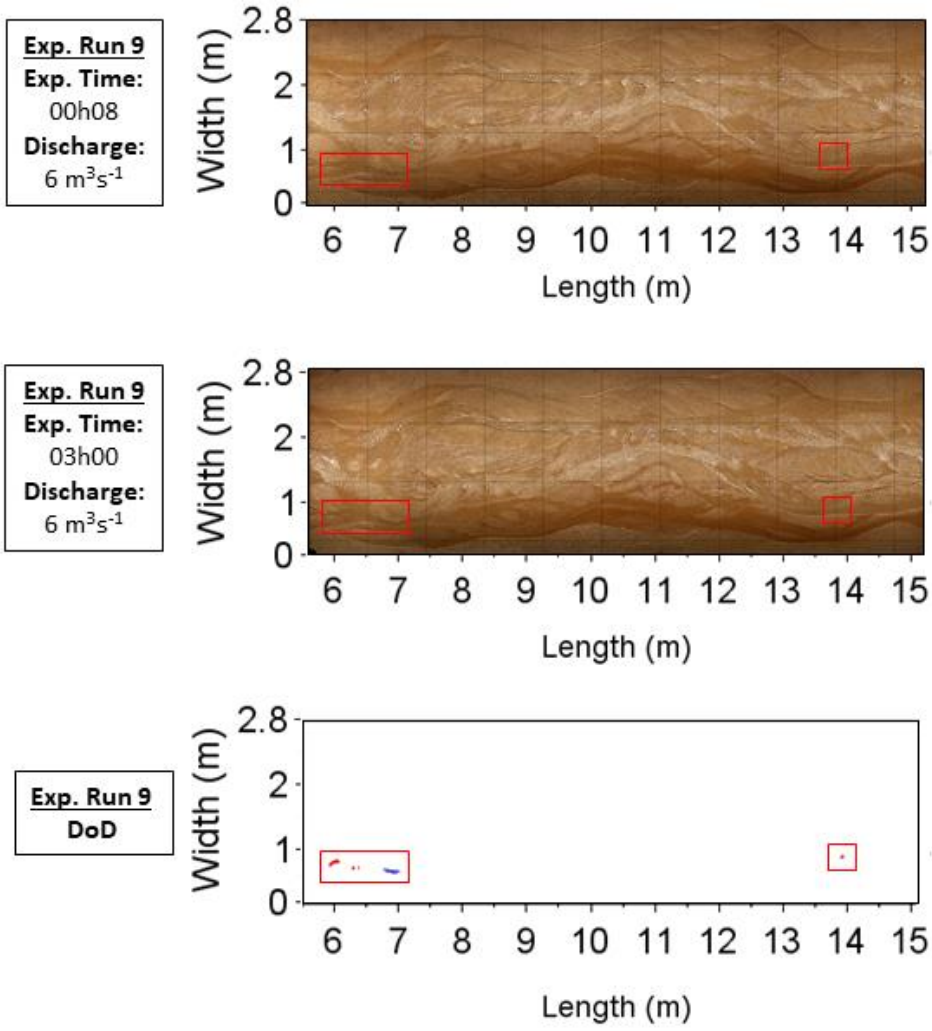

Figure 7.6: An example small morphological change detected where no planform change was observed, captured in experimental run 9, highlighted in the red boxes.

Flume experiments also allowed for observations to be made of bedload transport and the collection of bedload samples to see the grain size distribution to determine if all grain sizes were being transported at different measured areas of planform change. Grain size distributions showed no real trend between samples collected at different discharges. We can therefore expect that as substantial areas of planform change occur, the same grain size distribution is able to be transported. This has important implications for the application of planform measurements as a surrogate method for estimating rates of bedload transport in the field. Planform change can be a reliable method for directly measuring bedload transport in the context of the Sunwapta, with no adjustment of the grain size needed as part of prediction, answering research question #4.

Different planform configurations were found to alter the relationship, as discussed in Section 6.3.3.4. Areas of planform change measured and total bedload transport weights were found to have a more significant relationship when Experiments 11-12 were not included. A similar situation is possible in the field setting when a braided channel hits a valley wall or human interference. This is seen on the Sunwapta River where the primary channel has migrated into the highway, blocking further migration and reducing rates of planform change (Figure 7.7). While these braided configurations are possible they are seen to produce a different relationship to morphological change. As pattern processes change from a braided condition to local scour in a fixed channel, the planform/bedload relationship also changes. This was observed during Experimental run 11 and 12 which saw the primary channel hit the flume wall producing different morphological conditions and increased rates of sediment transport.

Figure 7.7: The current braided configuration of the Sunwapta River where the primary channel is seen to lie against the highway, reducing the rate of planform change.

While variable, the range of sediment weights transported was seen to increase in relation to an increase in the ABI up to an ABI of 3. ABI shows the extent of bedload transport within a braided network correlated to the area of change. Larger areas of planform change measured in the field would therefore be expected to have bedload transported in more channels. Only two observations were made of four active channels, both found to record a lower sediment weight than the highest weights at lower discharges. This may show that as flow is separated among more channels, the energy is divided, and while bedload is occurring in more channels, the total load may be lower.

This highlights one aspect of the variation in rates of bedload transport at different discharges and in relation to channel pattern.

7.3 Planform change and active width

The relationship between planform and morphological change can be compared in the field with previous studies related to topographic changes in a braided river. Previous studies on Sunwapta River have focused on 2-3 week periods of intense field work collecting measurements such as the active width and discharge (Ashmore et al. 2011) over this time but not at a longer temporal scale of study like the use of time-lapse imagery provides. The active width was measured for 2-3 week periods in 1999 and 2003 where repeated cross-sectional surveys were completed measuring areas of erosion and deposition in relation to peak discharge. This allows measurements of the area of planform change made in the field to be compared to previous morphological measurements which were also collected daily in relation to the daily peak discharge at the same study reach. Areas of planform change can be converted to determine the area that underwent planform change by dividing the area by the reach length. This allowed planform measurements of the river width to undergo change to be compared to morphological measurements of the active width, defined as the area of bed over which bedload flux and short-term morphological change occur.

2012 recorded 3 daily hydrographs with a width of planform change that exceeded 20% of the wetted width, which is higher than measured in any other years. 2003 and 2012 recorded measurements of a width of planform change or active width that was between 10-16% of the wetted width while 2003 and 2013 only saw widths of change below 10% (Figure 7.8). While similar peak flows were recorded, different years showed different potential for producing a planimetric or morphological change. Overall, widths of planform change (and therefore areas of planform change) measured in 2012 and 2013 lined up with morphological measurements made in 1999 and 2003, showing a similar threshold discharge for change and a similar proprtional area of change.

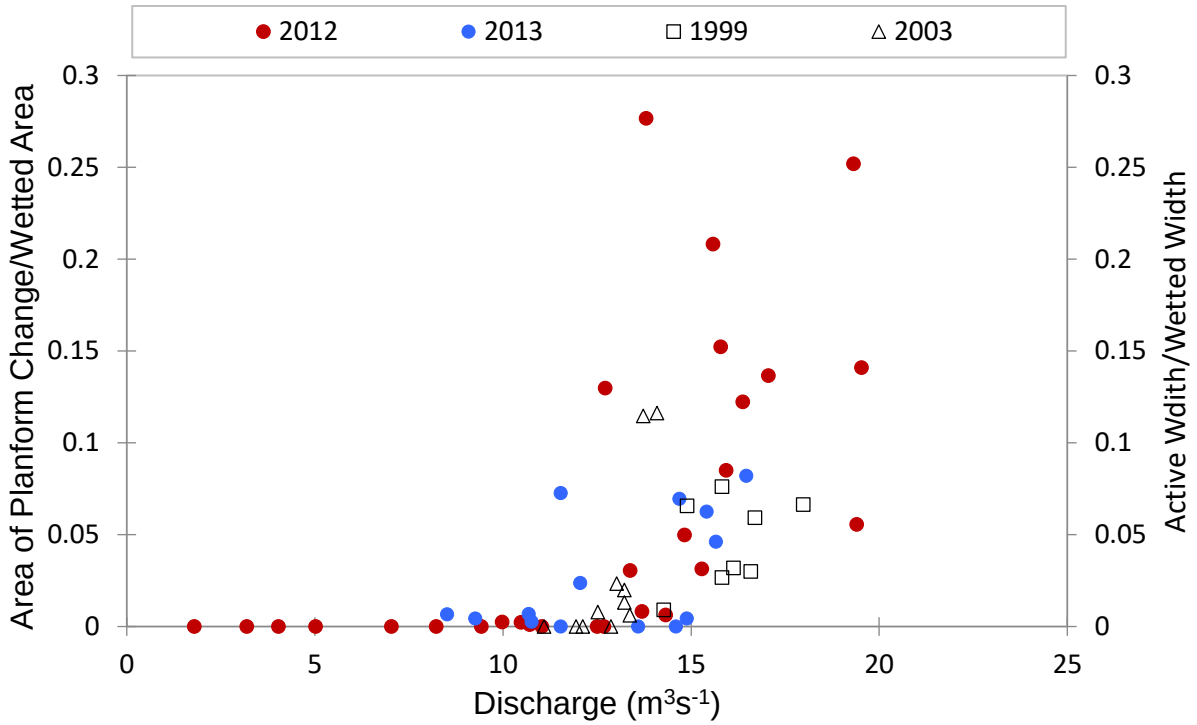

Figure 7.8: The relationship between active width/wetted area for previous measurements in 1999, 2003 and developed for this research for 2012 and 2013.

7.4 Planform change and bedload in gravel-bed braided rivers

Understanding of braided rivers and the complexity of these systems has been developed in the past 30 years (Ashmore, 2013). A large area of research has focussed on understanding the dynamic nature of these systems and rates of morphological change and bedload transport, related to different discharges. Field measurements of topographic changes in a braided river have typically focussed on measurements of morphological change, calculated through rates of erosion and deposition (Goff & Ashmore, 1994; Bertoldi et al. 2010; Ashmore et al. 2011) and through high resolution surveys of the topography to generate DEMs (Brasington et al. 2000; Lane et al. 2002; Hicks et al. 2003; Westoby, 2012; Tarolli, 2014; Wheaton et al. 2013; Micheletti et al. 2015; Smith et al. 2016). Due to the complicated nature of braided systems, field data is difficult to collect and is therefore widely spaced in time or covers only very limited all periods of time at higher temporal frequency.

Studies have turned to laboratory flumes where braided processes have been modelled successfully and the majority of knowledge on braided river morphodynamics and bedload transport has been

generated (Ashmore 1982; Ashmore, 1988; Ashmore, 1991; Young and Davies, 1990; Warburton, 1996; Schvidchenko and Kopaliani, 1998; Bertoldi et al. 2006, 2009; Ashmore et al. 2011; Mao, 2012; Peirce, 2017). The studies of Mao (2012) and Peirce (2017) also studied the effects of a hydrograph on rates of bedload transport but discharge was stopped between hydrograph steps, therefore utilizing a constant-flow to collect measurements. This research has extended these studies as well other laboratory data of braided rivers by modelling experiments using an unsteady flow, which has seldom been done previously. Many studies completed in the laboratory setting have recorded the river planform throughout experiments to understand how the planform and morphology are adjusted through experiments but areas of planform change have not been quantified in a systematic way. In this thesis, measurements of planform and morphological change as well as bedload transport were collected over the entire hydrograph, capturing the unsteady flow and providing a better comparison of braided river dynamics in a laboratory setting to the dynamic nature of these systems in the field.

The planform of braided rivers has been studied in the field with studies typically focussing on detailed planform mechanics over short time frames at a high frequency (Arscott et al. 2002; Bertoldi et al. 2009; Bertoldi, 2012) or the long term study of historical planform changes with widely spaced measurements (multiple years) (Warburton et al. 1993; Luchi et al. 2007; East, 2017). The planform dynamics of braided systems have been studied in relation to different flow events with direct measures of bedload transport and morphological change but areas of planform have not been systematically completed, prior to Middleton, 2015 (Surian et al. 2009; Bertoldi et al. 2010).

This research has therefore extended the knowledge of braided rivers by quantifying the relationship between planform change, morphological change and bedload transport in a braided river and shown the significant correlation between these three measurements of change. This highlights the close connection and the potential to use one measure as a surrogate measure for others. The measurement of planform change therefore potentially provides a way of estimating rates of bedload transport in the field more easily and cheaply than for direct bedload measurements or detailed morphological change. Measurements of change could be collected throughout the meltwater season and provided a continuous and high-frequency record of planform changes and thus possible estimated rates of bedload transport. While planform change mapping

has been shown to be potentially reliable in the case of the Sunwapta River, similar studies are needed on other gravel-bed braided rivers to better determine the generality of the correlation between planform change and bedload transport gravel-bed braided rivers, especially for other types of discharge regimes.

Chapter 8

8 Summary and Conclusions

Daily measurements of planform change in the proglacial braided Sunwapta River were made using high frequency oblique time lapse images during the summer meltwater period. Selected daily hydrographs were then reproduced in a small-scale physical model to extend the field data to simultaneous observations of planform change, bedload, bedload grain size distribution and morphological change in relation to daily discharges of different magnitudes. The reanalysis of planform changes in the field from Middleton (2015) improved the accuracy of planform change measurements and data were extended by measuring area of change in relation to wetted area. This reanalysis showed no large areas of planform change to occur below 11 m^3s^{-1} with only select days found to record small areas of change and most daily hydrographs having zero observable areas of planform change. Areas of planform change were found to be variable at discharges greater than 11 m^3s^{-1} but consistent planform change occurred at discharges greater than 17 m^3s^{-1}.

Planform measurements made in the physical model were found to produce similar equivalent areas of change to areas of planform change measured in the field prototype. Automated measurement of planform change is problematic and at present manual identification of changes is necessary to achieve reliable results.

Areas of planform change quantified in the physical model were found to have a significant, positive relationship to the total volume of morphological change produced and total weight of bedload transported over a replicated daily event hydrograph. The relationship between variations in bedload transport rate and morphological change were consistent with previous studies of braided rivers (Ashmore et al. 2011; Peirce, 2017). Results showed some of the variability in rates of change is produced due to different styles of braiding configurations. When braiding processes shifted from braiding to local scour in a fixed channel the relationship between the rate of bedload transport and areas of planform change was different. This shift in braiding configurations was documented in the laboratory setting but is also possible in the field setting as braided channels adjust and are impacted by both natural and anthropogenic influences.

The strong positive correlation between planform change and bedload for a hydrograph event indicates that areas of planform change would provide a potential surrogate method for measuring rates of bedload transport in the context of the Sunwapta River, with the potential to apply this methodology to other gravel-bed braided rivers. The full mobility of grain size distributions at different discharges indicates that no adjustment is needed to also infer the grain size distribution of the predicted bedload transport from measured areas of planform change. These measurements have lead to insights into braided processes and provided an understanding of the connections between planform change, morphological change and bedload transport.

The prediction of both bedload transport and rates of channel adjustment are key issues in fluvial geomorphology and the study of braided rivers specifically (Gomez, 1991; Church, 2010; Luchi et al. 2007). This study shows the close relationship between the river planform, morphology and rates of bedload transport and proposes an alternative method to monitor rates of transport and channel adjustment simultaneously by inferring rates of bedload transport based on areas of planimetric change. This would allow these changes to be continuously monitored in a cost-effective manner. Therefore this research has important implications moving forward for braiding river management and has practical applications that will benefit not only geomorphologists but engineers, ecologists and river managers. Due to the complicated nature of braided rivers, historically the morphology has been drastically altered to provide a control on these systems. Across the world, and in Europe specifically, a large push has occurred for the restoration of these areas (Luchi et al 2007). The understanding of these systems is therefore becoming increasingly important and an understanding of the rates of bedload transport and how the channel planform position is subsequently altered are invaluable for producing the successful restoration of these systems and in providing process-based restoration targets.

In conclusion, this research has extended the understanding of braiding planform dynamics by quantifying areas of change at a high-frequency throughout a range of discharge conditions in a proglacial river.

8.1 Future Research

The results from the analysis of experiments conducted in the physical model showed the potential for future areas of study. The same data set used for field and flume analysis can be extended in

many ways to increase our understanding of the relationship between bedload transport, morphological and planform change and to further investigate the similarity between the field prototype and physical model.

Measurements were conducted over daily hydrograph periods but the analysis of the temporal variability of individual sediment samples over hydrograph experiments showed the limited stages at which substantial rates of bedload transport were possible. The high-frequency of time-lapse imagery from the both the field and flume setting, documenting planform changes would allow rates of planform change to be measured at a higher frequency, multiple times on the rising and falling limb of a daily hydrograph. This could potentially narrow the range and decrease the variability of discharges capable of producing planimetric changes and determine the amount of time capable of producing change on a daily basis.

The comparison of field prototype and physical model can be further analyzed using a range of different methodologies which were not the focus of this thesis. A comparison of the styles of planform/morphological change produced at different discharges and the potential of different configurations to drive planform change may yield interesting results and uncover some of the variability of rates of change. The planform and morphological features of these configurations could then also be measured in both locations to determine the similarity between the size of features in field prototype and physical model. Other potential analyses include the further measurement of Active Braiding Intensity (ABI) and Braiding Intensity (BI) to increase the accuracy of the inferred ABI rate from observations completed of sediment movement. ABI and BI measurements could be completed for both the field and flume setting using an image analysis program to map out channels using time-lapse imagery and active channels using DoDs at multiple cross sections.

This study aimed to capture the natural variability of braided river systems by modelling hydrographs using unsteady discharge compared to the majority of physical model experiments run at a constant discharge (Young & Davies, 1990). While this approach attempted to fill this research gap much more research is needed in physical models, replicating field conditions of braided systems. This would help develop a better understanding of the errors associated with scaling time from the field prototype to model, which is not well understood. For experimental work to be fully justified (Schumm et al. 1987), results need to be applied to a field setting which

needs to be completed more often to understand scaling impacts when modelling specific field prototypes in a physical model.

2012 saw two periods of peak discharges exceeding 17 m^3s^{-1} while this only occurred on one occasion in 2013. These higher flow periods were also seen to be longer in 2012 with more peak flows produced. 2012 saw two extended flow periods during which peak discharges were above 17m^3s^{-1} for 5 subsequent days in July and again for 3 subsequent days in August. 2013 however only saw one such extended flow period but only two days recorded discharges greater than 17 m^3s^{-1}. This is also reflected in the rates of planform change as 2012 produced higher areas of change, on more daily hydrograph measurements. This may show the potential for increased rates of change in relation to an increase in the number of peak flow days noted by Haines (2012). A long-term study of planform changes over daily hydrographs each meltwater season may show a further trend in this relationship.

8.2 Concluding Statements

In conclusion, the research presented found that:

1) Automated detection of planform changes in the field setting of a proglacial gravel-bed braided river were not reliable.
2) Areas of planform change, volumes of morphological change and total bedload transport over a daily hydrograph were significantly correlated over hydrograph experiments in the physical model.
3) Equivalent areas and styles of planform change measured in the physical model were comparable to the equivalent areas and styles planform change measured on the field prototype, Sunwapta River, providing validation of the physical model.
4) Measurement of planform change provided a comparable measurement of bedload transport on the Sunwapta River but may miss small ‘background’ transport at lower discharges when no changes are observed in the river planform.

This has confirmed previous knowledge of the planform dynamics of gravel-bed braided rivers and extends the study of Middleton (2015) by increasing the accuracy of the measurement of planimetric change in the field and relating equivalent areas of planform change to simultaneous measurements of bedload transport and volumes of morphological change over hydrograph experiments in the physical model.

References

Ashmore, P. (1982). Laboratory modelling of gravel braided stream morphology. *Earth Surface Processes and Landforms, 7,* 201-225.

Ashmore, P. E. (1988). Bed load transport in braided gravel-bed stream models. *Earth Surface Processes and Landforms, 13,* 677-695.

Ashmore, P. (1991) a. Channel morphology and bed load pulses in braided, gravel-bed streams. *Geografiska Annaler. Series A, Physical Geography, 73,* 37-52.

Ashmore, P. (1991) b. How do gravel bed rivers braid? *Canadian Journal of Earth Sciences, 28,* 236-341.

Ashmore, P. (1993) Anabranch confluence kinetics and sedimentation processes in gravel-braided streams. *Geological Society Special Publication, 75,* 129-146.

Ashmore, P. (2009). Intensity and characteristic length of braided river channel patterns. *Canadian Journal of Civil Engineering*, 36, 1656-1666.

Ashmore, P. 2013. Morphology and dynamics of braided rivers. In, Shroder, J. (Editor in Chief) Wohl, E. (Ed.) Treatise on Geomorphology. Academic Press, San Diego, CA vol. 9, Fluvial Geomorphology, pp 289-312.

Ashmore, P., & Church, M. (1998). Sediment transport and river morphology: a paradigm for study. In *Gravel-Bed Rivers in the Environment* (pp. 115–148).

Ashmore, P. & Sauks, E. (2006). Prediction of discharge from water surface width in a braided river with implications for at-a-station hydraulic geometry. *Water Resources Research, 42.* 1-11.

Ashmore, P., Bertoldi, W., & Gardner, T. J. (2011) Active width of gravel-bed braided rivers. *Earth Surface Processes and Landforms, 36,* 1510-1521.

Ashmore, P., & Rennie, C. D. (2013). Gravel-bed rivers: from particles to patterns. *Earth Surface Processes and Landforms*, 217-220.

Ashworth, P.J., Best, J.L., Jones, M. (2004) Relationship between sediment supply and avulsion frequency in braided rivers. *Geology, 32 (1)* 21-24.

Ashworth, P.J., Best, J.L. & Jones, M. (2007). The relationship between channel avulsion, flow occupancy and aggradation in braided rivers: insights from an experimental model. *Sedimentology, 54.* 497-513.

Arscott, D.B., Tockner, K., van der Nat, D., Ward, J.V. (2002). *Ecosystems, 5,* 802-814.

Bennett, S.J., Ashmore, P., McKenna Neuman, C. (2015). Transformative geomorphic research using laboratory experimenttion. *Geomorphology, 244,* 1-8.

Bertoldi, W. (2012). Life of a bifurcation in a gravel-bed braided river. *Earth Surface Processes and Landforms, 37,* 1327-1336.

Bertoldi, W., Amplatz T., Miori S., Zanoni L. & Tubino M. (2006a). Bed load fluctuations and channel processes in a braided network laboratory model. Proceedings of the International Conference on Fluvial Hydraulics-River Flow 2006 (Eds. Ferreira RML, Alves CTL, Leal GAB, Cardoso AH), London, Taylor & Francis, vol. 1, 937-945

Bertoldi, W., Gurnell, A., Surian, N., Tockner, K., Zanoni, L., Ziliani, L. & Zolezzi, G. (2009) Understanding reference processes: linkages between river flows, sediment dynamics and vegetated landforms along the Tagliamento River, Italy. *River Research and Applications, 25,* 501-516.

Bertoldi, W., Miori S., Salvaro M., Zanoni L. & Tubino M. (2006b). Morphological description of river bifurcations in gravel-bed braided networks. Proceedings of the International Conference on Fluvial Hydraulics-River Flow 2006 (Eds. Ferreira RML, Alves CTL, Leal GAB, Cardoso AH), London, Taylor & Francis, vol. 2, 1311-1318.

Brasington, J., Rumsby, B.T. & Mcvey. R.A. (2000). Monitoring and modelling morphological change in a braided gravel-bed river using high resolution GPS-based survey. *Earth Surface Processes and Landforms, 25,* 973-990.

Bridge, J.S. (1993). The interaction between channel geometry, water flow, sediment transport and deposition in braided rivers. *Geological Society, London, Special Publications,* 75 (1):13.

Chandler, J., Ashmore, P., Paola, C., Gooch, M., & Varkaris, F. (2002). Effective application of automated digital photogrammetry for geomorphological research. *Earth Surface Processes and Landforms, 24*(1), 51–63.

Chew, L.C. & Ashmore, P.E. (2001). Channel Adjustment and a test of rational regime theory in a proglacial braided stream. *Geomorphology, 37,* 43-63.

Church, M. (2010). Gravel-Bed Rivers. In T. Burt, & R. Allision, *Sediment Cascades: An Integrated Approach* (pp. 241-269). Hoboken: Wiley.

Church, M. & Gilbert, R. (1975). Proglacial Fluvial and Lacustrine Environments. *Glaciofluvial and Glaciolacustrine Sedimentation, 23,* 22-100.

Dietrich, J. T. (2016). Riverscape mapping with helicopter-based Structure-from-Motion photogrammetry. *Geomorphology, 252,* 144–157.

East, A.E., Jenkins, K.J., Happe, P.J., Bountry, J.A., Beechie, T.J., Mastin. M.C., Sankey, J.B., & Randle, T.J. (2017). Channel-planform evolution in four rivers of Olympic National Park, Washington, USA: the roles of physical drivers and trophic cascades. *Earth Surface Processes and Landforms, 42,* 1011-1032.

Egozi, R. & Ashmore, P. (2008) Experimental analysis of braided channel pattern response to increased discharge. *Journal of Geophysical Research, 114*. 1-15.

Fonstad, M. A., Dietrich, J. T., Courville, B. C., Jensen, J. L., & Carbonneau, P. E. (2013). Topographic structure from motion: A new development in photogrammetric measurement. *Earth Surface Processes and Landforms*, *38*(4), 421–430.

Gardner, J.T. & Ashmore, P.E. (2011) Geometry and grain-size characteristics of the basal surface of a braided river deposit. *Geology, 39 (3),* 247-250.

Goff, J.R. & Ashmore, P. (1994). Gravel transport and morphological change in braided Sunwapta River, Alberta Canada. *Earth Surface Processes and Landforms, 19*, 195-212.

Gran, K. & Paola, C. (2001). Riparian vegetation controls on braided stream dynamics. *Water Resources Research, 37(12),* 3275-3283.

Gomez, B. (1991). Bedload transport. *Earth-Science Reviews*, 31(2), 89-132.

Haines, H.A. (2012). Changes in the hydrological regime in the Upper Bow and Upper Athabasca Watersheds during the 20th century. Master's Thesis. Department of Geography, University of Western Ontario, London.

Haschenburger, J.K. (2013). Tracing river gravels: Insights into dispersion from a long-term field experiment. *Geomorphology, 200,* 121-131.

Hicks, D.M., Duncan, M.J., & Walsh, J.M. (2002). New views of the morphodynamics of large braided rivers from high-resolution topographic surveys and time-lapse video. *The Structure, Function and Management Implications of Fluvial Sedimentary Systems* (IAHS-AISH Publication no. 276_2002).

Hicks, D. M., Duncan, M.J., Lane, S. N., Tal, M., & Westaway, R. (2008). Contemporary morphological change in braided gravel-bed rivers: new developments from field and laboratory studies, with particular reference to the influence of riparian vegetation. In H. Habersack, H. Piegay, & M. Rinaldi (Eds.), Gravel Bed Rivers VI: From Process Understanding to River Restoration (pp. 557-586). Amsterdam: Elsevier.

Hicks, D. M., Westaway, R., & Lane, S. (2003). A bird's-eye assessment of gravel movement in large braided rivers. *Water and Atmosphere, 11(1),* 21-23.

Hoey, T. B. & Sutherland, A. J. (1991) Channel morphology and bedload pulses in braided rivers: a laboratory study. *Earth Surface Processes and Landforms, 16*, 447-462.

Hundey, E.J. & Ashmore, P.E. (2009). Length scale of braided river morphology. *Water Resources Research, 45,* 1-9.

Javernick, L., Brasington, J., Caruso, B., Hicks, M. & Davies, T. (2012). Creating High Quality DEMs of Large Scale Fluvial Environments Using Structure-from-Motion. *Poster presented at American Geophysical Union Fall Meeting, California, USA,* December 3-7, 2012.

Javernick, L., Brasington, J., & Caruso, B. (2014). Modeling the topography of shallow braided rivers using Structure-from-Motion photogrammetry. *Geomorphology*, *213*, 166–182.

Kasprak, A., Wheaton, J. M., Ashmore, P., Hensleigh, J. W., & Peirce, S. (2015). The relationship between particle travel distance and channel morphology : Results from physical models of braided rivers. *Journal of Geophysical Research F: Earth Surface, 120*(1), 55–74.

Kussner, B. D. 1995. Variation in bedload transport: Sunwapta River, Alberta. Master's Thesis. Department of Geography, University of Western Ontario, London.

Leduc, P., Ashmore, P., & Sjogren, D. (in press). Technical note: Stage and water width measurement of a mountain stream using a simple time-lapse camera. *Hydrology and Earth Systems Sciences.*

Lajeunesse, E., Malverti, L. & Charru, F. (2010). Bed load tranpsort in turbulent flow at the grain scale: Experiments and modeling. *Journal of Geophysical Research, 115,* F04001.

Liu, Y., Métivier, F., Lajeunesse, É., Lancien, P., Narteau, C., Ye, B. & Meunier, P. (2008) Measuring bedload in gravel-bed mountain rivers: averaging methods and sampling strategies. *Geodinamica Acta 21/1-2,* 81-92.

Luchi, R., Bertoldi, W., Zolezzi, G., Tubino, M. (2007). Monitoring and predicting channel change in a free-evolving, small Alpine river: Ridanna Creek (North East Italy). *Earth Surface Processes and Landforms, 32,* 2104-2119.

Mao, L., Cooper, J.R. & Frostick, L.E. (2011). Grain size and topographical differences between static and moble armour layers. *Earth Surface Processes and Landforms, 36,* 1321-1334.

Mao, L. (2012). The effect of hydrographs on bedload transport and bed sediment spatial arrangement. *Journal of Geophysical Research (117),* 1-16.

McKenna Neuman, C., Ashmore, P., & Bennett, S.J. (2013). Laboratory and Experimental Geomorphology: Examples from Fluvial and Aeolian Systems. In J. Shroder (Ed.), *Treatise on Geomorphology* (pp. 325-348). San Diego: Academic Press.

Meesuk, V., Vojinovic Z., Mynett, A.E. & Abdullah, A.F. (2015). Urban flood modelling combining top-view LiDAR with ground-view SfM observations. *Advances in Water Resources, 75,* 105-117.

Micheletti, N., Chandler, J. H., & Lane, S. N. (2015a) Structure from Motion (SfM) Photogrammetry, Photogrammetric heritage, *2,* 1–12.

Micheletti, N., Chandler, J. H., & Lane, S. N. (2015)b. Investigating the geomorphological potential of freely available and accessible structure-from-motion photogrammetry using a smartphone. *Earth Surface Processes and Landforms, 40*(4), 473–486.

Metivier, F. & Meunier, P. (2003). Input and output mass flux correlations in an experimental braided stream. Implications on the dynamics of bedload transport. *Journal of Hydrology, 271,* 22-38.

Middleton, L. (2015). Braiding Channel Pattern Dynamics in a Proglacial River. BSc Thesis. Department of Geography, University of Western Ontario.

Meunier, P., Metivier, F., Lajeunesse, E., Meriauz, A.S., & Faure, J. (2006). Flow pattern and sediment transport in a braided river: The "torrent de St Pierre" (French Alps). *Journal of Hydrology, 330,* 496-505.

Mueller, E. R., & Pitlick, J. (2014). Sediment supply and channel morphology in mountain river systems: 2. Single thread to braided transitions. *Journal of Geophysical Research: Earth Surface, 119,* 1516-1541.

Papangelakis, E., & Hassan, M.A. (2016). The role of channel morphology on the mobility and dispersion of bed sediment in a small gravel-bed stream. *Earth Surface Processes and Landforms, 41,* 2191-2206.

Peakall, J., Ashworth, P., & Best, J. (1996). Physical Modelling in Fluvial Geomorphology: Principles, Applications and Unresolved Issues. In B. L. Rhoads, & C. E. Thorn (Ed.), The Scientific Nature of Geomorphology: Proceedings of the 27th Binghamton Symposium in Geomorphology (pp. 221-253). John Wiley & Sons Ltd.

Piégay, H., Grant, G., Nakamura, F., & Trustrum, N. (2006). Braided river management from assessment of river behaviour to improved sustainable development. In G. H. Sambrook Smith, J. L. Best, C. S. Bristow, & G. E. Petts (Eds.), *Braided Rivers: Process, Deposits, Ecology and Management* (pp. 257-276). Malden, MA: Blackwell Publishing Ltd.

Peirce, S. E. K. (2017). Morphological Bedload Transport in Gravel-Bed Braided Rivers. PhD Thesis. Department of Geography, Univseristy of Western Ontario.

Robert, A. (2003). Flow and sediment dynamics in curved, braided, and confluent channels. In *River Processes* (pp. 129-167). New York, NY: Routledge.

Sapozhnikov, V.B. and Foufoua-Georgiou, E. (1997). Experimental evidence of dynamic scaling and indications of self-organized criticality in braided rivers. *Water Resources Research 33(8),* 1983-1991.

Schmidt, L. J. & Potyondy, J. P. (2004). Quantifying channel maintenance instream flows: an approach for gravel-bed streams in the Western United States. Gen. Tech. Rep. RMRS-GTR-128. Fort Collins, CO: U.S. Department of Agriculture, Forest Service, Rocky Mountain Research Station. 33 p.

Schumm, S. A., Mosley, M. P., & Weaver, W. E. (1987). *Experimental Fluvial Geomorphology*. New York: John Wiley & Sons Ltd.

Shvidchenko, A. B. & Kopaliani, Z. D. (1998) Hydraulic modeling of bed load transport in gravel-bed Laba River. *Journal of Hydraulic Engineering, 124,* 778-785.

Smith, M. W., Carrivick, J. L., & Quincey, D. J. (2016). Structure from motion photogrammetry in physical geography. *Progress in Physical Geography, 40(2),* 247-275.

Smith, M. W., Carrivick, J. L., Hooke, J., & Kirkby, M. J. (2014). Reconstructing flash flood magnitudes using "Structure-from-Motion": A rapid assessment tool. *Journal of Hydrology, 519*(PB), 1914–1927.

Smith, N.D. (1964). Sedimentology and Bar Formation in the Upper Kicking Horse River, a Braided Outwash Stream. *The Journal of Geology, 82,* 205-223.

Surian, N., & Cisotto, A. (2007). Channel adjustments, bedload transport and sediment sources in a gravel-bed river, Brenta River, Italy. *Earth Surface Processes and Landforms, 32,* 1641–1656.

Varkaris, F.C. 2002. Variability in bedload sediment transport estimates, Sunwapta River, Alberta, Canada. Master's Thesis. Department of Geography, University of Western Ontario, London.

Tal, M., Gran, C., Bray Murray, A., Paola, C., & Hicks, D.M. (2004). Riparian Vegetation as a Primary Control on Channel Characteristics in Multi-thread rivers. From: Riparian Vegetation and Fluvial Geomorphology; Water Science and Application, Vol. 8, Bennett SJ, Simon A (eds). American Geophysical Union: Washington, DC; 43–58.

Tal, M., & Paola, C. (2010). Effects of vegetation on channel morphodynamics: results and insights from laboratory experiments. *Earth Surface Processes and Landforms, 35,* 1014-1028.

Tamminga, A.D., Eaton, B.C. & Hugenholtz, C.H. (2015). UAS-based remote sensing of fluvial change following an extreme flood event. *Earth Surface Processes and Landforms.*

Tarolli, P. (2014). High-resolution topography for understanding Earth surface processes: Opportunities and challenges. *Geomorphology, 216,* 295–312.

Warburton, J. (1996a). Active braidplain width, bed load transport and channel morphology in a model braided river. *Journal of Hydrology (NZ), 35 (2),* 258-285.

Warburton, J. (1996b). A brief review of hydraulic modelling of braided gravel-bed rivers in New Zealand. *Journal of Hydrology (NZ), 35(2),* 157-173.

Warburton J. & Davies, T. (1994) Variability of bedload transport and channel morphology in a braided river hydraulic model. *Earth Surface Processes and Landforms, 19,* 5, 403-421.

Warburton, J., Davies, T.R.H., & Mandl, M.G. (1993). A meso-scale field investigation of channel change and floodplain characteristics in an upland braided gravel-bed river, New Zealand. *From* Nest, J.L. & Bristow, C.S. (eds), 1993, *Braided Rivers,* Geological Society Special Publication No. **75,** pp. 241-255.

Westoby, M.J,, Brasington, J., Glasser, N.F., Hambrey, M.J. & Reynolds, J.M. (2012). 'Structure from-Motion' photogrammetry: A low cost, effective tool for geoscience applications. *Geomorphology, 179,* 300-314.

Wheaton, J. M., Brasington, J., Darby, S. E., Kasprak, A., Sear, D. & Vericat, D. (2013). Morphodynamic signatures of braiding mechanisms as expressed through change in sediment storage in a gravel-bed river. *Journal of Geophysical Research: Earth Surface, 118,* 759-779.

Williams, R.D., Brasington, J., Vericat, D., & Hicks, D.M. (2014). Hyperscale terrain modelling of braided rivers: fusing mobile terrestrial laser scanning and optical bathymetric mapping. *Earth Surface Processes and Landforms, 39,* 167-183.

Williams, R.D., Rennie, C.D., Brasington, J., Hicks, D.M., Vericat, D. (2015) Linking the spatial distribution of bedload transport to morphological change during high-flow events in a shallow braided river. *Journal of Geophysical Research, Earth Surface, 120,* 604-622.

Woodget, A.S., Carbonneau, P.E., Visser, F., & Maddock, I.P. (2014). Quantifying submerged fluvial topography using hyperspatial resolution UAS imagery and structure from motion photogrammetry. *Earth Surface Processes and Landforms, 40,* 47-64.

Wohl, E. (2013). Field and Laboratory Experiments in Fluvial Geomorphology. In J. Shroder (Ed.), *Treatise on Geomorphology* (pp. 679-693). San Diego: Academic Press.

Yalin, M.S. (1971). Theory of hydraulic models. Macmillan, London.

Young. W.J & Davies, T.R.H. (1990). Prediction of bedload transport rates in braided rivers: a hydraulic model study. *Journal of Hydrology (NZ), 29 (2).* 75-92.

Young, W., & Warburton, J. (1996). Principles and practice of hydraulic modelling of braided gravel-bed rivers. *Journal of Hydrology (NZ), 35*(2), 175-198.

Appendices

Appendix A Structure from Motion Photogrammetry

Photogrammetry is a common method of deriving topographic data from overlapping images collected at multiple different viewpoints. Recently, technological advancements have greatly increased the use photogrammetry through a new method, Structure from Motion (SfM) which is heavily automated, greatly decreasing the amount of work and the expertise needed to produce topographic data (Micheletti et al. 2015). Fluvial surfaces pose more problems for SfM and for remote sensing overall but multiple studies have used this method successfully to demonstrate fluvial topography in different ways. These studies have focused on completing surveys in ephemeral rivers or at low flow periods to obtain as much topographic data as possible (Fonstad, 2013; Smith et al. 2014; Dietrich, 2016), or combining SfM with other methods to produce a full Digital Elevation Model (DEM) of submerged and unsubmerged areas (Javernick et al. 2014; Meesuk, 2015; Woodget, 2015).

The majority of imagery can be used to input into SfM software and high resolution outputs can be achieved with consumer grade cameras. Image data sets have even been collected through images downloaded from the internet or through raw video footage. At short ranges low-cost cameras such as those imbedded in smart phones had comparable point cloud quality with no significant differences shown from those taken with a more expensive, digital SLR camera (Micheletti et al. 2015b; Smith et al. 2016). At longer survey ranges above 100 m such as in aerial platforms, the highest results can be achieved using a digital SLR camera equipped with a fixed focus lens (Micheletti et al. 2015a; Smith et al. 2016).

The application of SfM in braided river research

While problems for fluvial topographic surveys like partial inundation, high sediment mobility and complex topography exist in all areas of fluvial geomorphology, these are especially true for braided river systems due to their complex and high energy nature (Javernick et al. 2012). Braided rivers, commonly found in mountainous terrain offer an ideal location to implement SfM in fluvial geomorphology allowing surveys to be performed remotely using UAVs (Ashmore, 2013, Smith et al. 2016). Alternatively in alpine terrain, surrounding cliff ledges or valley slopes could be used to obtain images from a higher view point as done in Smith et al. 2014.

SfM Field Studies

While SfM can currently only survey submerged areas that are shallow, it can be combined with other methods to produce a full topographic survey of a braided river network. Javernick et al. 2014 used SfM in combination with optical bathymetric modeling to model two study reaches (1.6 and 1.7 km long) of the Ahuriri River in New Zealand. The final outputs produced were a detrended DEM and the bathymetric modeled water depth. Overall over three km of river reach were surveyed with results indicating that geo-registration errors of 0.04 m (planar) and 0.10 (elevation) can be achieved with photographs taken from 600m and 800m. This study utilized a helicopter platform to obtain images allowing the large spatial extent of the river to be mapped. As shown in Smith et al. 2016 however this also reduces the resolution and less error would be observed at smaller scales from shorter distances.

Tamminga et al. 2015 completed topographic surveys of the Elbow River, Southern Alberta of a braided/wandering one km reach. While the topographic survey recorded was with traditional photogrammetry, similar approaches could be applied using SfM. Using SfM to record topographic data of braided rivers at low flow would provide a cheaper alternative to traditional photogrammetry and produce outputs of similar accuracy. Orthomosaics produced through SfM would allow for assessments of planform and morphological change in a braided river after an extreme flood event. This could allow for measurements of lateral expansion, which would show which channel features remain or were eroded away and potentially where areas of erosion and deposition may be. The DEMs would not show topographic changes in areas currently inundated unless they were quite shallow, when subject to extreme floods all areas of the river channel would have been inundated. Once water levels reside however, much of the bed is exposed, allowing DEMs to be obtained of these areas. This could potentially lead to the ability to measure volumes of sediment eroded, bedload transport rates and the volume of sediment eroded from the banks due to lateral expansion.

SfM Flume Studies

Due to the complexity of braided river systems, research has often turned towards the use of physical models, such as flumes to better understand braiding processes. While not commonly done, SfM can be used in a laboratory setting to derive DEMs, DoDs and stitched orthomosaics. Due to the close proximity setting, high accuracy is achievable using SfM and the ability to stop

water allows DEMs to be derived of the entire river bed once it has dried between experiments. Kasprak et al. 2014 used SfM in a flume to measure particle travel distance with tracers and volumes of sediment eroded during experimental runs.

Appendix B Bubbler Sensor System

"Bubbler" sensors are used widely by the WSC and operated using a digital sensor that measures the amount of gas pressure that is required to generate a bubble at the end of a submerged orifice line (Figure B-1). The pressure that is required to create the bubble is then proportional to water head height above the orifice and therefore is the equivalent to the water level stage.

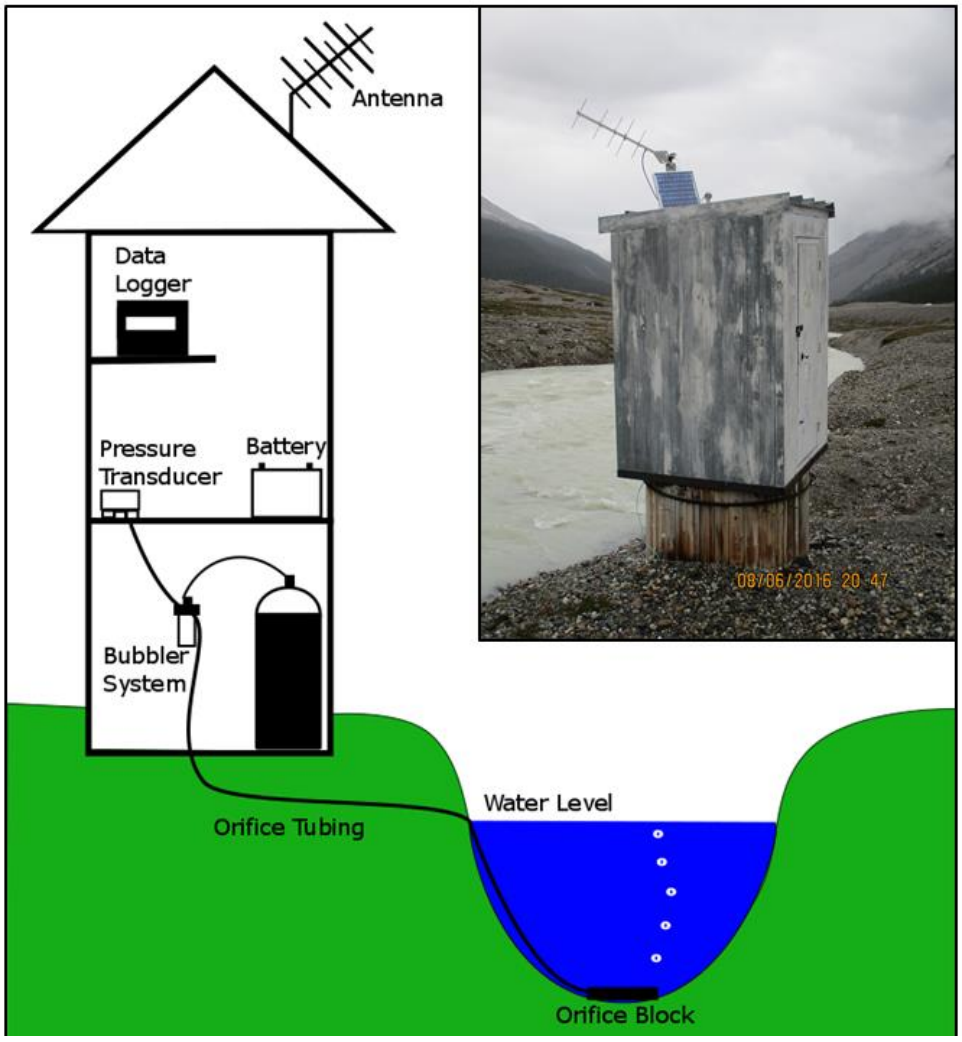

Figure B.1: A diagram of the typical model of a Pressure Bubbler Sensor operating system with the WSC operating system set-up on the Sunwapta River, immediately downstream of Sunwapta Lake. Adapted from Water Survey of Canada.

Appendix C Slope

The slope remained at 1.5% throughout all experimental runs to replicate the slope of the Sunwapta study reach, determined by Froude scaling. Slope was determined using a Leica TCA 1800 total station with the survey method adapted from Gardner, 2009. This involved two surveys to be completed from two different locations with three external control points located on the laboratory walls. These points were recorded at the beginning and at the end of each survey to ensure accuracy (<0.002”) of coordinates and survey orientation. Within the flume, 18 coded targets were distributed on the side of both walls two meters apart and surveyed from both locations. The average horizontal and vertical angles were converted to a 3D (xyz) position using trigonometry.

Appendix D Estimation of Flume Discharge

The estimated discharge was calculated by using a custom-built pool attached to the edges of the weir with a vertical scale on both the upstream and downstream end where the water height could be read. Over a series of slope and discharge settings, the time it took to fill the pool was measured. The height of water in the head tank could then be linearly related to the discharge flowing over the weir. While several sources of error exist, this was minimized by running each measurement three times and having the same person at each station throughout measurements. Discharge values have an estimated error of ~5% based on the relative error shown in Table 4.1.

Table D.1: The relative error in discharge measurements in the flume as a function of the head tank water height.

Relative Error	**Q (ls^{-1})**
Mean	0.045
Minimum	0.001
Maximum	0.15
Standard Deviation	0.44

Appendix E Summary of Linear Correlation

Two types of regression have been used to understand different relationships throughout this thesis. Both power and linear functions report the root-mean-square error (RMSE) as an indication of the measure of difference between variables. The 95th confidence interval of the mean confidence interval of the prediction are indicated where applicable on linear functions.

Select linear relationships have been further explored to determine the correlation between two variables using Pearson's Correlation Analysis. The summary statistics of these relationships is provided below; n is the number of observations, the min., max., and mean values represent the minimum, maximum and average results, SD is the standard deviation, PCC is the Pearson's correlation coefficient and the p-values are computed using $\alpha = 0.05$.

Table E.1: Summary of statistics of the original areas of planform change measured and the same daily hydrograph re-measured.

	n	Min	Max	Mean	SD	PCC	P-value
Original Measured Areas of Planform Change (m^2)	19	0	2357.683	358.275	635.173	0.994	< 0.0001
Re-Measured Areas (m^2)	117	0	0	0	0		

Table E.2: Summary of statistics for the areas of planform change measured in the field on daily hydrographs with peaks below 11 m^3s^{-1} .

	n	Min	Max	Mean	SD	PCC	P-value
Measured Areas of Planform Change (m^2)	117	0	80.994	2.073	9.292	1	0
Zero Slope	117	0	0	0	0		

Table E.3: Summary of statistics for the areas of planform change and volumes of morphological change over hydrographs in the physical model.

	n	Min	Max	Mean	Standard Deviation	PCC	P-value
Areas of Planform Change (m^2)	12	0	6.957	2.314	2.524	0.928	< 0.0001
Volumes of Morphological Change (m^3)	12	0.008	0.211	0.079	0.070		

Table E.4: Summary of statistics for the areas of planform change and total bedload transported over hydrograph experiments 1-12 in the physical model.

	n	Min	Max	Mean	Standard Deviation	PCC	P-value
Areas of Planform Change (m^2)	12	0	6.957	2.314	2.524	0.586	0.004
Total Bedload Transport Weight (kg)	12	1.065	116.782	29.429	39.104		

Table E.5: Summary of statistics for the areas of planform change and total bedload transported over hydrograph experiments 1-10 in the physical model.

	n	Min	Max	Mean	Standard Deviation	PCC	P-value
Areas of Planform Change (m^2)	10	0	6.957	2.283	2.688	0.820	0.0003
Total Bedload Transport Weight (kg)	10	1.065	116.782	29.429	39.104		

Appendix F Summary of Boxplots

Box plots in the thesis displayed the median weight with the central horizontal bars, the first and third quartiles as the lower and upper limit of the box respectively and the mean weight as a black cross. The minimum and maximum weights are identified in the black diamond with the maximum weights all outliers, lying above the whisker showing the third quartile + 1.5 x the inter-quartile range. The summary statistics of the one box plot (Figure 6.13) are provided below.

Table F.1: Summary of statistics for the sediment weights transported at different observed Active Braiding Intensities.

Statistic	**Active Braiding Intensity**			
	0	1	2	3+
# of observations	16	61	30	25
Min.	0.370	1.130	6.677	5.517
Max.	127.427	453.020	1166.367	1166.330
1st Quartile	2.859	9.010	43.319	68.190
Median	6.215	24.377	126.795	183.003
3rd Quartile	28.561	83.914	262.317	469.410
Mean	20.912	63.181	204.191	285.037
Variance (n-1)	1074.070	7880.809	65092.287	83204.265
Standard deviation (n-1)	32.773	88.774	255.132	288.451

Curriculum Vitae

Name:	Lara Middleton
Post-secondary Education and Degrees	University of Western Ontario London, Ontario, Canada 2011-2015 BA University of Western Ontario London, Ontario, Canada 2015-Present MSc
Honours and Awards	Brian Luckman Award, 2016-2017 Dean's Honour List, 2014-2015
Related Work Experience	Teaching Assistant The University of Western Ontario 2015-2017 Research Assistant The University of Western Ontario 2014-2016
Conferences and Publications	**Middleton, L.** (2015). *Braiding Channel Pattern Dynamics in a Proglacial River*. BSc Thesis. Department of Geography, University of Western Ontario. **Middleton, L.** *The Sunwapta River*. Guest lecture presented to Geography 2071, University of Western Ontario, London, Ontario. February 10, 2016. **Middleton, L**., Ashmore, P., Leduc, P. 2016. *Braiding planform dynamics in a proglacial river*. Poster presented at

the CMOS and CGU Joint Scientific Congress, Fredericton, New Brunswick. May 29-June 2 2016.

Middleton, L., Ashmore, P., Leduc, P. 2016. *Braiding planform dynamics in a proglacial river*. Poster presented at the CGU Eastern Section Meeting, Guelph, Ontario. February 4, 2016.